Chapter 4: Thin airfoils and finite wings

Nomenclature for airfoils and wings

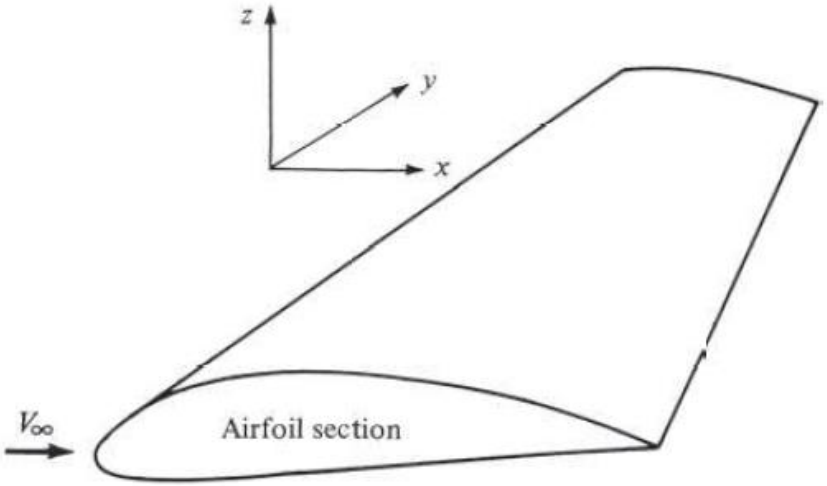

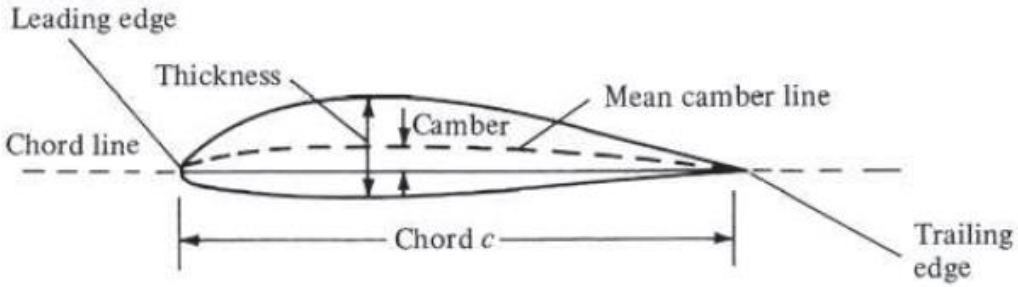

Airfoils

NACA airfoils: developed by the National Advisory Committee for Aeronautics (NACA) starting from the late 1920s.

Four-digit series:
First digit: maximum camber as % of chord.

Second digit: distance of maximum camber from the airfoil leading edge in tenths of the chord.

Last two digits: maximum thickness of the airfoil as % of chord.

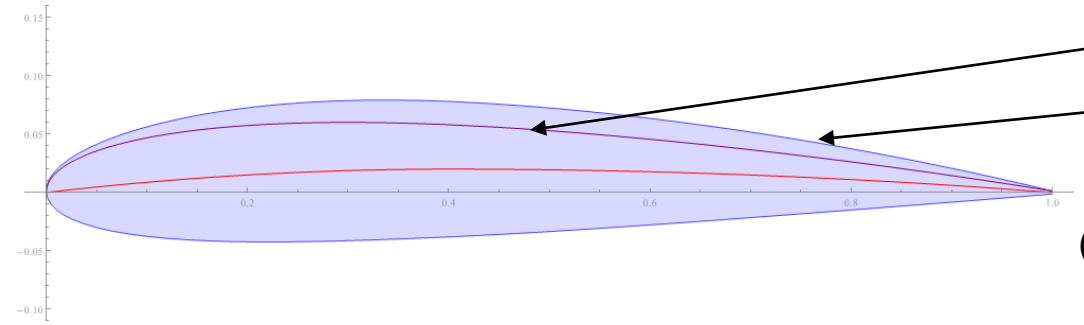

NACA0012

NACA2412

(careful about the “American convention” on airfoil thickness)

Airfoils

NACA airfoils: after the four-digit series, NACA developed the five-, six-, seven- and eight-digit series, typically aiming to maximize the extent of laminar flow above and below the wing.

DLR, ONERA, TsAGI … and many more!

An extensive database (almost 1600 entries!) of airfoil designs is available on the dedicated website of the Aerospace Engineering Department of the University of Illinois at Urbana-Champaign: https://m-selig.ae.illinois.edu/ads.html

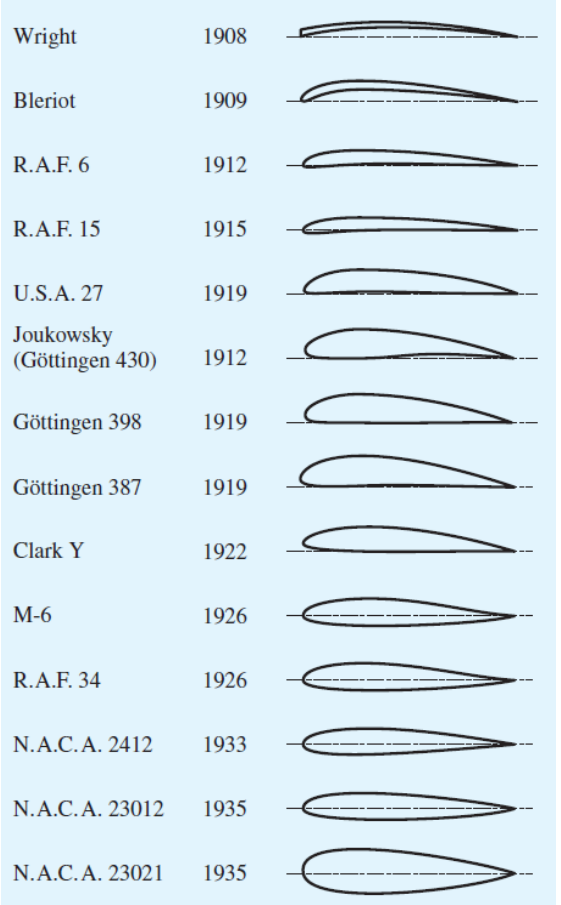

Wing configuration: monoplane

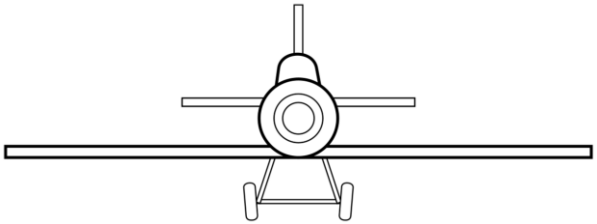

low wing

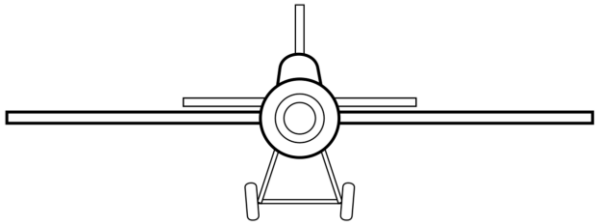

mid wing

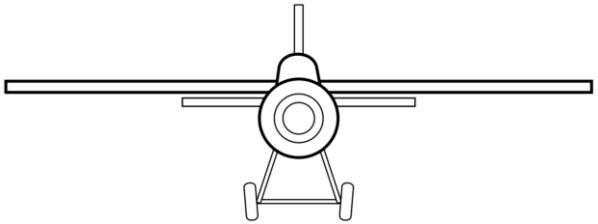

shoulder wing

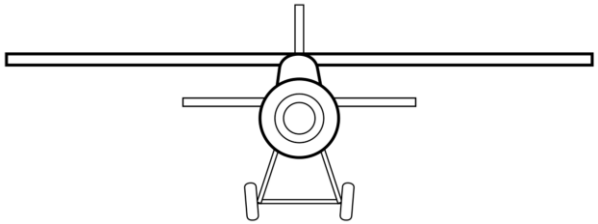

high wing

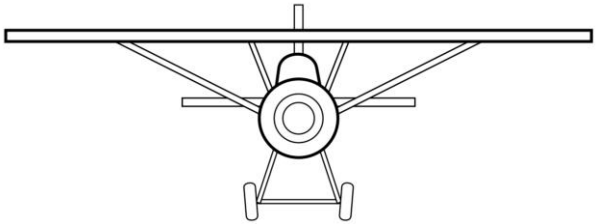

parasol wing
(by the use of struts or pylon)

Wing configuration: biplane

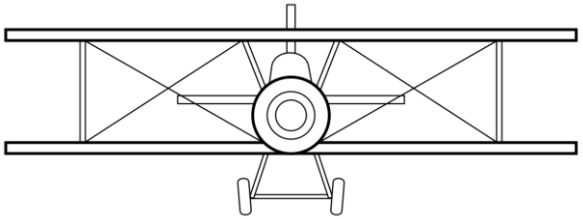

two wing planes of similar size (ex. Wright Flyer I)

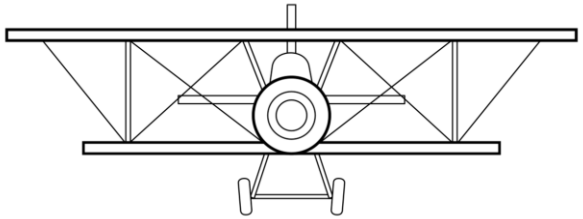

unequal span biplane
(ex. Curtiss JN-4 Jenny)

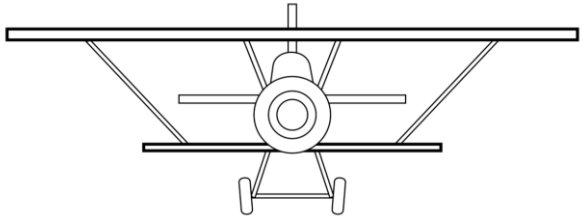

sesquiplane
(ex. Nieuport 17)

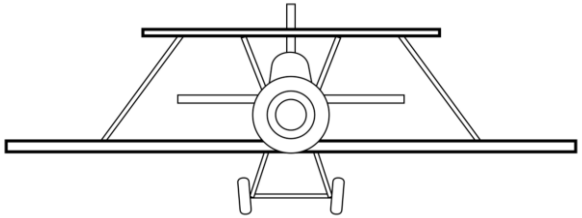

inverted sesquiplane
(ex. Fiat C.R.1)

Wing configuration: biplane

On May 5th, 1925, Mario de Bernardi, piloting a FIAT C.R.1, achieved the world record speed over a 500 km distance, flying at an average speed of 254 km/h.

Wing configuration: multiplane

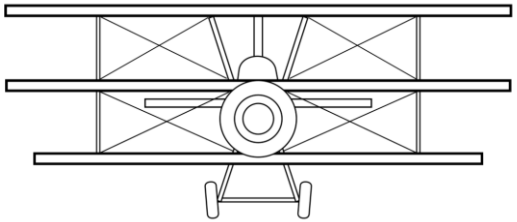

triplane
(ex. Fokker DR.I)

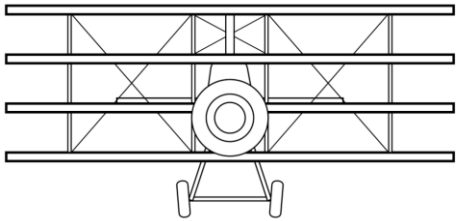

quadriplane
(ex. Armstrong Whitworth F.K.10)

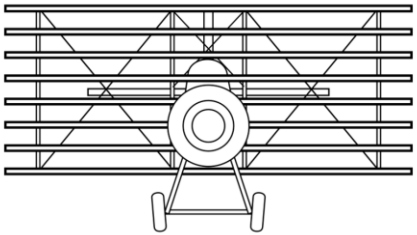

multiplane
(ex. Caproni CA.60 Transaereo)

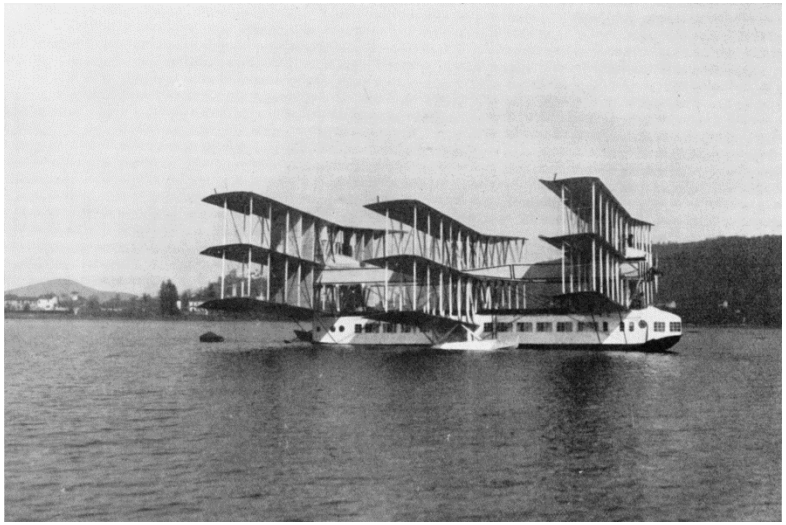

Wing configuration: closed wing

Merging or joining structurally the two wing planes at or near the tips stiffens the structure and can reduce induced drag

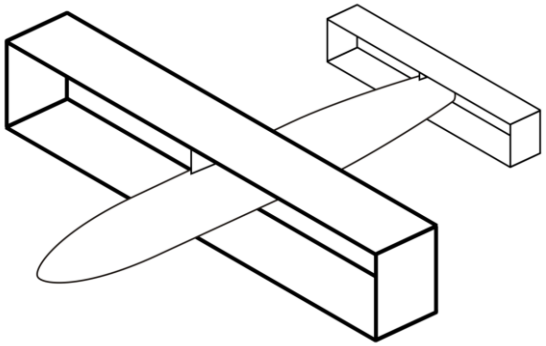

box wing
(ex. Santos-Dumont's 14-bis)

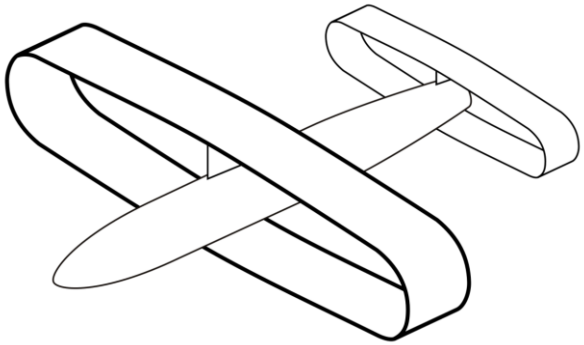

annular box wing
(ex. Blériot III)

Wing planform: aspect ratio AR

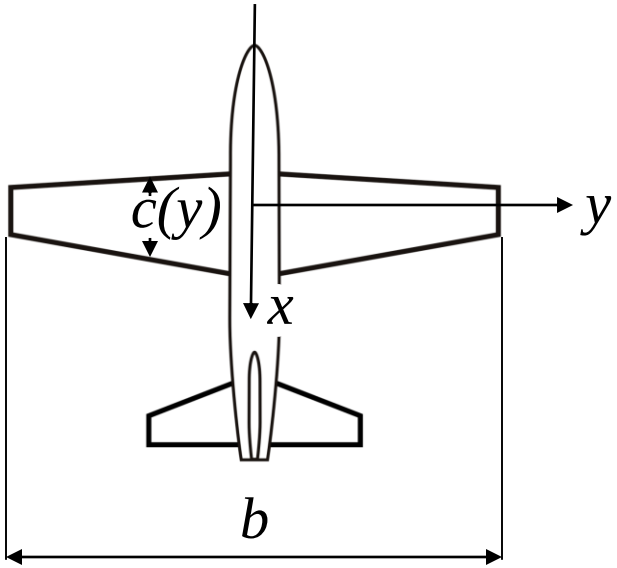

mean chord: $\bar{c} = \dfrac{\int_{-b/2}^{b/2} c(y)\,\mathrm{d}y}{b}$

planform area: $S = b\,\bar{c}$

aspect ratio: $AR = \dfrac{b^2}{S} = \dfrac{b}{\bar{c}}$

Wing planform: aspect ratio AR

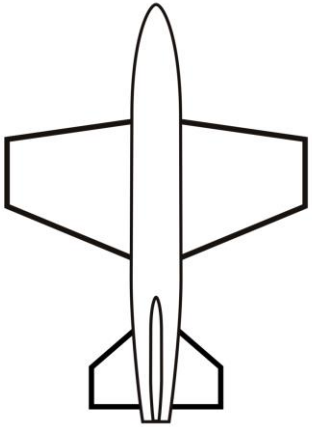

low AR
(structurally efficient and high roll rate, ex. Lockheed F-104 Star Fighter)

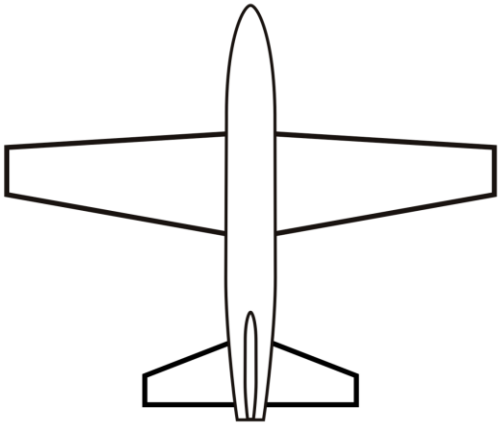

moderate AR
(general purpose, ex. Lockheed P-80 Shooting Star)

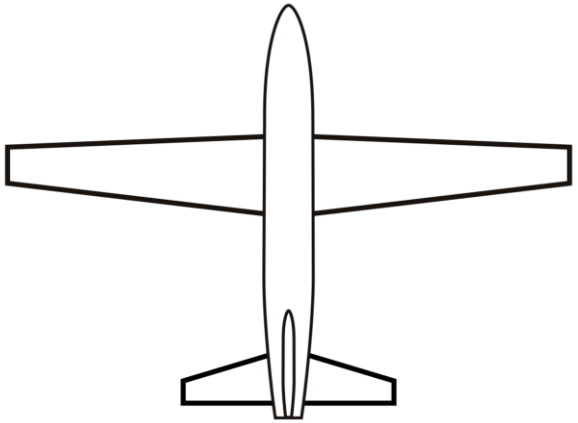

high AR
(aerodynamically efficient, ex. Bombardier Dash 8)

Wing planform: chord variation along y

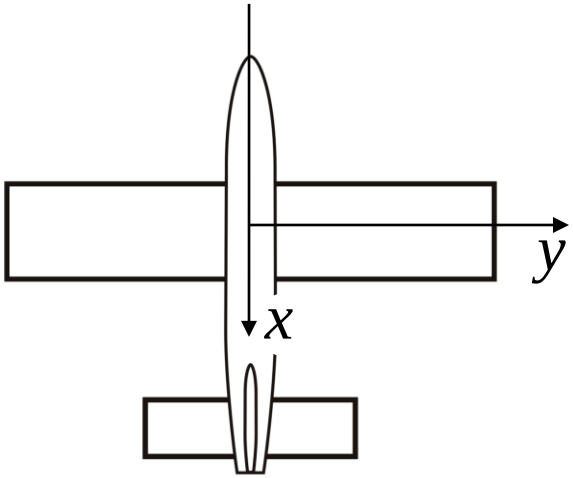

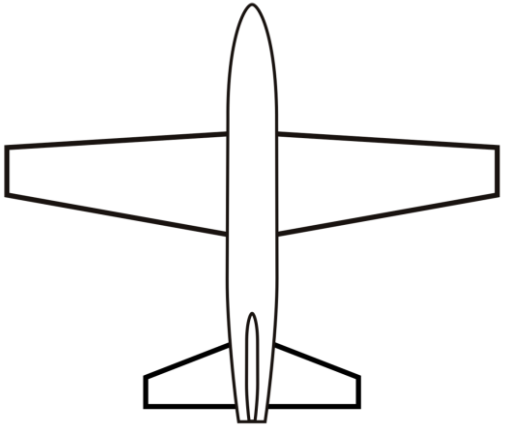

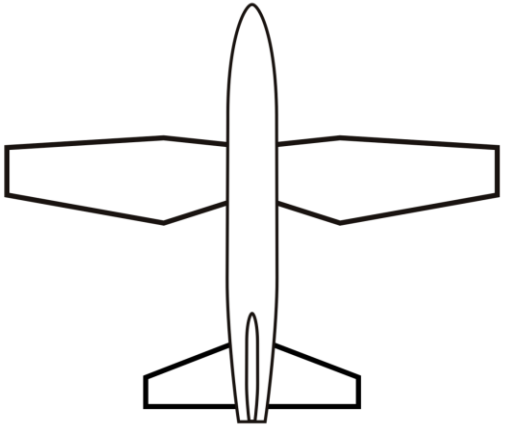

constant chord or rectangular wing (low cost but not efficient, ex. Piper J-3 Cub)

tapered wing, trapezoidal (c decreases with y, ex. Grumman F4F Wildcat)

compound tapered (ex. Westland Lysander army cooperation aircraft)

Wing planform: chord variation along y

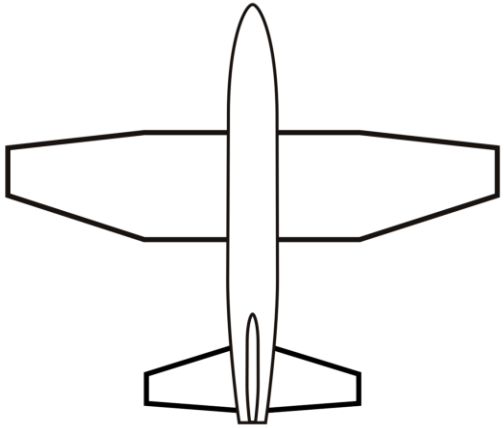

constant chord w/ tapered outer section (ex. many Cessna)

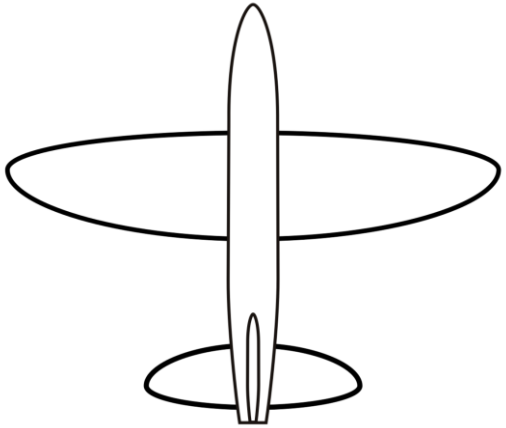

elliptical wing (ex. Supermarine Spitfire)

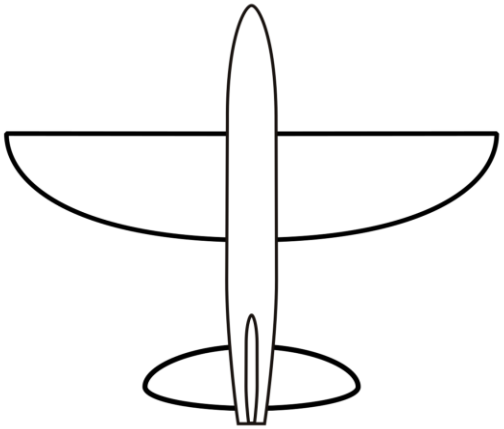

semi-elliptical wing (only LE or TE have elliptical shape, ex. Seversky P-35)

Supermarine Spitfire

Probably the most famous British fighter aircraft of WWII, it continued in service for many years after the war. Designed by R.J. Mitchell, the aircraft's elliptical wing had a thin cross-section to permit achieving high speeds.

According to John D. Anderson, Jr., the choice of the elliptic shape had "*nothing to do with aerodynamics*" …

Wing planform: wing sweep

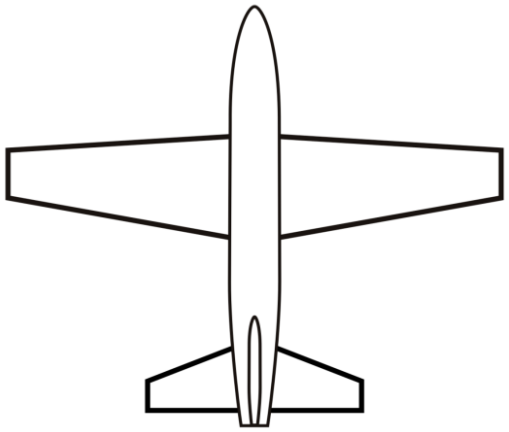

straight

structurally efficient wing for low speed designs, ex. Lockheed P-80 Shooting Star

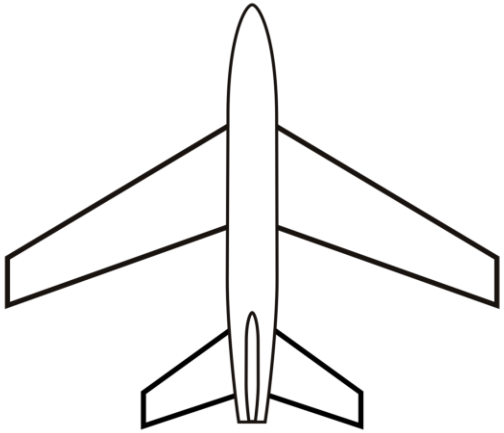

swept back

high subsonic and early super-sonic designs, ex. Hawker Hunter

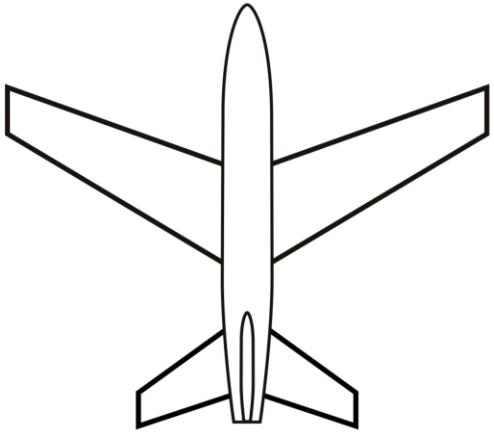

forward swept

low drag at transonic speeds, but aero-elastic problems, ex. Sukhoi Su-47

Wing planform: wing sweep

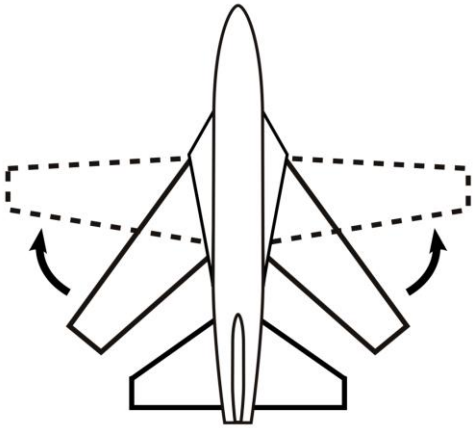

swing-wing

ex. a few military aircrafts, such as the General Dynamics F-111 Aardvark

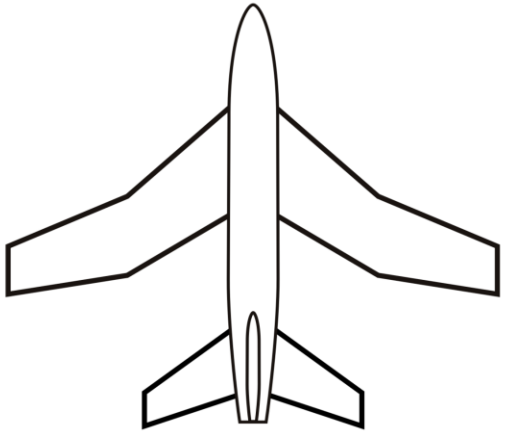

crescent

different sweep on outer and inner sections, compromise between shock delay and spanwise flow control, ex. Handley Page Victor

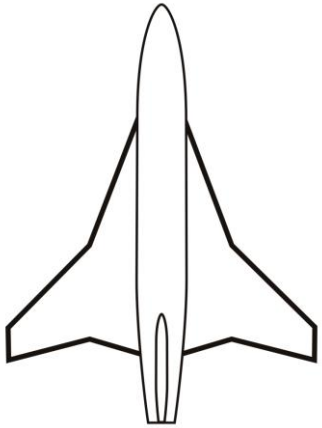

cranked arrow

prototypes by General Dynamics F16-XL

Wing twist

Aerodynamic feature to adjust the lift distribution along wing span.

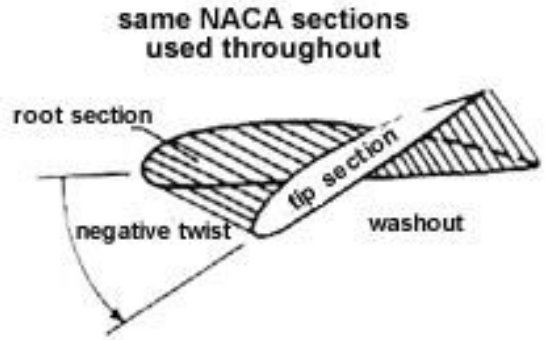

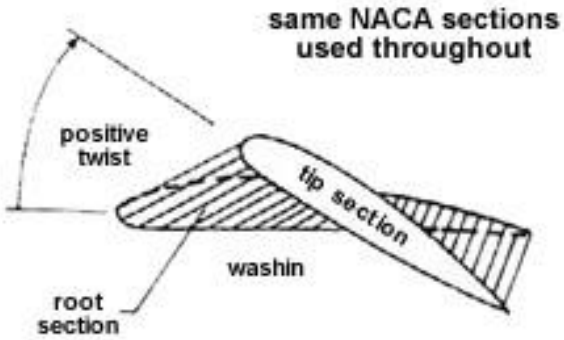

geometric twist

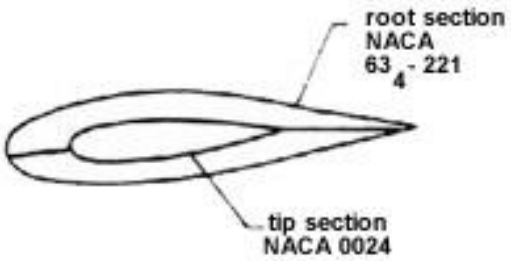

aerodynamic twist

Dihedral and anhedral

Angling the wings up or down spanwise from root to tip can help to resolve various design issues, such as stability and control in flight.

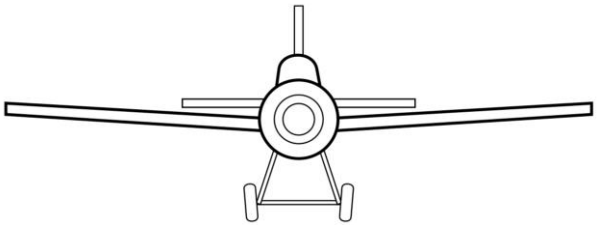

dihedral

improved lateral stability, ex. Boeing 737

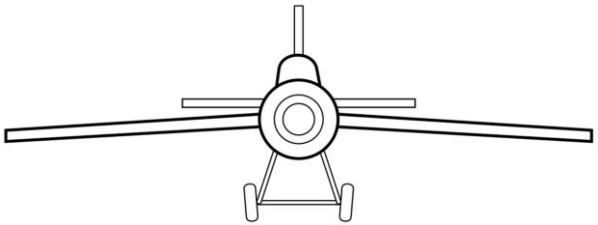

anhedral

improved maneuverability ex. Boeing B-52 Strato-fortress

Minor independent surfaces

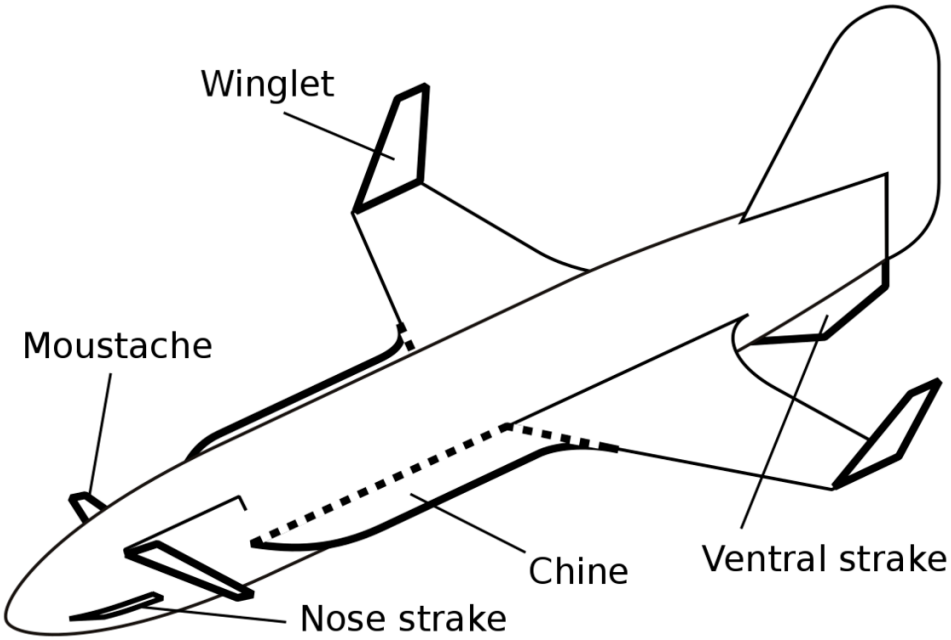

Winglet: a small vertical fin at the wingtip, usually turned upwards. Reduces the size of vortices shed by the wingtip, and hence also tip drag.

Strake: a small surface, typically longer than it is wide and mounted on the fuselage. Strakes may be located at various positions in order to improve aerodynamic behavior. Leading edge root extensions (**LERX**) are also sometimes referred to as wing strakes.

Control surfaces

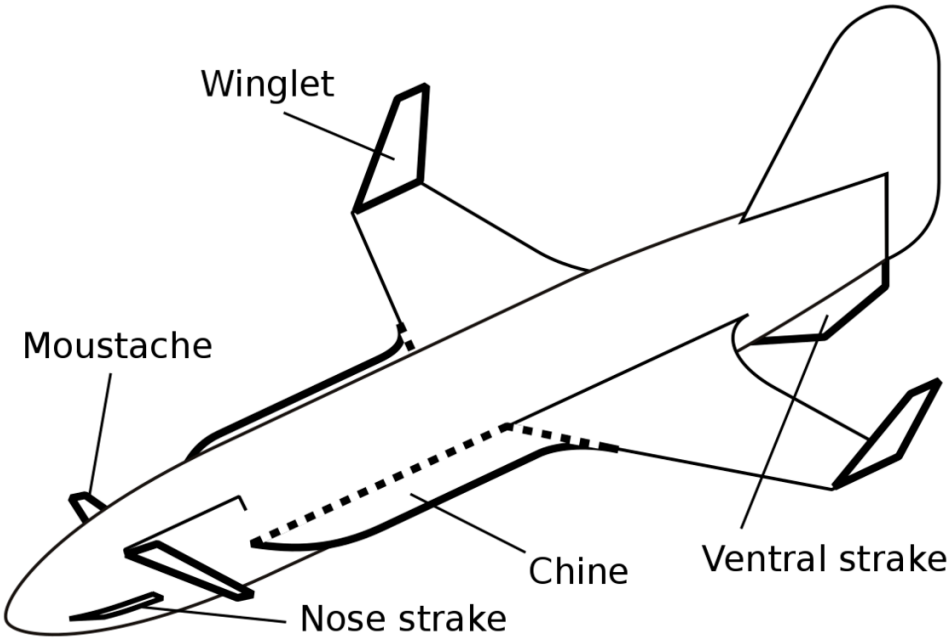

Chine: long, narrow sideways extension to the fuselage, blending into the main wing. It improves low speed (high angle of attack) handling, provides extra lift at supersonic speeds for minimal increase in drag. Ex. Lockheed SR-71 Blackbird191.

Moustache: small high-aspect-ratio canard surface having no movable control surface. Typically is retractable for high speed flight. Deflects air downward onto the wing root, to delay the stall. Ex. Dassault Milan192 and Tupolev Tu-144193.

Control surfaces: high lift devices

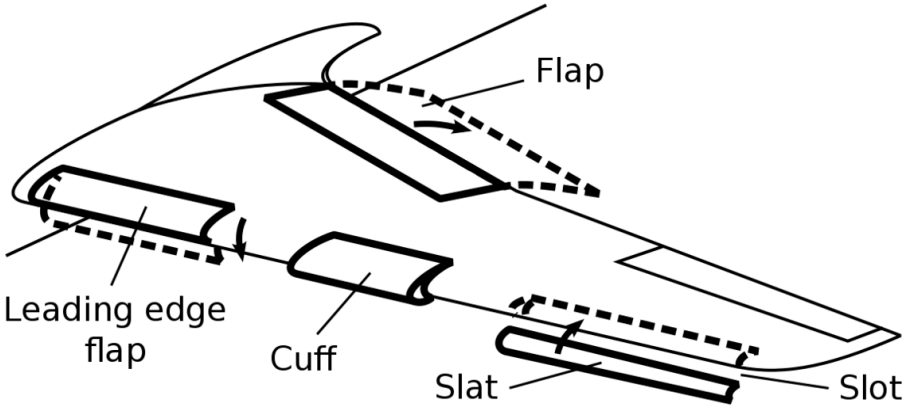

Slat and **slot**: a leading edge slat is a small airfoil extending in front of the main leading edge. The spanwise gap behind it forms a leading-edge slot. Air flowing up through the slot is deflected backwards by the slat to flow over the wing, allowing the aircraft to fly at lower air speeds without flow separation or stalling. A slat may be fixed or retractable.

Flap: a hinged aerodynamic surface, usually on the trailing edge, which is rotated downwards to generate extra lift and drag.

Cuff: fixed aerodynamic device which introduces a sharp discontinuity at the LE, typically to improve low-speed characteristics.

Control surfaces: devices to delay stall

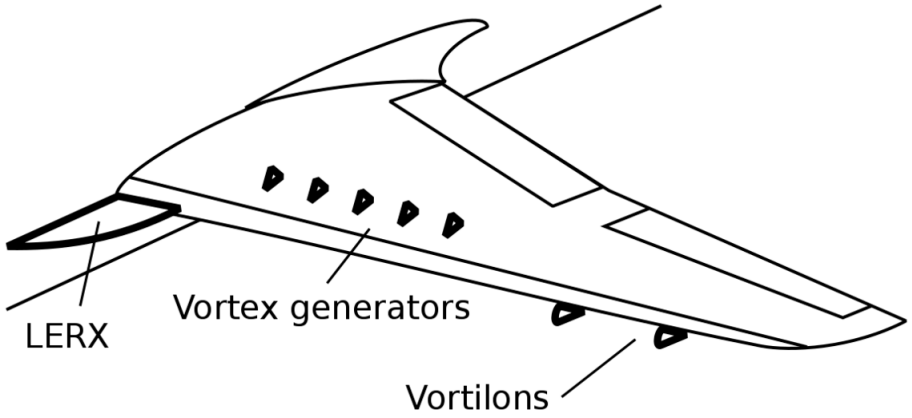

Vortex generator: small protrusion on the upper leading wing surface; usually, several are spaced along the span of the wing. They increase drag at all speeds.

Vortilon: one or more flat plates attached to the underside of the wing near its outer leading edge. At low speeds, it creates a vortex which energizes the boundary layer over the wing.

Leading-edge root extension (LERX): placed forward of the leading edge. The primary reason for adding a LERX is to improve the airflow at high angles of attack and low airspeeds, to improve handling and delay stall.

Control surfaces: drag reduction devices

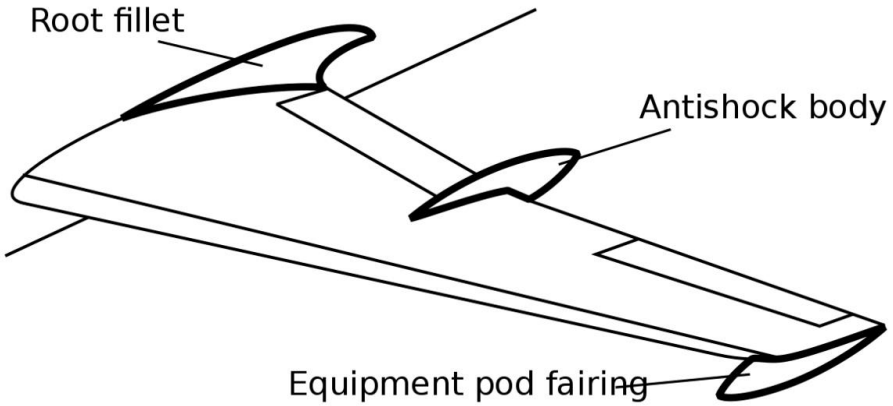

Anti-shock body: a streamlined pod shape added to the leading or trailing edge of an aerodynamic surface, to delay the onset of shock stall and reduce transonic wave drag. Examples include the *Küchemann carrots* on the wing trailing edge of the Handley Page Victor B.2.

Fillet: a small curved infill at the junction of two surfaces, such as a wing and fuselage, blending them smoothly together to reduce drag.

Fairings of various kinds, such as blisters, pylons and wingtip pods, whose only aerodynamic purpose is to produce a smooth outline and reduce drag.

Axis of control of an airplane

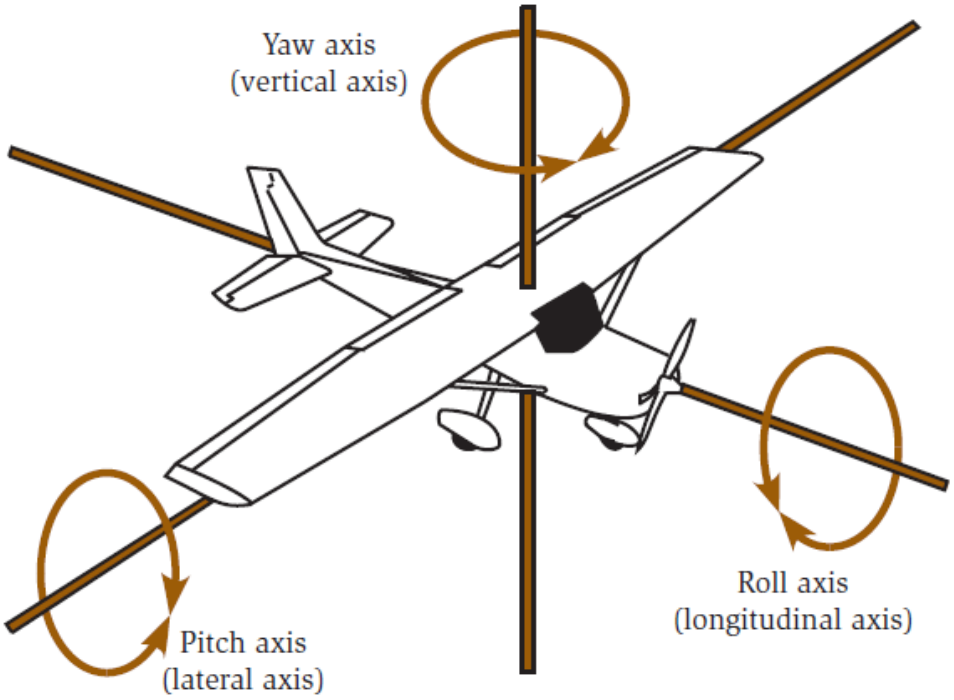

The three axes go through the center of gravity (balance point) of the airplane.

Ailerons control rotation about the roll axis

Elevators control the pitch of an airplane, and thus the angle of attack of the wing.

The rudder controls yaw.

Parts definition

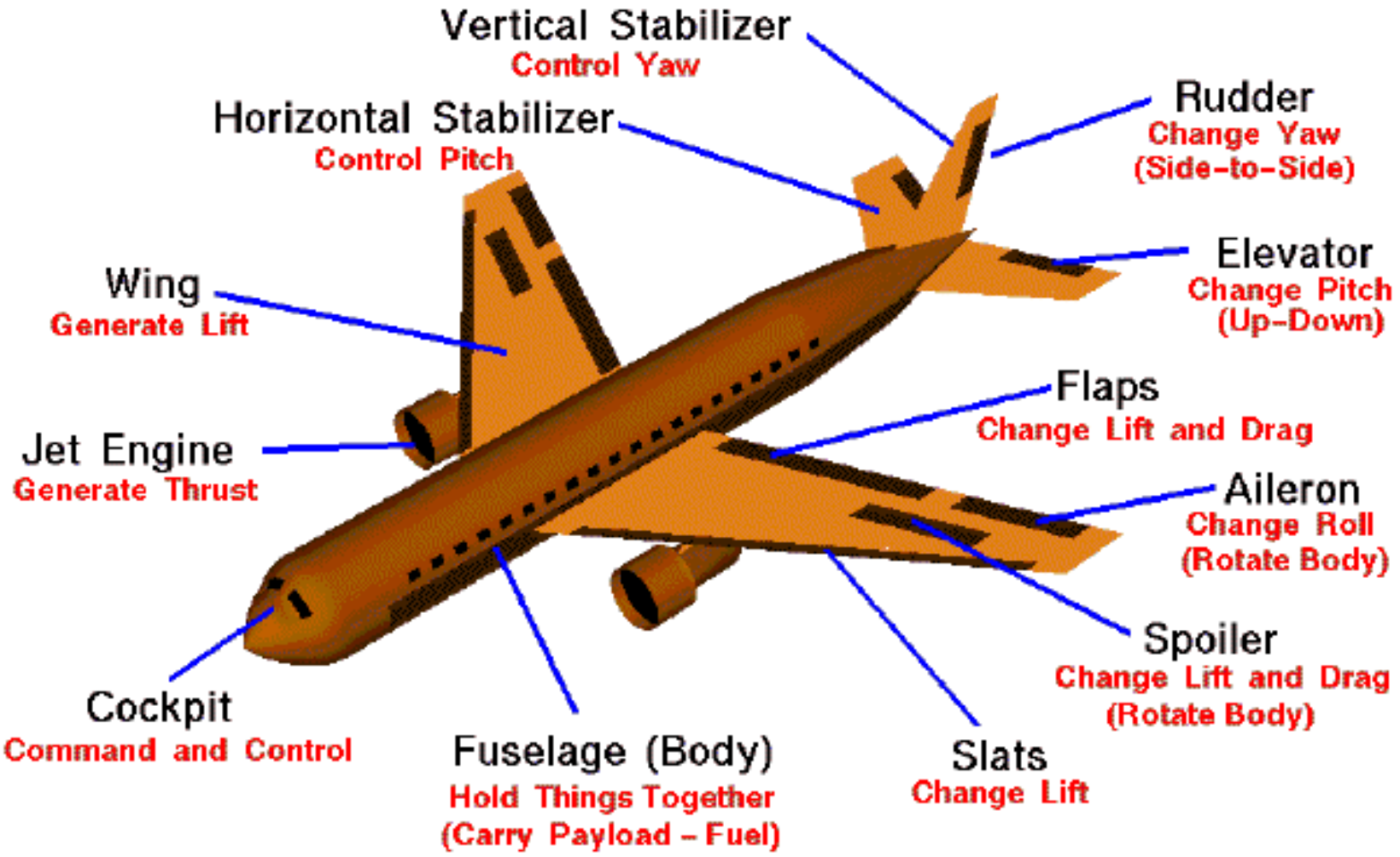

Ailerons

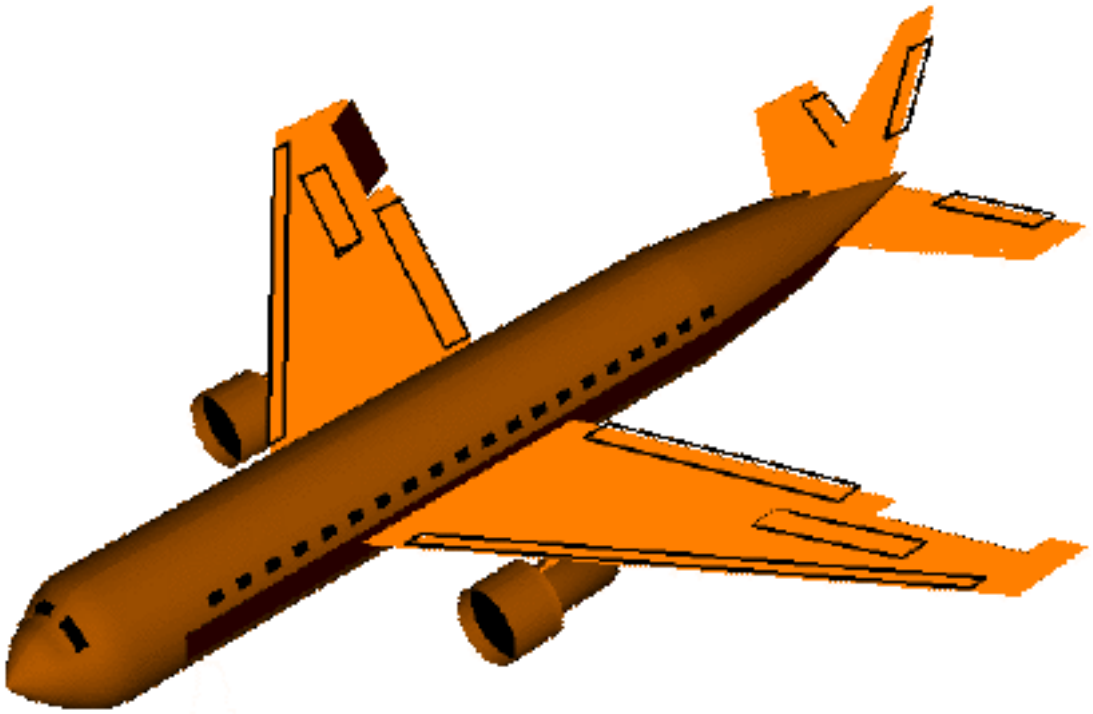

Elevators

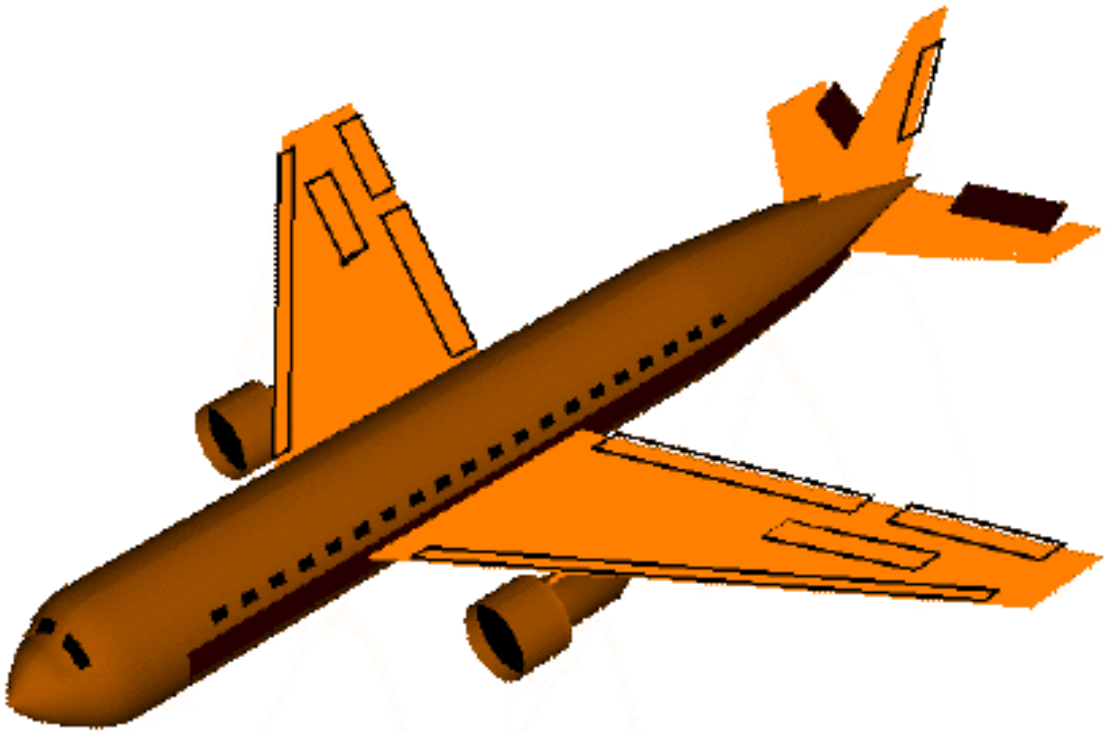

Rudder

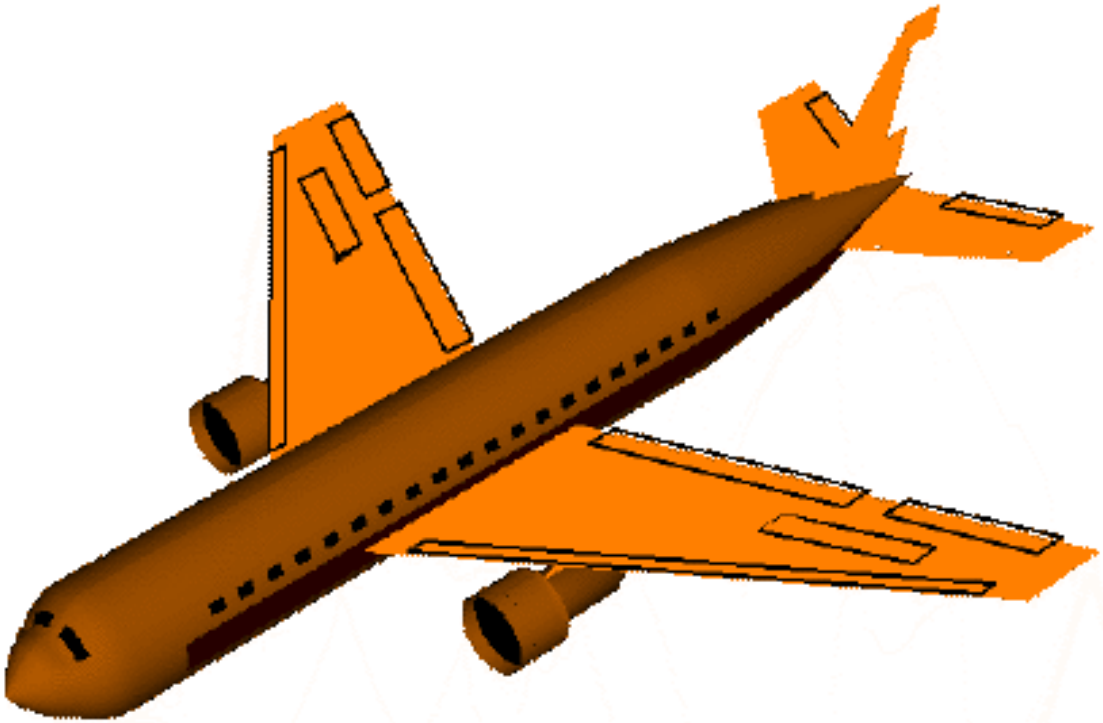

One spoiler

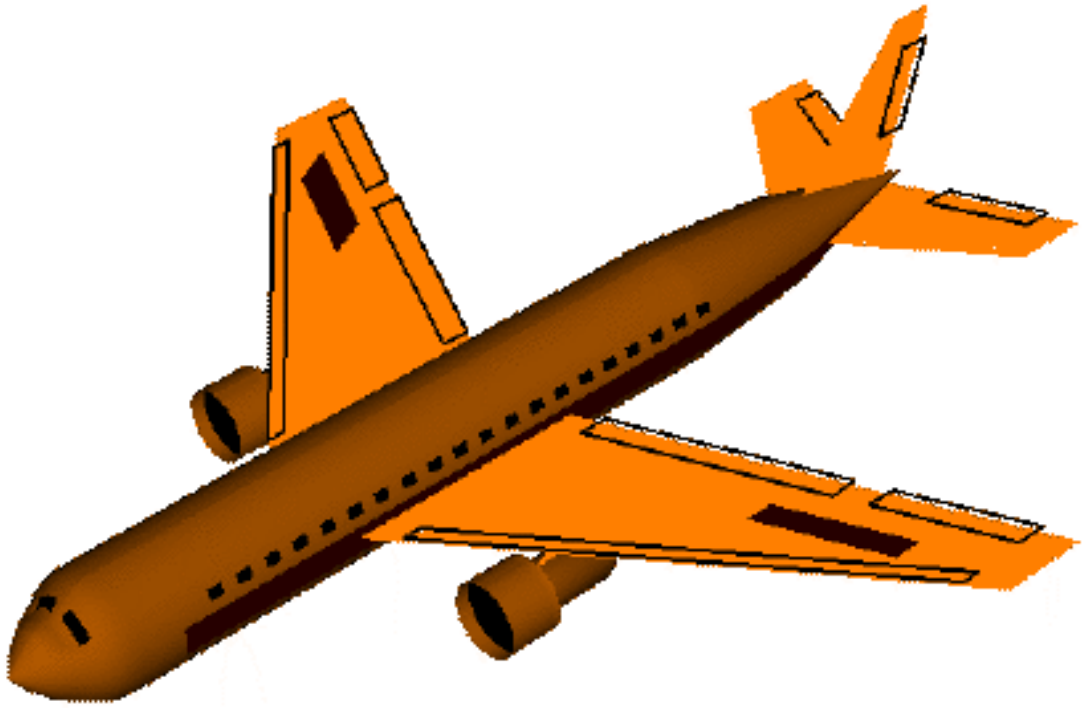

Both spoilers

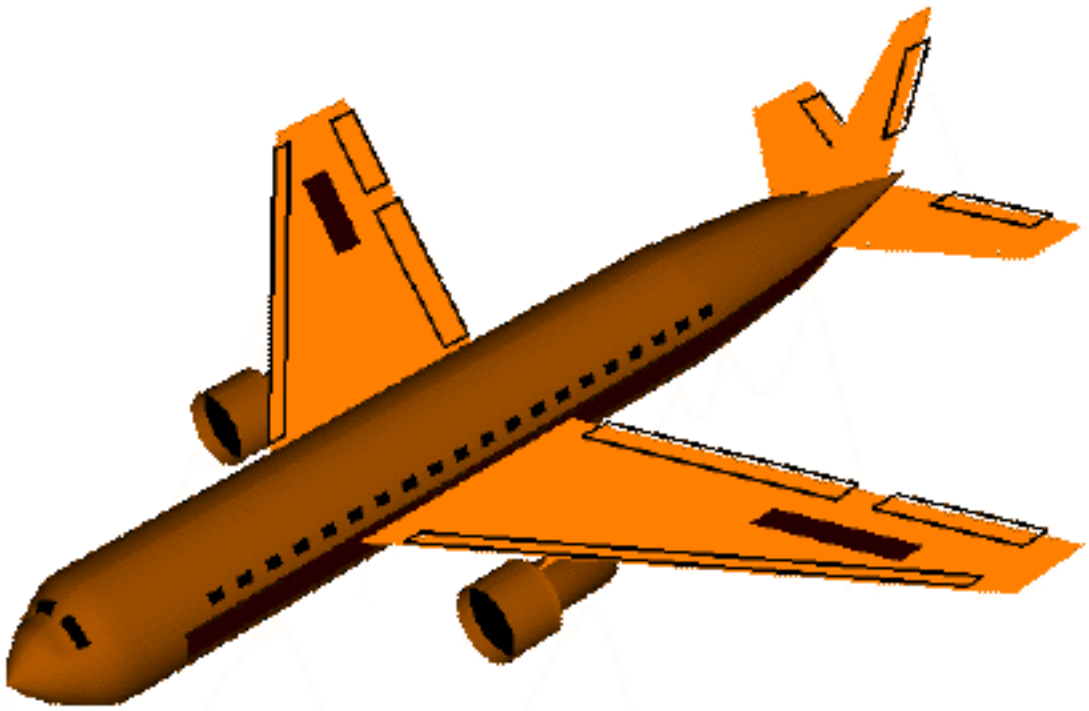

Flaps/slats

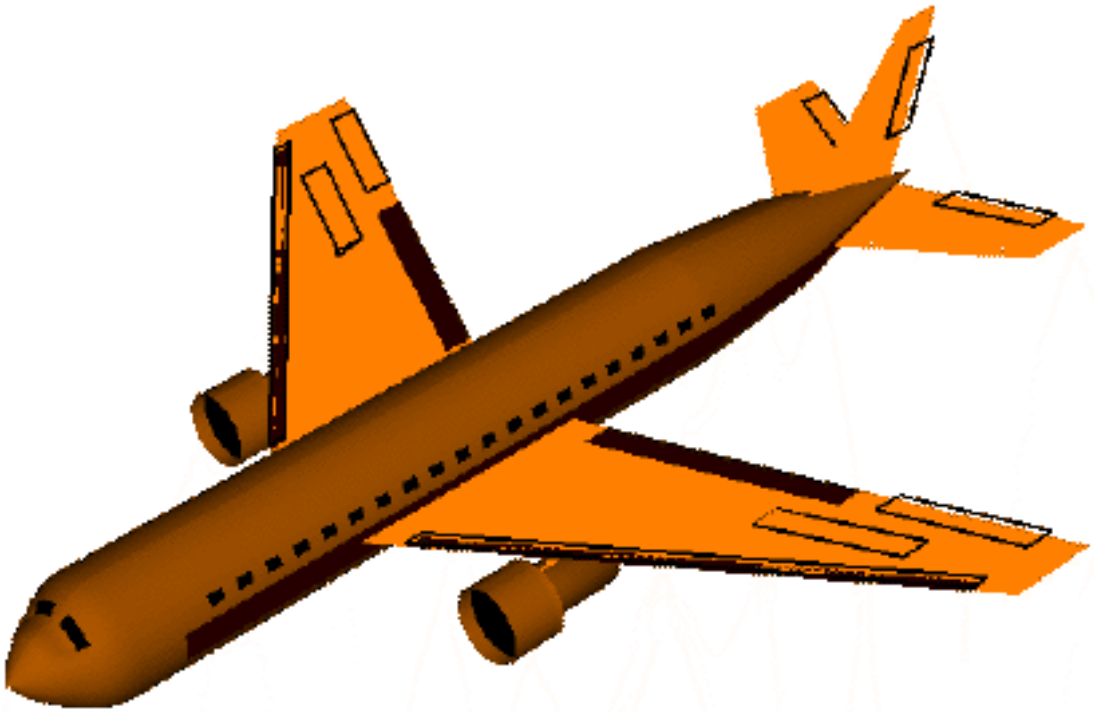

Flaps/slats

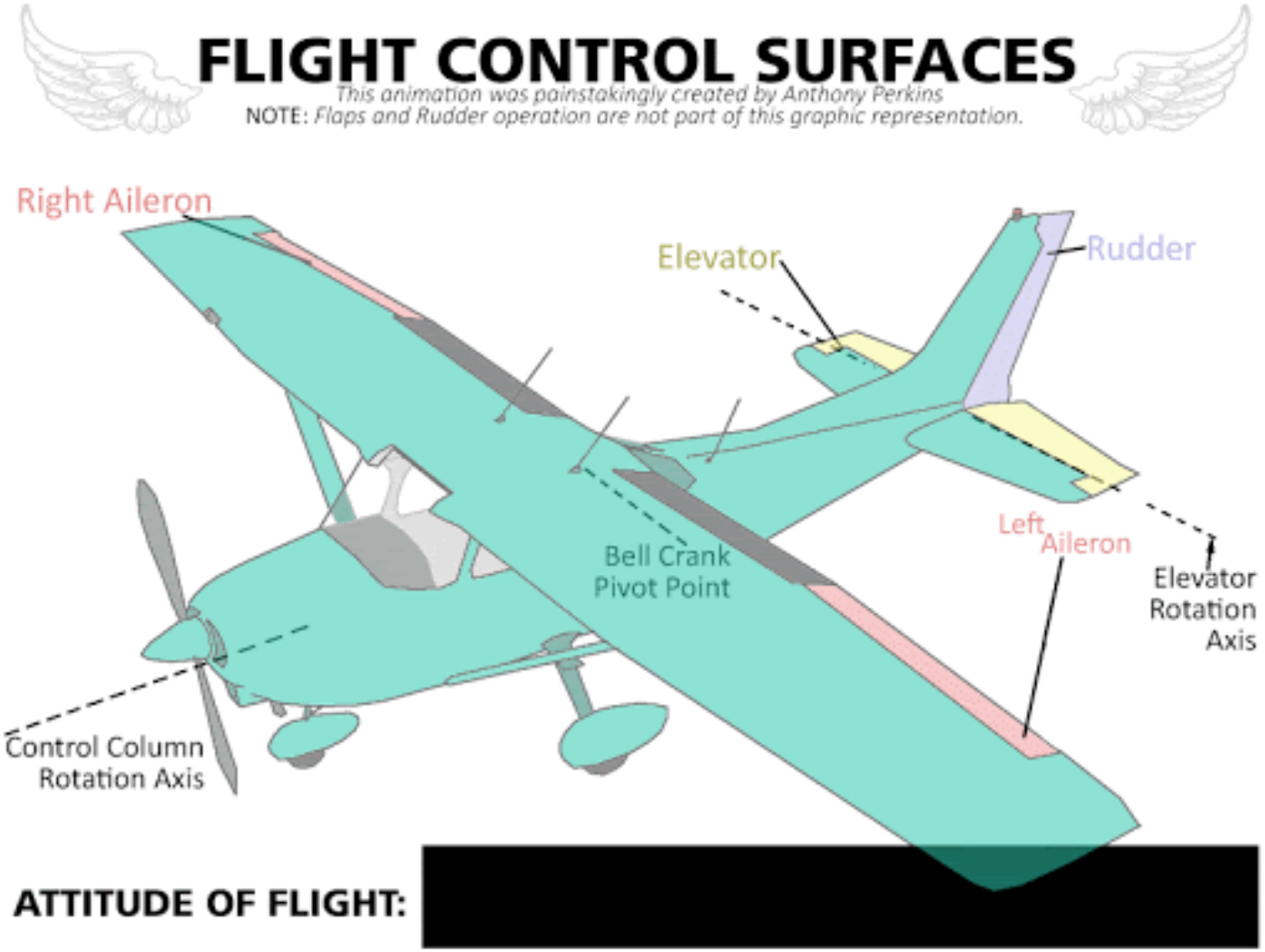
FLIGHT CONTROL SURFACES
This animation was painstakingly created by Anthony Perkins
NOTE: Flaps and Rudder operation are not part of this graphic representation.
Right Aileron
Elevator
Rudder
Left Aileron
Bell Crank Pivot Point
Elevator Rotation Axis
Control Column Rotation Axis
ATTITUDE OF FLIGHT:

The vortex filament

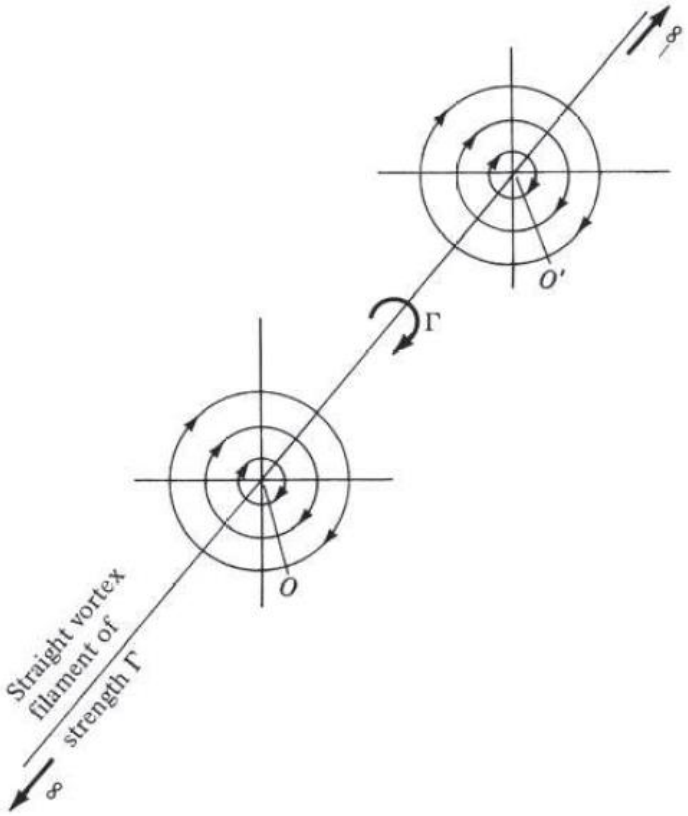

Aerodynamic convention: positive circulation is **clockwise**

(this is different from what we had in ch. 3)

The vortex sheet

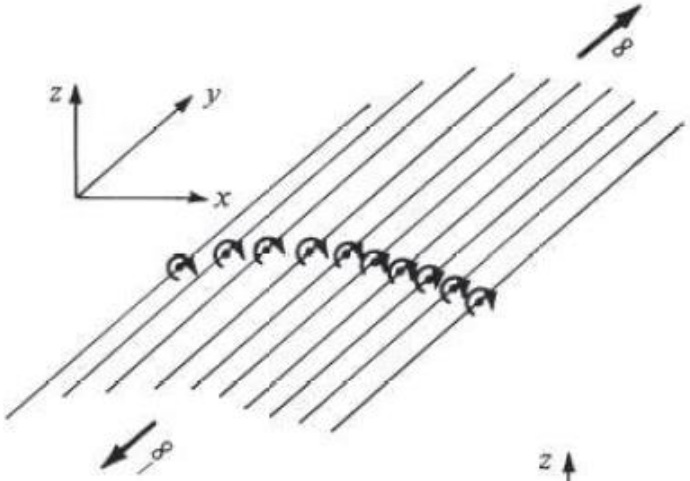

Vortex sheet in perspective

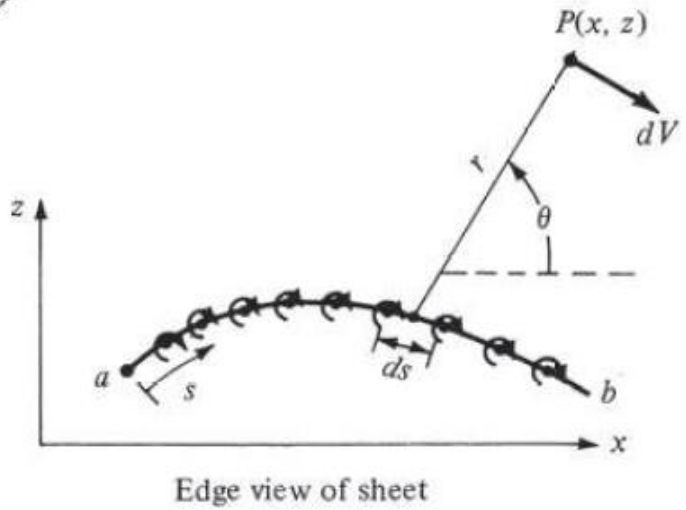

Edge view of sheet

$\gamma = \gamma(s)$ strength of the vortex sheet *per unit length*

The vortex sheet

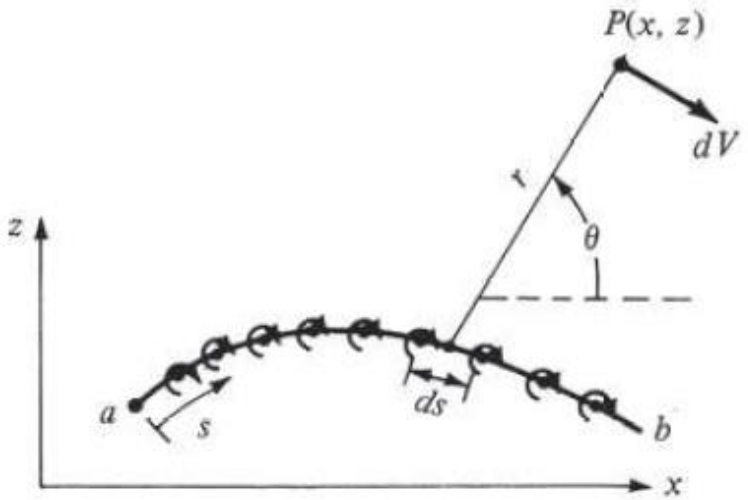

The infinitesimal portion ds of the vortex sheet induces on point P in the flow a velocity of magnitude

$$|\mathrm{d}V| = \frac{|\mathrm{d}\Gamma|}{2\pi r}$$

$\mathrm{d}\Gamma = \gamma\, \mathrm{d}s$ circulation over infinitesimal segment $\mathrm{d}s$

The vortex sheet

For a vortex sheet there is a discontinuous change in the *tangential component* of velocity across the sheet, while the normal component is preserved across the sheet.

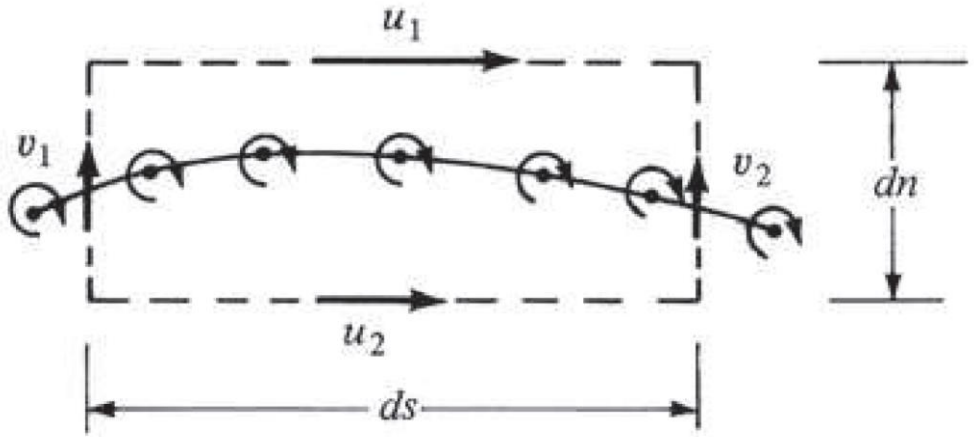

$$\Gamma = u_1\,\mathrm{d}s - v_2\,\mathrm{d}n - u_2\,\mathrm{d}s + v_1\,\mathrm{d}n$$
$$= (u_1 - u_2)\,\mathrm{d}s + (v_1 - v_2)\,\mathrm{d}n = \gamma\,\mathrm{d}s$$

The vortex sheet

For $\mathrm{d}n \to 0$ we have

$$\gamma = u_1 - u_2$$

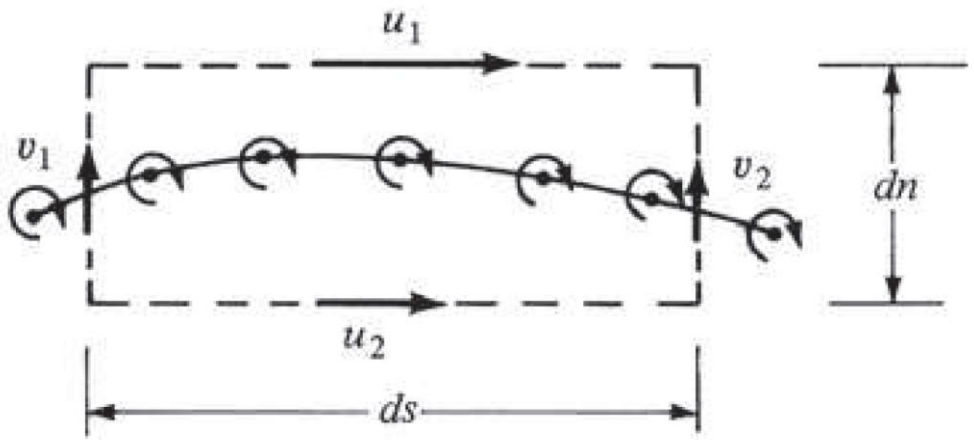

The local jump in tangential velocity across the vortex sheet is equal to the local sheet strength

How to use a vortex sheet?

An airfoil surface or the camber line can be replaced by a vortex sheet of variable strength (L. Prandtl, 1912-1922)

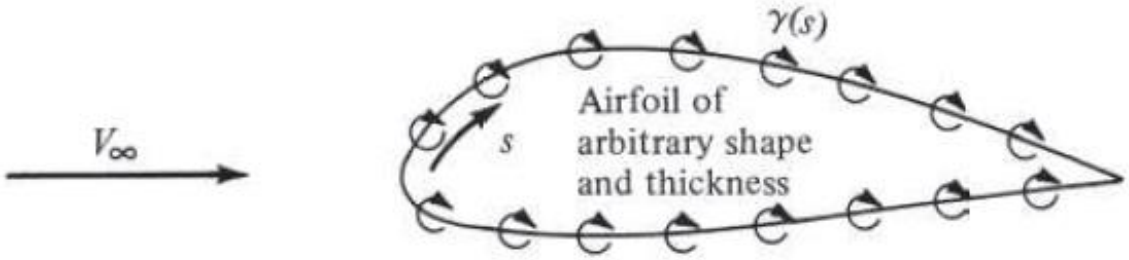

(note the similarity with the concept of a boundary layer!)

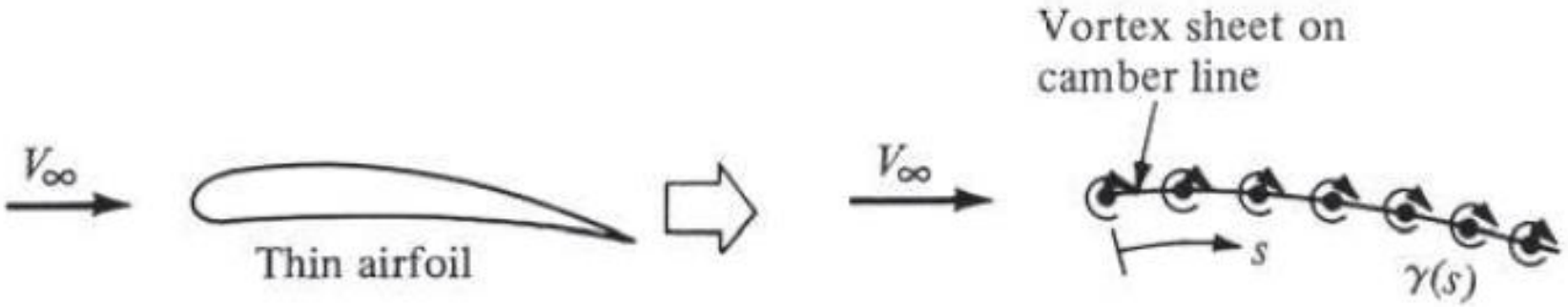

Kutta (yet again!)

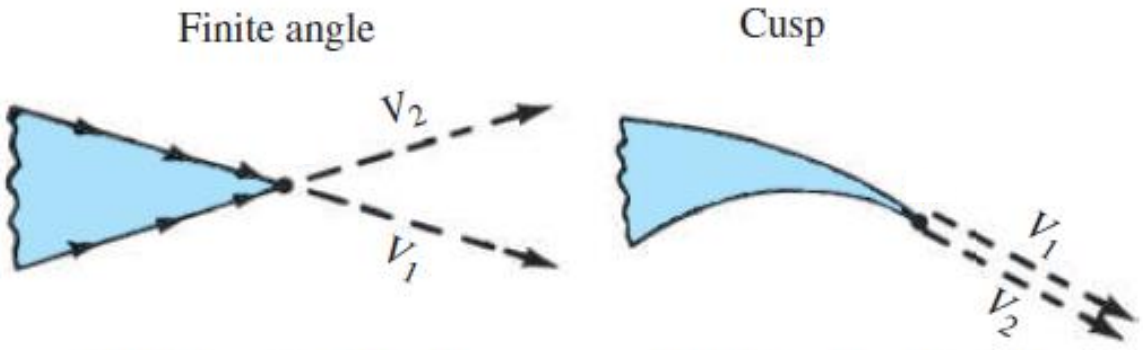

At the trailing edge velocity and pressure (!) are unique, hence:

$$\gamma(TE) = 0$$

Thin airfoil theory

A *thin* airfoil can be modeled as a vortex sheet on the camber line. Goal: find the distribution of $\gamma(s)$ that renders the camber line a streamline of the flow and such that the Kutta condition is satisfied.

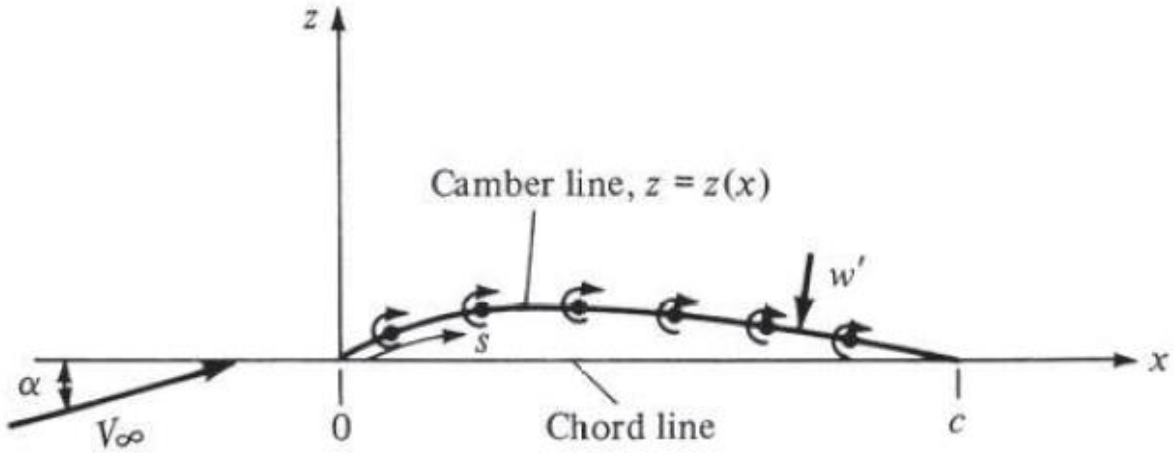

$$\gamma = \gamma(s)$$

Thin airfoil theory

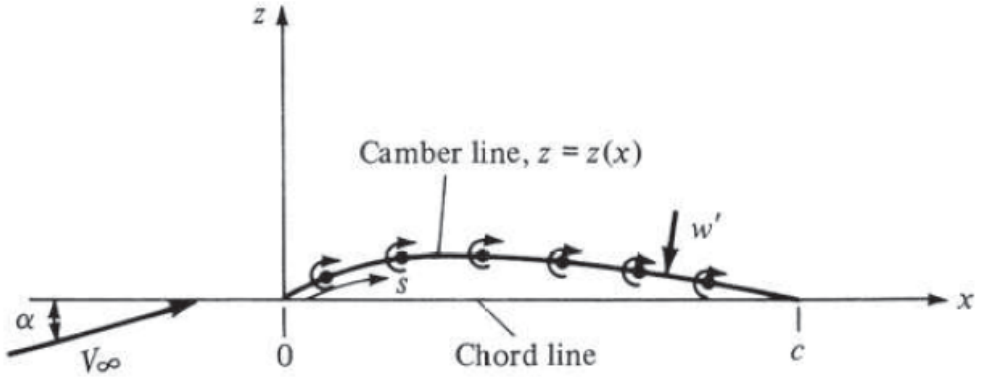

(a) Vortex sheet on the camber line

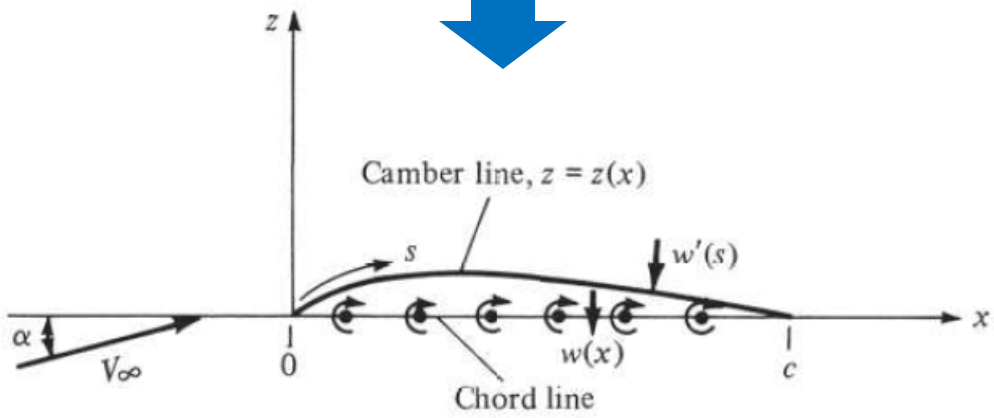

(b) Vortex sheet on the chord line

$$\gamma = \gamma(x)$$

Thin airfoil theory

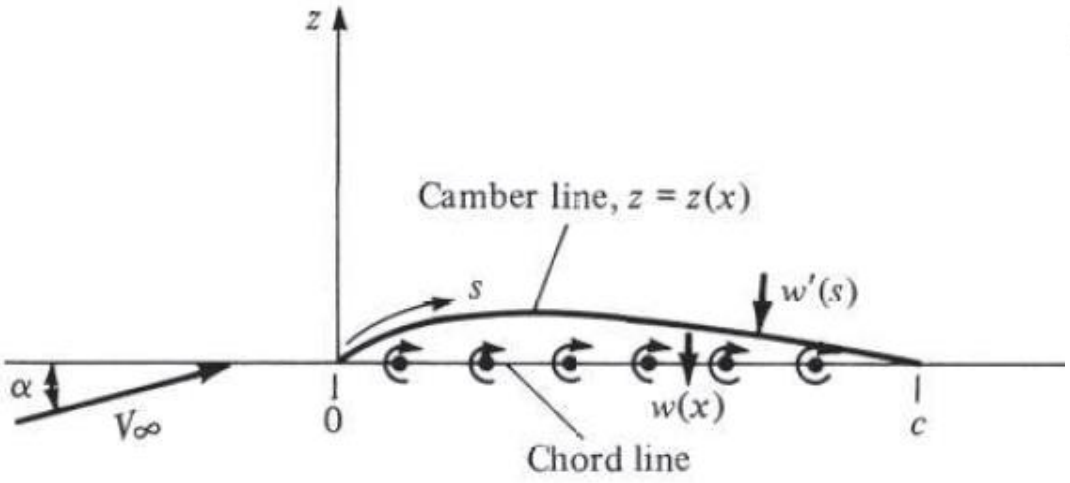

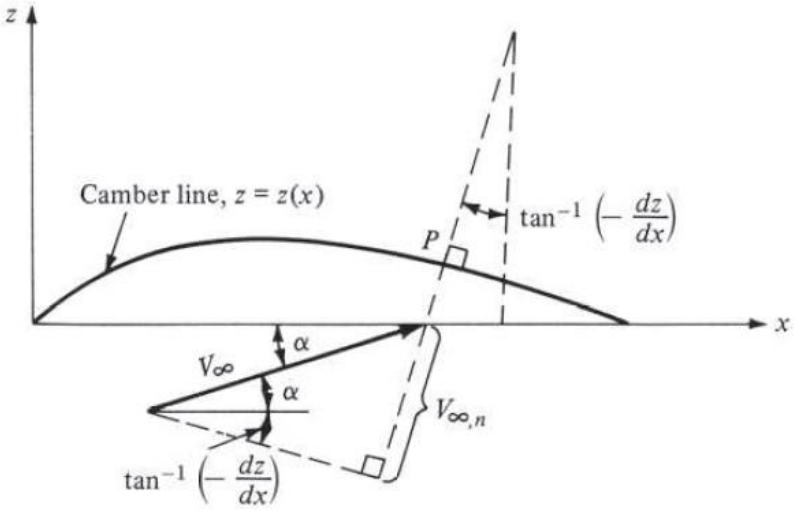

$$V_{\infty,n} + w'(s) = 0$$

$$V_{\infty,n} = V_\infty \sin\left[\alpha + \tan^{-1}\left(-\frac{dz}{dx}\right)\right]$$

$$w'(s) \approx w(x)$$

$$V_{\infty,n} \approx V_\infty \left(\alpha - \frac{dz}{dx}\right)$$

Thin airfoil theory

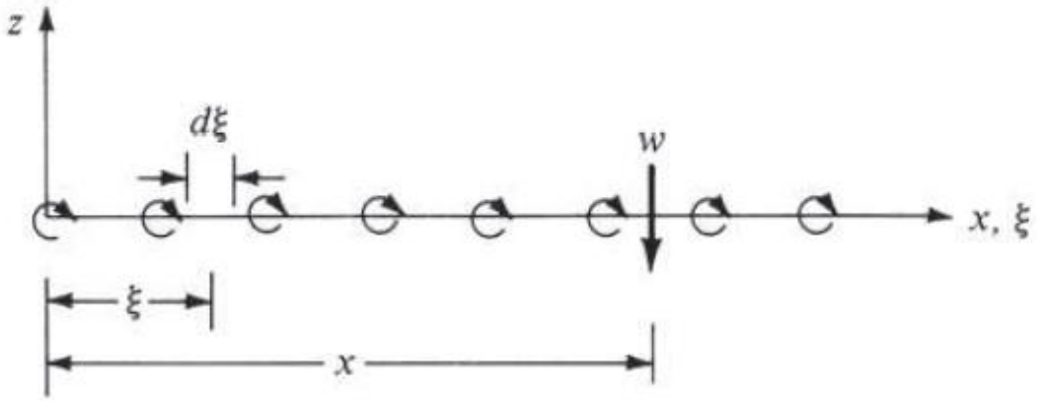

$$w(x) = -\int_0^c \frac{\gamma(\xi)\,d\xi}{2\pi(x-\xi)}$$

(– sign because in direction opposite to that of z-axis)

$$\frac{1}{2\pi}\int_0^c \frac{\gamma(\xi)\,d\xi}{x-\xi} = V_\infty\left(\alpha - \frac{dz}{dx}\right)$$

Fundamental equation of thin airfoil theory

$$\gamma(c) = 0$$

(α in radians!)

Thin airfoil theory

Once $\gamma = \gamma(x)$ is found, we can easily find the total circulation, $\Gamma = \int_0^c \gamma(x)\,\mathrm{d}x$, and then from the KJ theorem the lift on the airfoil: $L' = \rho\, V_\infty\, \Gamma$

(notice that now clockwise circulation is positive)

Thin airfoil theory: the **symmetric** airfoil

If the thin airfoil is symmetric $z(x) = 0$ and $\frac{\mathrm{d}z}{\mathrm{d}x} = 0$

$$\frac{1}{2\pi}\int_0^c \frac{\gamma(\xi)\,d\xi}{x-\xi} = V_\infty \alpha$$

Transformation: $\xi = \frac{c}{2}(1-\cos\theta) \longrightarrow d\xi = \frac{c}{2}\sin\theta\, d\theta$

$\theta = 0$ (LE, $\xi = 0$)

$\theta = \pi$ (TE, $\xi = c$)

$x = \frac{c}{2}(1-\cos\theta_0)$ x is a some point on the chord line

Thin airfoil theory: the symmetric airfoil

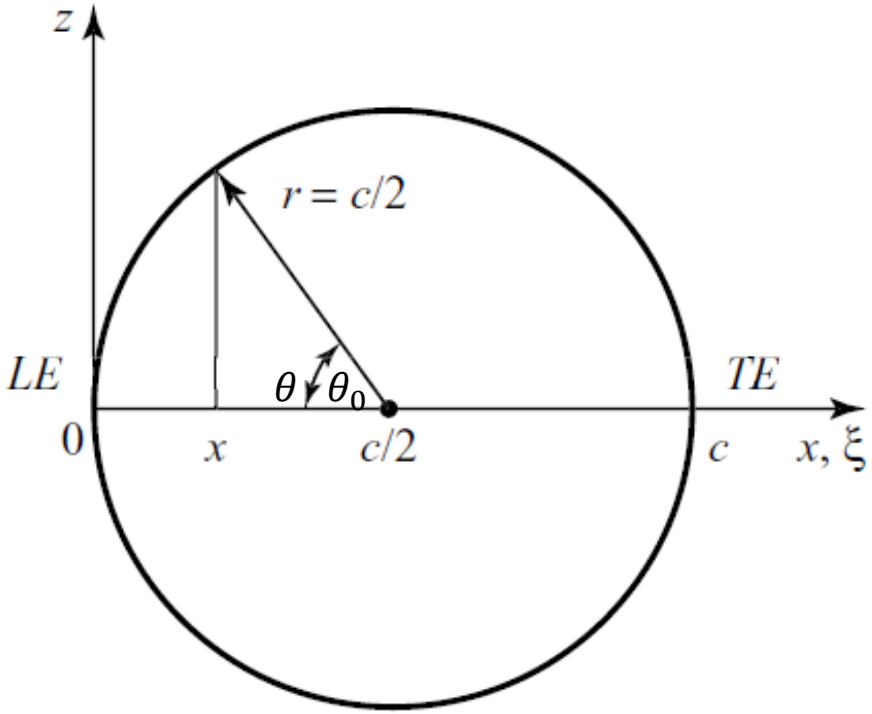

The transformation variable

Thin airfoil theory: the symmetric airfoil

$$\frac{1}{2\pi}\int_0^{\pi}\frac{\gamma(\theta)\sin\theta\,d\theta}{\cos\theta-\cos\theta_0}=V_\infty\alpha$$

From the mathematical theory of integral equations a solution can be found:

$$\boxed{\gamma(\theta)=2\alpha V_\infty\frac{(1+\cos\theta)}{\sin\theta}}$$

(verify the solution by yourselves, using Glauert's first integral, and verify also that Kutta condition is satisfied)

Thin airfoil theory: Glauert's integrals

$$\int_0^{\pi} \frac{\cos(n\theta)}{\cos\theta - \cos\theta_0}\,\mathrm{d}\theta = \frac{\pi \sin(n\theta_0)}{\sin\theta_0}$$

$$\int_0^{\pi} \frac{\sin(n\theta)\sin\theta}{\cos\theta - \cos\theta_0}\,\mathrm{d}\theta = -\pi\cos(n\theta_0)$$

Thin airfoil theory: the symmetric airfoil

$$\gamma(\theta) = 2\alpha V_\infty \frac{(1+\cos\theta)}{\sin\theta}$$

$$\cos\theta = 1 - \frac{2\xi}{c}$$

$$\sin\theta = 2\sqrt{\frac{\xi}{c}\left(1-\frac{\xi}{c}\right)}$$

$$\gamma(\xi) = 2\alpha V_\infty \frac{1-\frac{\xi}{c}}{\sqrt{\frac{\xi}{c}\left(1-\frac{\xi}{c}\right)}} = 2\alpha V_\infty \sqrt{\frac{c}{\xi}-1}$$

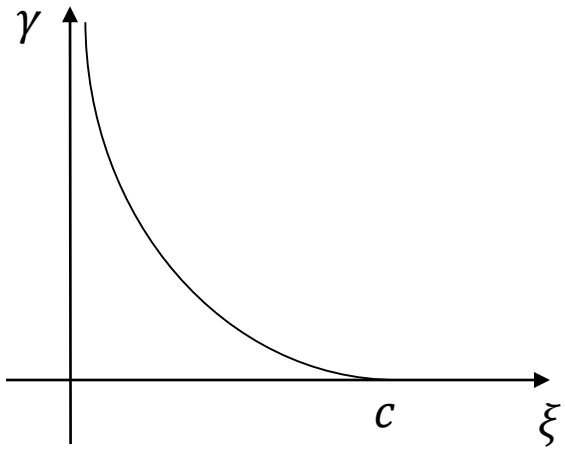

$$\Gamma = \int_0^c \gamma(\xi)\,\mathrm{d}\xi$$

Thin airfoil theory: the symmetric airfoil

$$\Gamma = \int_0^c \gamma(\xi)\,\mathrm{d}\xi = \int_0^\pi 2\alpha\, V_\infty \frac{1+\cos\theta}{\sin\theta}\,\frac{c}{2}\sin\theta\,\mathrm{d}\theta$$

$$= \alpha\, c\, V_\infty \int_0^\pi (1+\cos\theta)\,\mathrm{d}\theta = \pi\,\alpha\, c\, V_\infty$$

(clockwise circulation)

KJ theorem: $L' = \rho\, V_\infty\, \Gamma = \pi\,\alpha\, c\,\rho\, V_\infty^2 \quad \rightarrow \quad c_l = 2\,\pi\,\alpha$

(same result found already for the Joukowski airfoil!)

lift slope: $a_0 = \frac{\mathrm{d}c_l}{\mathrm{d}\alpha} = 2\,\pi$

$2\,\pi$ *rad* $^{-1}$ = 0.10966227 *degree* $^{-1}$

Thin airfoil theory: the symmetric airfoil

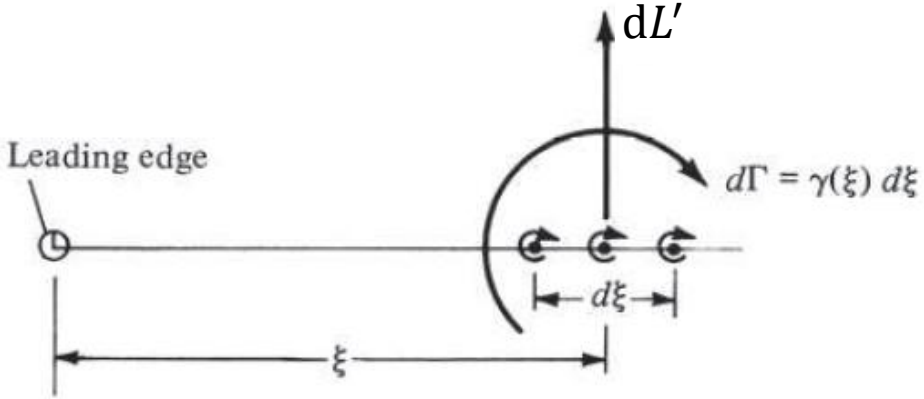

$$M'_{\mathrm{LE}} = \int_0^c -\xi \; \mathrm{d}L'$$

$$= -\rho \, V_\infty \int_0^c \xi \; \gamma(\xi) \, \mathrm{d}\xi = \cdots = -\frac{1}{4} \, \pi \, \alpha \, \rho \, V_\infty^2 \, c^2$$

$$\longrightarrow \qquad c_{m\,\mathrm{LE}} = -\frac{\pi \, \alpha}{2} = -\frac{c_l}{4}$$

Thin airfoil theory: the symmetric airfoil

$$c_{m\,c/4} = c_{m\,\mathrm{LE}} + \frac{c_l}{4}$$

(see slide 20 of ch. 1!)

$$c_{m\,c/4} = 0$$

$x = c/4$ is both CP and AC for the thin symmetric airfoil

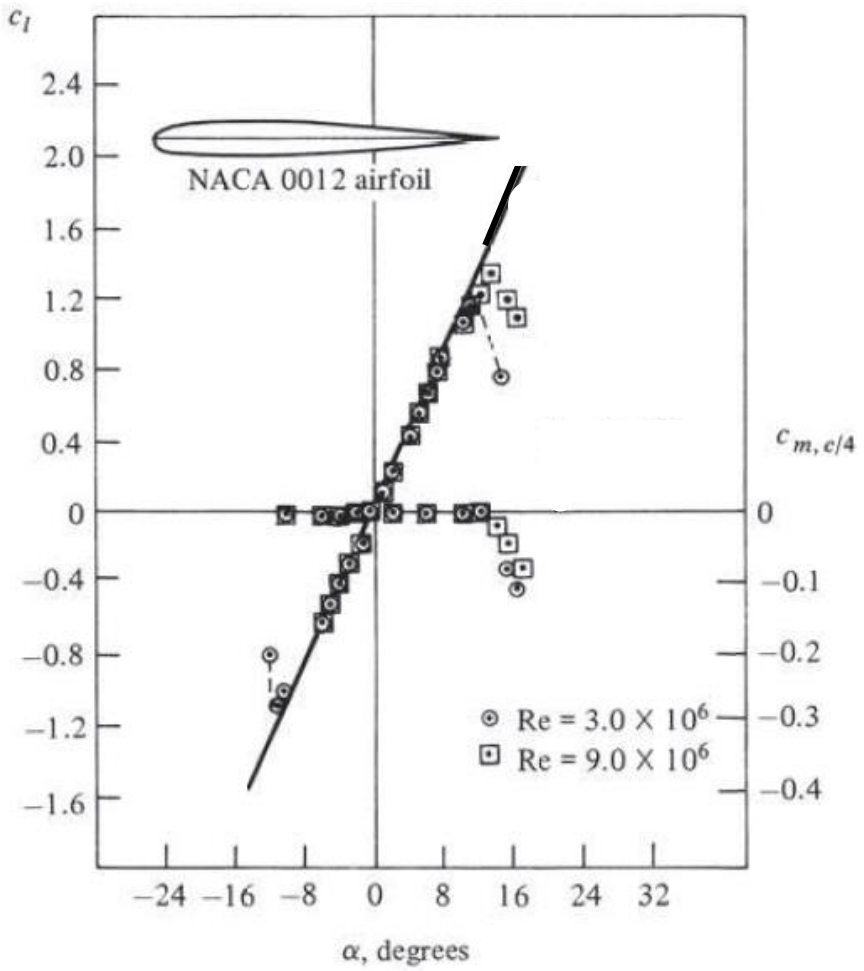

Thin airfoil theory: the symmetric airfoil

We can now refine a bit the qualitative argument presented in ch. 3, slide 29.

$$\gamma(x) = u_1 - u_2$$

$$\mathrm{d}L' = \rho\, V_\infty\, \gamma(x)\, \mathrm{d}x \approx \mathrm{d}F_p$$

$$= (p_2 - p_1)\, \mathrm{d}x$$

Bernoulli: $p_2 - p_1 = \frac{1}{2}\rho(u_1^2 - u_2^2) \approx \rho\, V_\infty\, \gamma(x)$

$$\longrightarrow \quad u_1 \approx V_\infty + \frac{\gamma}{2}, \quad u_2 \approx V_\infty - \frac{\gamma}{2}$$

$$u_1 \approx V_\infty + \alpha\, V_\infty \sqrt{\frac{c}{x} - 1}, \quad u_2 \approx V_\infty - \alpha\, V_\infty \sqrt{\frac{c}{x} - 1}$$

Thin airfoil theory: the symmetric airfoil

$$u_1 \approx V_\infty \left[1 + \alpha \sqrt{\frac{c}{x} - 1}\right] \neq 0 \qquad \forall x \text{ for } \alpha \geq 0$$

$$u_2 \approx V_\infty \left[1 - \alpha \sqrt{\frac{c}{x} - 1}\right] = 0 \quad \text{when} \quad \frac{x}{c} = \frac{\alpha^2}{\alpha^2+1}$$

When α is sufficiently small, the stagnation point on the pressure side of the airfoil has coordinate: $x_{stagn} \approx \alpha^2 c$

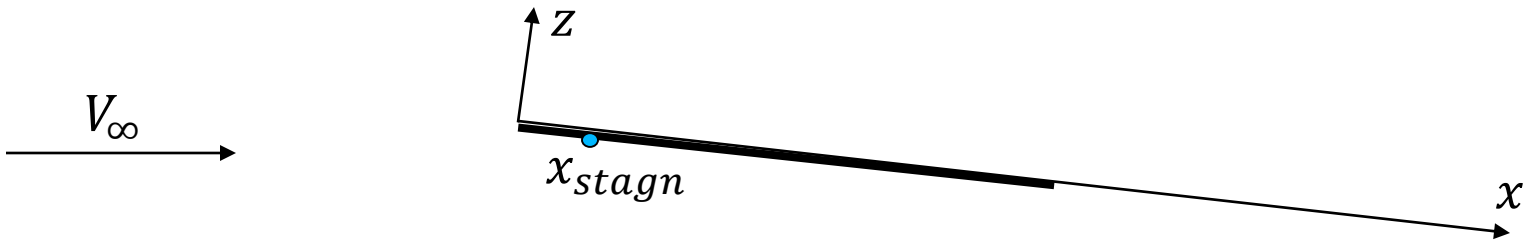

Thin airfoil theory: the **cambered** airfoil

Let us go back to the fundamental equation of thin airfoil theory (slide 43) which, in Glauert's coordinates, read:

$$\frac{1}{2\pi}\int_0^{\pi}\frac{\gamma(\theta)\sin\theta\,d\theta}{\cos\theta-\cos\theta_0}=V_\infty\left(\alpha-\frac{dz}{dx}\right)$$

together with Kutta condition: $\gamma(\pi)=0$

To express the solution we must rely on a Fourier cosine series expansion of the even function $\frac{dz}{dx}$

Fourier cosine series expansion

The Fourier cosine series expansion of a generic even function $f(x)$ is:

$$f(x) = \frac{1}{2}a_0 + \sum_{n=1}^{\infty} a_n \cos(nx)$$

with the coefficients given by

$$a_0 = \frac{1}{\pi}\int_{-\pi}^{\pi} f(x)\,dx = \frac{2}{\pi}\int_{0}^{\pi} f(x)\,dx$$

$$a_n = \frac{1}{\pi}\int_{-\pi}^{\pi} f(x)\cos(nx)\,dx = \frac{2}{\pi}\int_{0}^{\pi} f(x)\cos(nx)\,dx$$

Fourier cosine series expansion of $\frac{dz}{dx}$

The function $z = z(\theta_0)$ is odd (practical camber lines go to zero at LE and TE), so $^{dz}/_{dx}$ is an even function. The Fourier cosine series expansion of $\frac{dz}{dx}$ is written as:

$$\frac{dz}{dx} = (\alpha - A_0) + \sum_{n=1}^{\infty} A_n \cos(n\theta_0)$$

with the coefficients given by $(\alpha - A_0) = \frac{1}{\pi}\int_0^{\pi} \frac{dz}{dx}\, d\theta_0$

and $A_n = \frac{2}{\pi}\int_0^{\pi} \frac{dz}{dx} \cos(n\theta_0)\, d\theta_0$

Thin airfoil theory: the cambered airfoil

Inserting $\alpha - \frac{dz}{dx} = A_0 - \sum_{n=1}^{\infty} A_n \cos(n\theta_0)$ into the fundamental equation we have:

$$\frac{1}{2\pi V_\infty} \int_0^\pi \frac{\gamma(\theta) \sin\theta \, d\theta}{\cos\theta - \cos\theta_0} = A_0 - \sum_{n=1}^{\infty} A_n \cos(n\theta_0)$$

The result of this equation, satisfying Kutta condition, is:

$$\gamma(\theta) = 2V_\infty \left(A_0 \frac{1 + \cos\theta}{\sin\theta} + \sum_{n=1}^{\infty} A_n \sin n\theta \right)$$

Thin airfoil theory: the cambered airfoil

Assignement:

Verify that the given expression of $\gamma(\theta)$ satisfies the fundamental equation, using Glauert's second integral (slide 48). Verify also that Kutta condition is satisfied.

Note: for the limit case of symmetric airfoil $\left(\frac{dz}{dx} = 0\right)$ we have $A_0 = \alpha$ and $A_n = 0$, for $n = 1, 2, 3$ ... in this case the solution in slide 58 coincides with that of slide 47.

Thin airfoil theory: the cambered airfoil

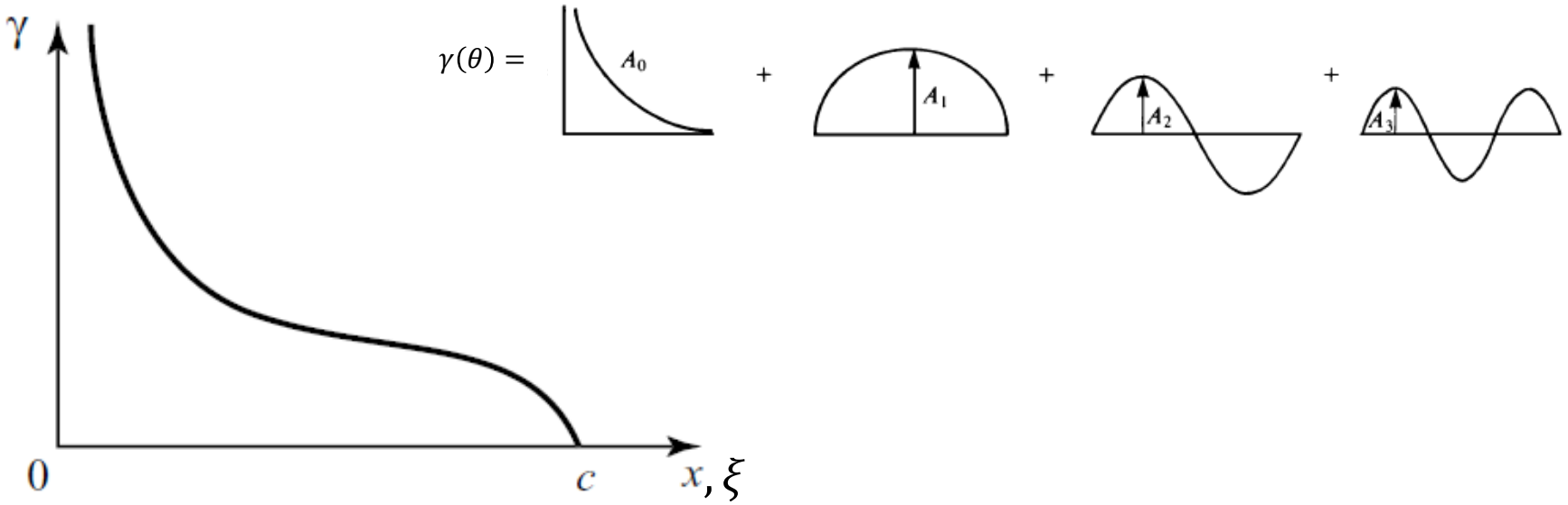

Generic form of the vortex sheet strength distribution, and schematic description of the first four terms in the series describing the circulation.

Thin airfoil theory: the cambered airfoil

Note: from slide 58 it is clear that at the LE, for $\theta \to 0$, it is $\sin\theta \to 0$ and the strength of the vortex sheet is locally singular ($\lim_{\theta\to 0} |\gamma| \to \infty$). The only way for this not to happen is that $A_0 = 0$. When this occurs the angle of attack is called *ideal* (because the local load at the LE vanishes). Thus

$$\alpha_{ideal} = \frac{1}{\pi}\int_0^{\pi} \frac{dz}{dx}\, d\theta_0$$

In this case the *ideal* lift coefficient is $c_l = \pi\, A_1$ (check slide 63). This is also called the *design lift coefficient*.

Thin airfoil theory: the cambered airfoil

Total circulation due to the vortex sheet:

$$\Gamma = \int_0^c \gamma(\xi)\, d\xi = \frac{c}{2} \int_0^\pi \gamma(\theta) \sin\theta\, d\theta$$

$$\Gamma = cV_\infty \left[A_0 \int_0^\pi (1 + \cos\theta)\, d\theta + \sum_{n=1}^{\infty} A_n \int_0^\pi \sin n\theta \sin\theta\, d\theta \right]$$

with

$$\int_0^\pi (1 + \cos\theta)\, d\theta = \pi$$

$$\int_0^\pi \sin n\theta \sin\theta\, d\theta = \begin{cases} \pi/2 & \text{for } n = 1 \\ 0 & \text{for } n \neq 1 \end{cases}$$

Thin airfoil theory: the cambered airfoil

$$\Gamma = c V_\infty \left(\pi A_0 + \frac{\pi}{2} A_1 \right)$$

KJ: $$L' = \rho V_\infty \Gamma = \rho V_\infty^2 c \left(\pi A_0 + \frac{\pi}{2} A_1 \right)$$

$$c_l = \frac{L'}{\frac{1}{2} \rho V_\infty^2 c} = 2\pi \left(A_0 + \frac{A_1}{2} \right)$$

$$= 2\pi \left[\alpha + \frac{1}{\pi} \int_0^\pi \frac{dz}{dx} (\cos\theta_0 - 1) \, d\theta_0 \right] = 2\pi \left(\alpha - \alpha_{l=0} \right)$$

Thin airfoil theory: the cambered airfoil

Lift slope: $a_0 = \frac{dc_l}{d\alpha} = 2\pi$

The lift slope is the same as for a symmetric airfoil!

The zero lift angle is:

$$\alpha_{l=0} = -\frac{1}{\pi}\int_0^{\pi} \frac{dz}{dx}(\cos\theta_0 - 1)\, d\theta_0$$

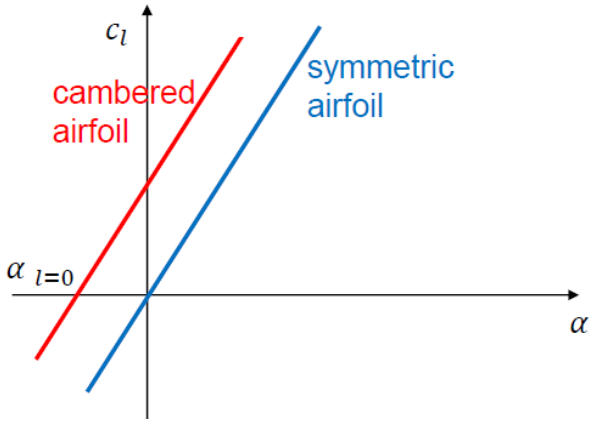

For symmetric airfoil $\alpha_{l=0} = 0$

Thin airfoil theory: the cambered airfoil

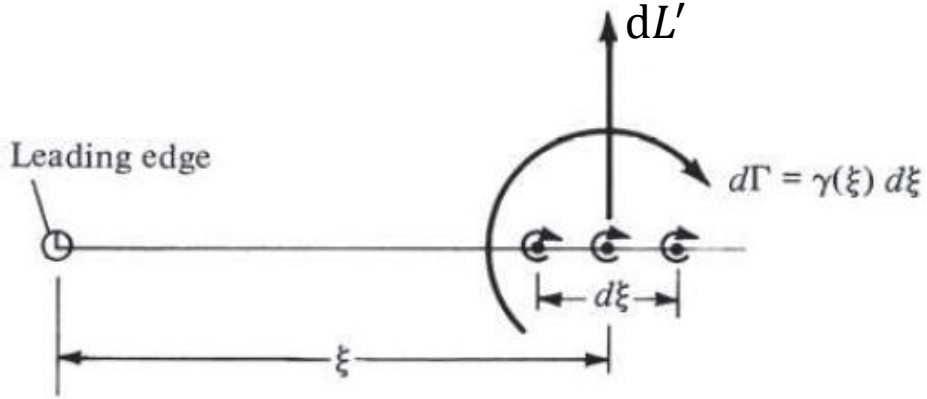

$$M'_{\mathrm{LE}} = \int_0^c -\xi \; \mathrm{d}L'$$

$$= -\rho \, V_\infty \int_0^c \xi \; \gamma(\xi) \, \mathrm{d}\xi = \cdots = -\frac{1}{4} \, \pi \, \rho \, V_\infty^2 \, c^2 \left(A_0 + A_1 - \frac{A_2}{2} \right)$$

$$\longrightarrow \quad c_{m\,\mathrm{LE}} = -\frac{\pi}{2}\left(A_0 + A_1 - \frac{A_2}{2} \right) = -\frac{c_l}{4} + \frac{\pi}{4}(A_2 - A_1)$$

Thin airfoil theory: the cambered airfoil

The moment coefficient for a cambered airfoil depends on only three Fourier series coefficients (function of angle of attack and camber).

Using the relation in slide 52 $\left(c_{m\,c/4} = c_{m\,\mathrm{LE}} + \frac{c_l}{4}\right)$ we have:

$$c_{m\,c/4} = \frac{\pi}{4}(A_2 - A_1)$$

Thus, the moment coefficient about quarter chord is independent of the angle of attack, which means that $x = c/4$ is the **aerodynamic center**.

Thin airfoil theory

For thin symmetric arfoil $x = c/4$ is **both** AC and CP.

For thin cambered airfoil $x = c/4$ is AC (but **not** CP since $c_{m\,c/4} \neq 0$ because of the airfoil camber) To find the center of pressure consider that the total moment about the CP vanishes, i.e.

$$M'_{\mathrm{CP}} = L'\,\Delta x + M'_{c/4} = 0$$

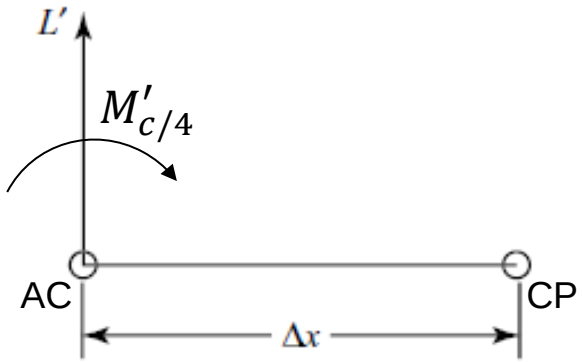

$$\frac{\Delta x}{c} = -\frac{c_{m\,c/4}}{c_l} = \frac{\pi}{4}\left(\frac{A_1 - A_2}{c_l}\right) \quad \rightarrow \quad x_{\mathrm{CP}} = \frac{c}{4} + \Delta x$$

(notice that x_{CP} changes with lift!)

Thin airfoil theory: comparison w/ exp

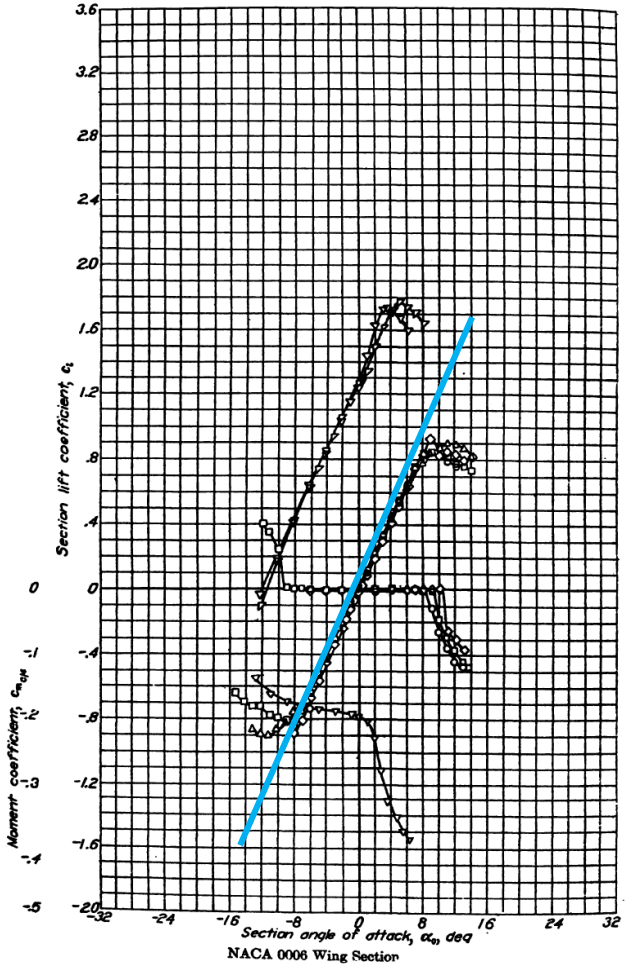

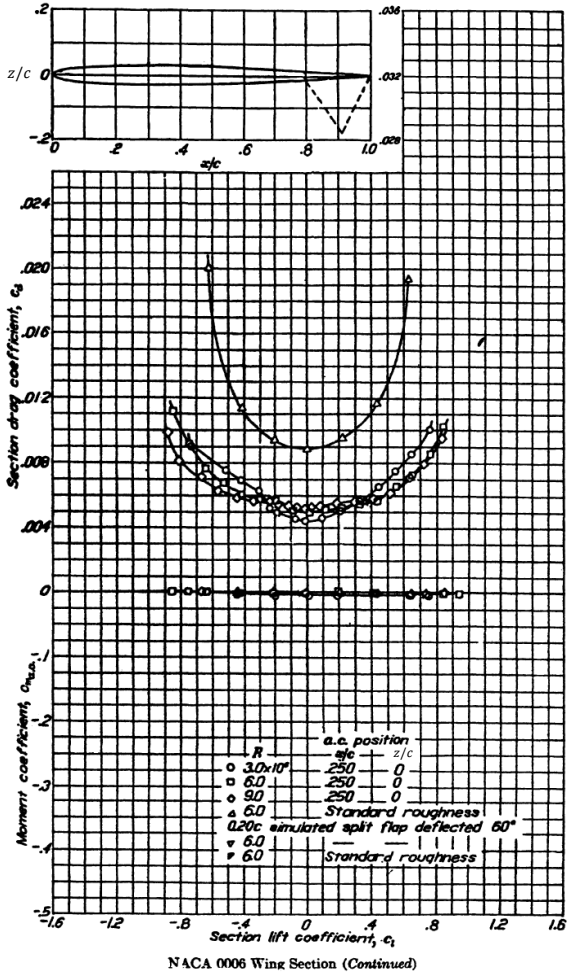

Abbott &
van Doenhoff

Thin airfoil theory: comparison w/ exp

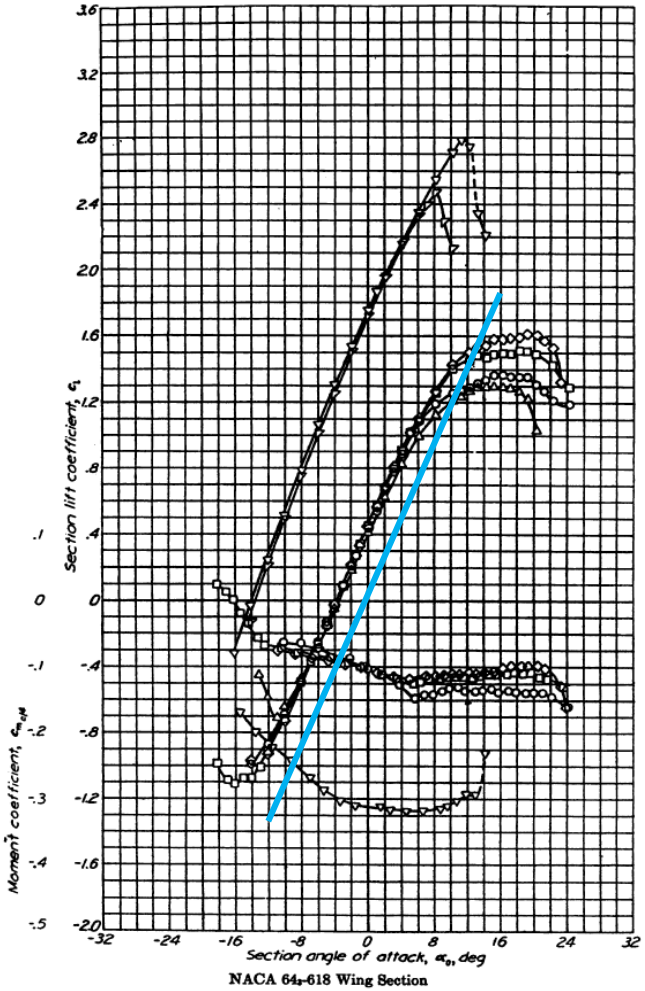

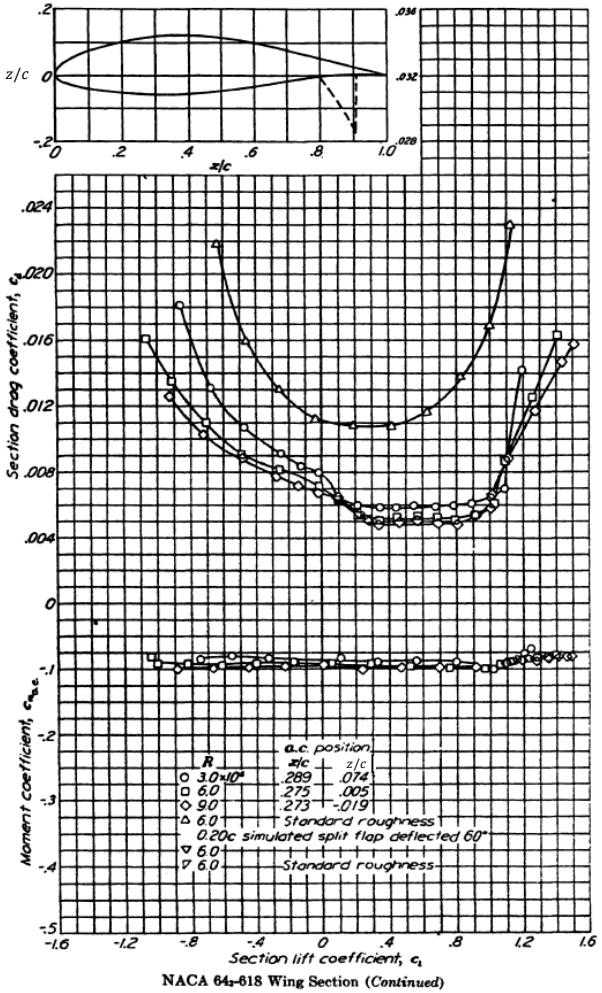

Abbott &
van Doenhoff

Thin (or thick?) airfoil: the AC

Thin airfoil theory should, in principle, not be applied if the thickness of the airfoil is large. For a thick airfoil the AC is not at $c/4$ (but close …)

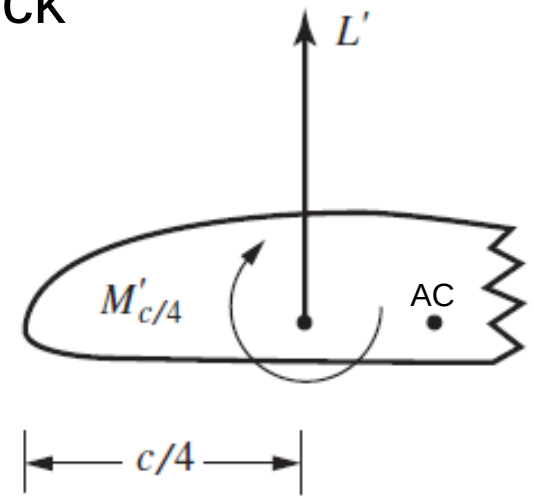

$$M'_{\mathrm{AC}} = M'_{c/4} + \left(x_{\mathrm{AC}} - \frac{c}{4}\right) L'$$

$$c_{m\,\mathrm{AC}} = c_{m\,c/4} + \left(\frac{x_{\mathrm{AC}}}{c} - \frac{1}{4}\right) c_l$$

$$\frac{dc_{m\,\mathrm{AC}}}{d\alpha} = 0 = \frac{dc_{m\,c/4}}{d\alpha} + \left(\frac{x_{\mathrm{AC}}}{c} - \frac{1}{4}\right)\frac{dc_l}{d\alpha} = m_0 + \left(\frac{x_{\mathrm{AC}}}{c} - \frac{1}{4}\right) a_0$$

$$\frac{x_{\mathrm{AC}}}{c} = \frac{1}{4} - \frac{m_0}{a_0}$$

(either larger or smaller than 1/4)

Thin (or thick?) airfoil: the AC

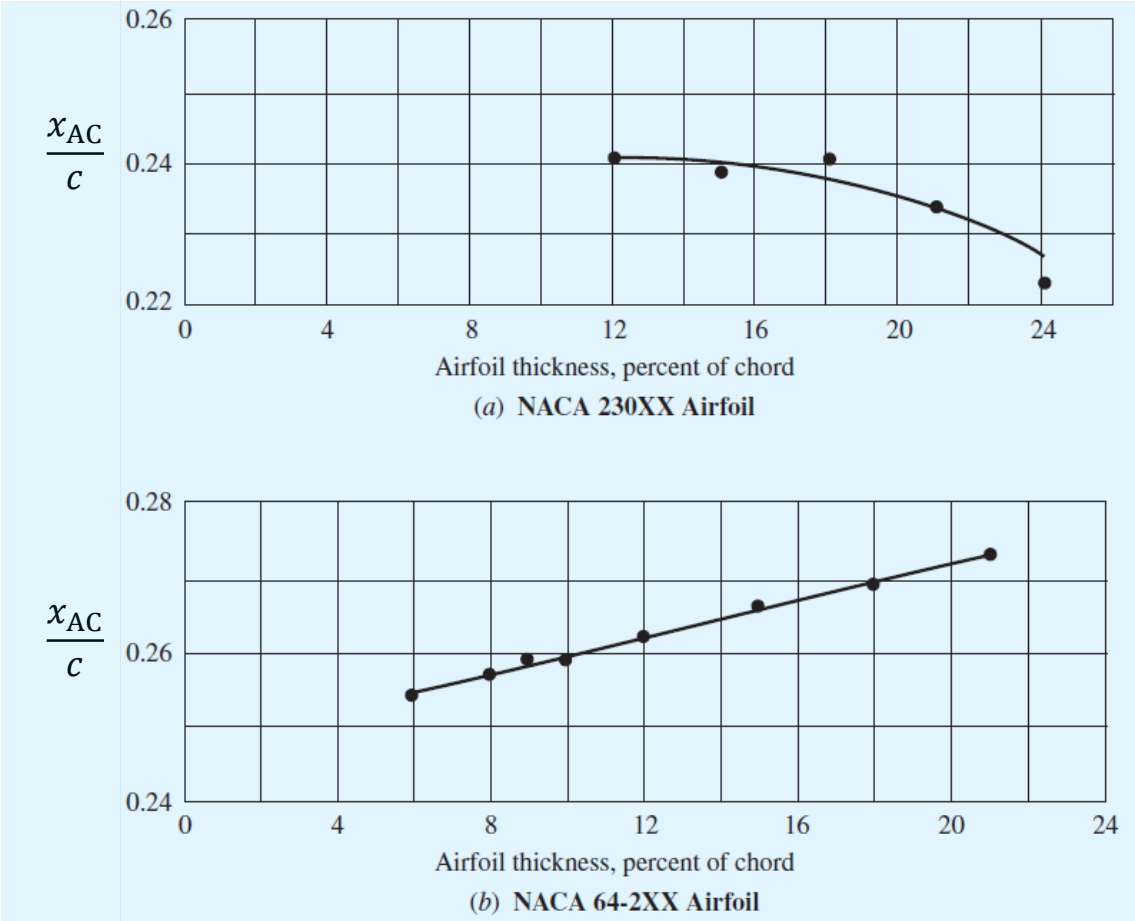

Thin airfoil theory: the effect of flaps

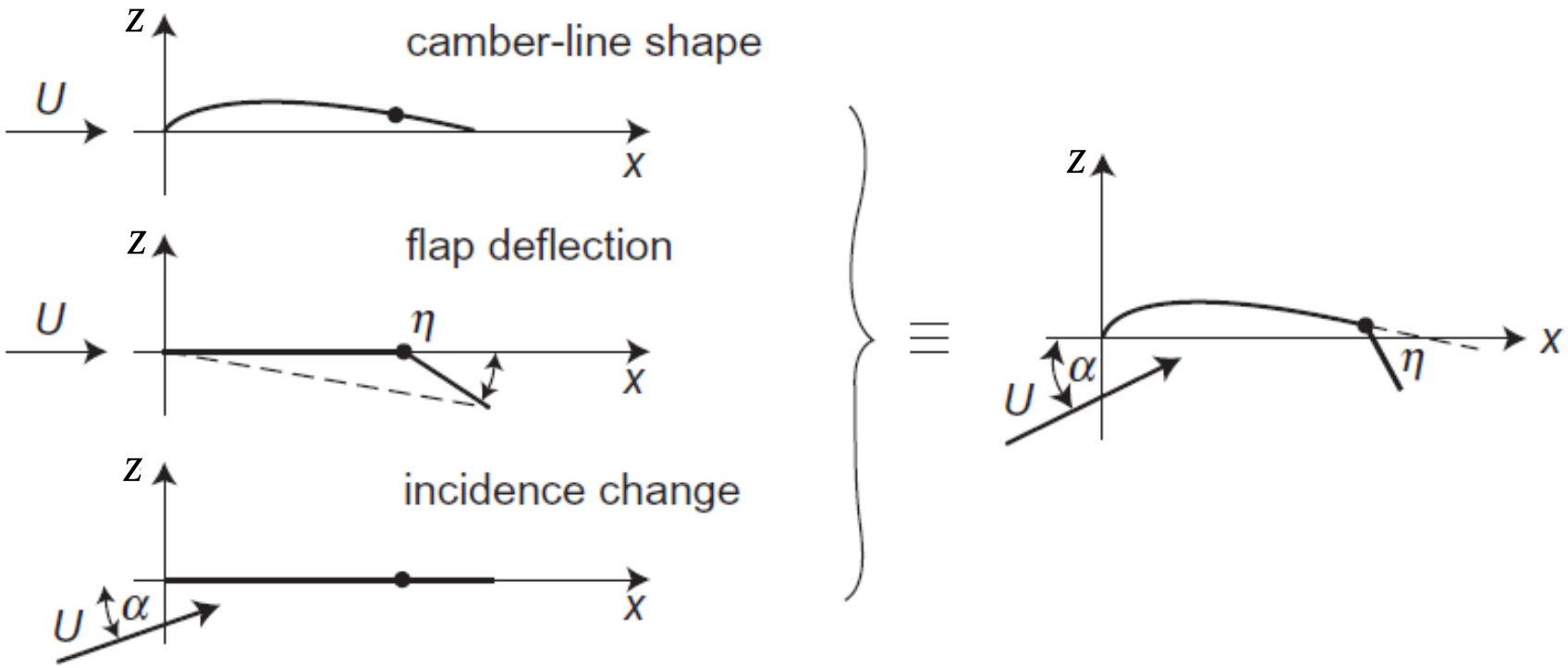

Thin airfoil theory: the effect of flaps

Flaps are the main mechanism to generate control forces on airplanes (cf. slides 68 and 69) since they change the effective camber of the airfoil/wing.

Deploying flaps has a minor effect on lift slope a_0, but:

- $\alpha_{l=0}$ is substantially decreased (+)
- max lift coefficient is increased (+)
- the angle of stall is reduced (–) (but this reduction is not large enough to detract from the advantages of shifting the lift curve to the left)

Thin airfoil theory: the effect of flaps

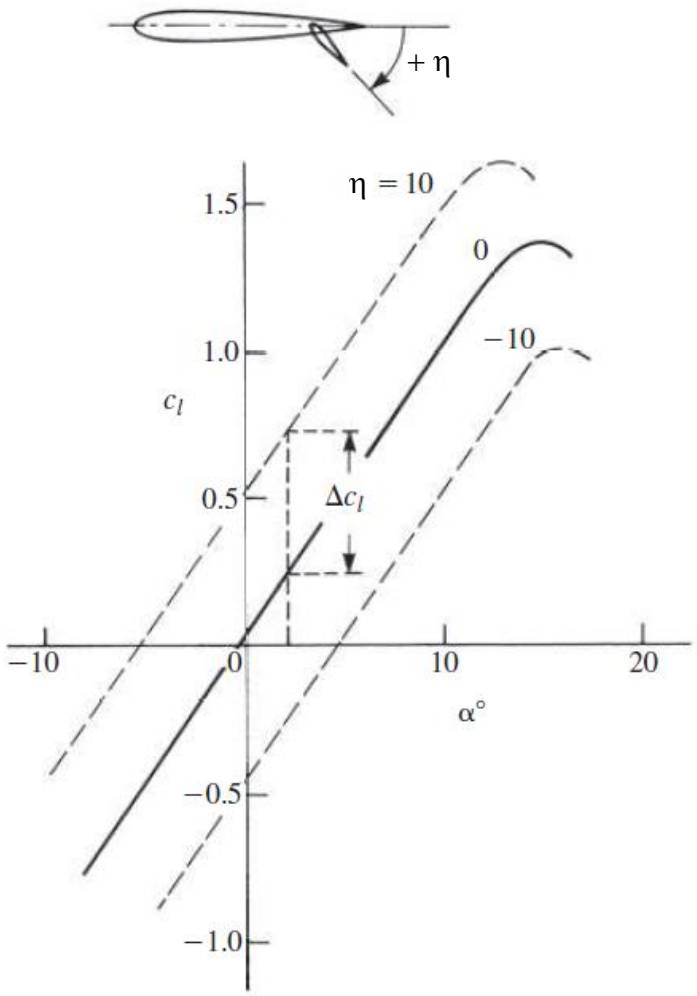

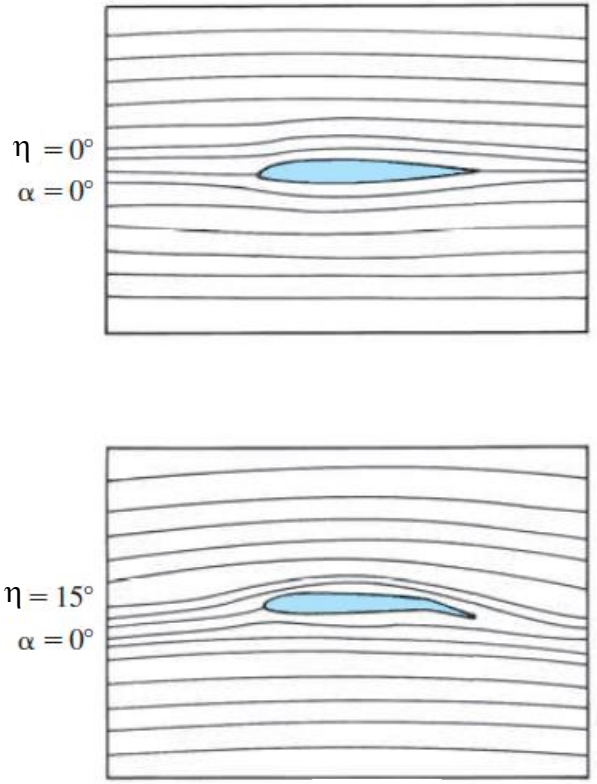

(for η ≠ 0 drag increases …)

Other HLD: the leading edge slat

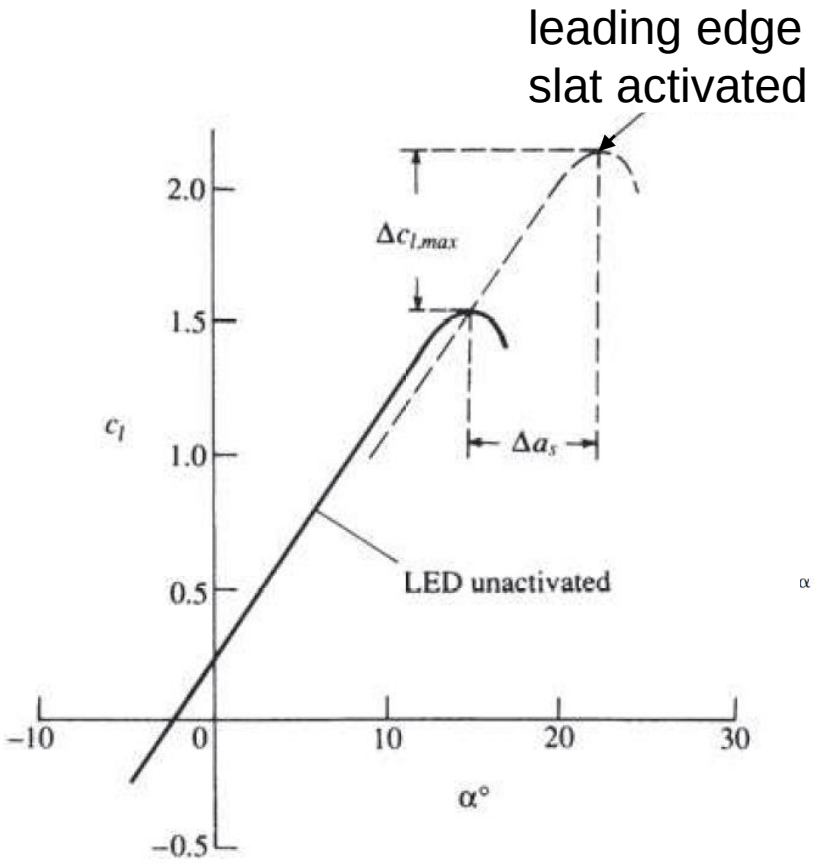

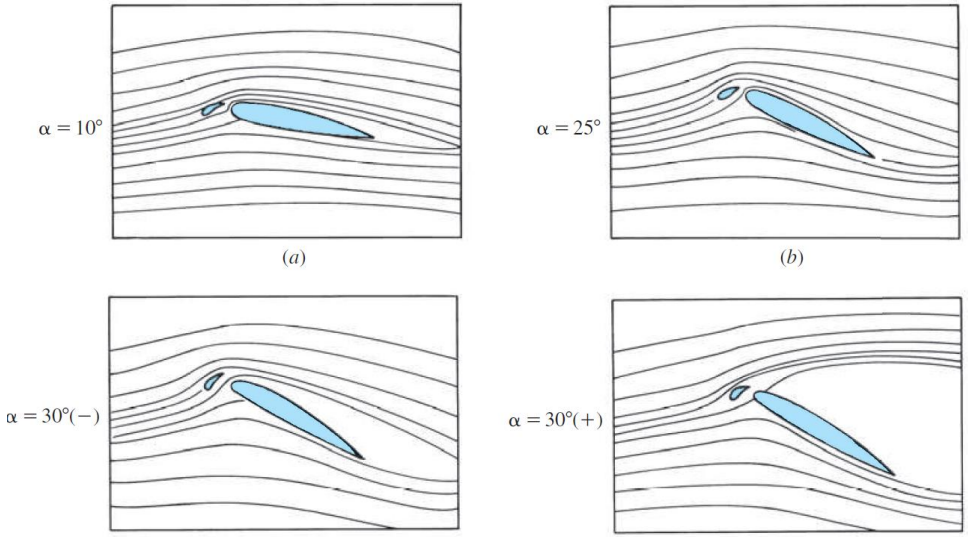

Other HLD

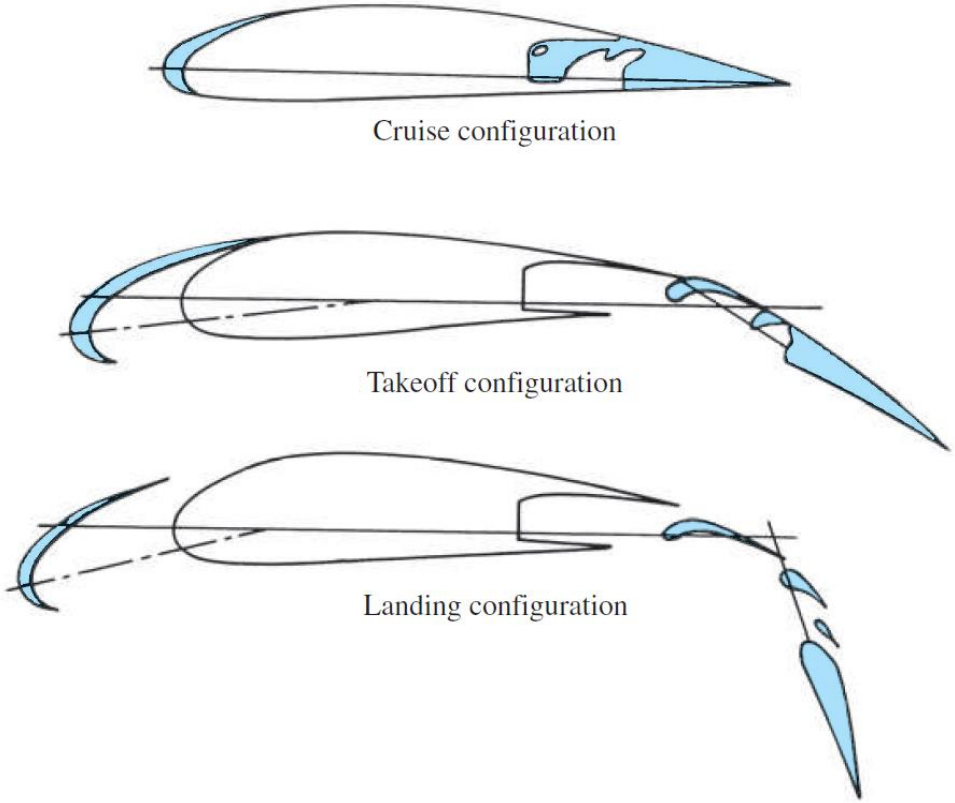

Airfoil with LE slat and TE multi-element flap

Other HLD

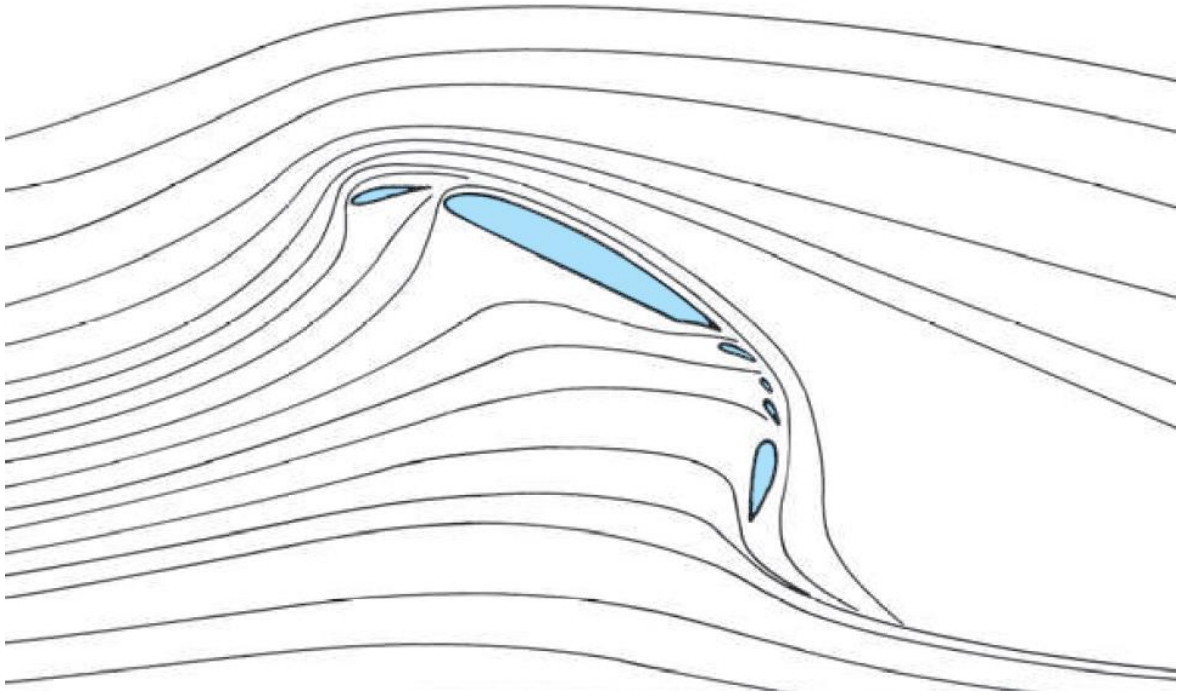

$$\alpha = 25^{\circ}$$

Thin airfoil theory

Exercises

1. Consider a thin airfoil, with mean camber line in the form of a circular arc, with mean camber given by $z = 4f\left[\frac{x}{c} - \left(\frac{x}{c}\right)^2\right]$, where f is the maximum camber. Find $\alpha_{l=0}$, c_l, $c_{m\,\mathrm{AC}}$, $c_{m\,\mathrm{LE}}$, x_{CP}, α_{ideal}, and the *design* lift coefficient.

2. For the thin airfoil of mean camber line given by $z = f\,\sin^2\theta_0$ (θ_0 defined as in slide 45), with f the maximum camber, answer the same question of the previous exercise.

3. Consider the airfoil with flap shown in the figure, with the chord c equal to the segment AC and h, $F < 1$. Answer the same question of ex. 1.

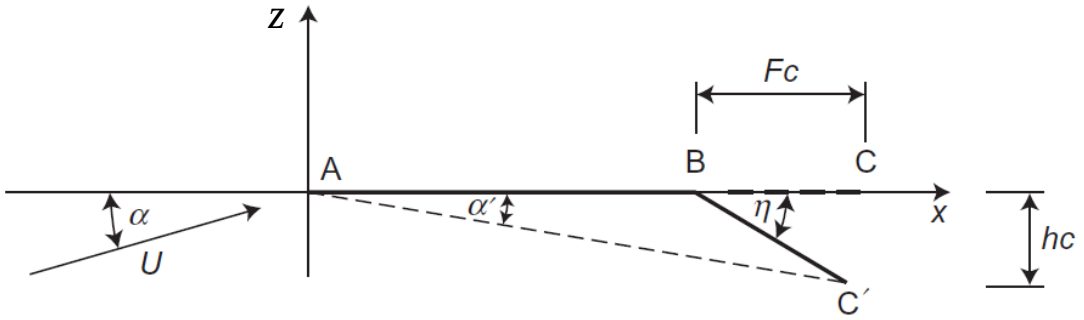

The numerical vortex panel method

The **panel method**, based on a distribution of potential sources (or doublets or vortices, and sometimes a combination of different singularities), is a common numerical technique to treat the flow over *non-lifting* or *lifting bodies.*

XFOIL (https://web.mit.edu/drela/Public/web/xfoil/) – and similar codes – are based on the vortex panel method. This differs from the *lumped vortex element method*. Panels, i.e. straight-line segments, have a surface distribution $\gamma(s)$ of vorticity. The strength of the vortex sheet on each panel of the airfoil must be determined.

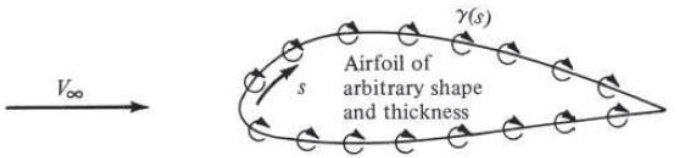

The numerical vortex panel method

Simple implementation: each of the N straight panels carries a vortex distribution of linearly varying strength between the end points of each panel. End point values are the unknowns of the problem: $\gamma_j \ \ (j = 1, 2, \ldots \mathrm{N} + 1)$, and are found by imposing that the body surface is a streamline of the flow, plus Kutta condition: $\gamma_1 = -\gamma_{\mathrm{N}+1}$.

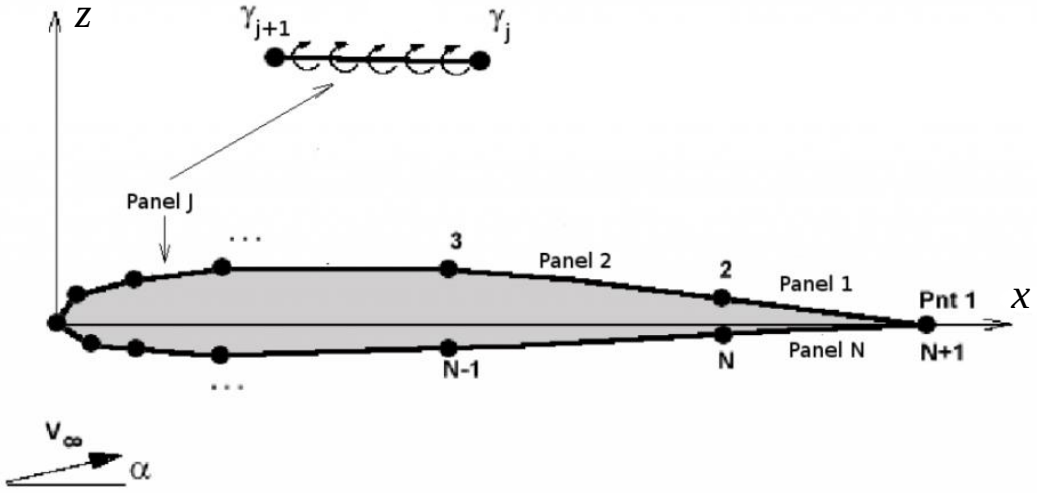

The numerical vortex panel method

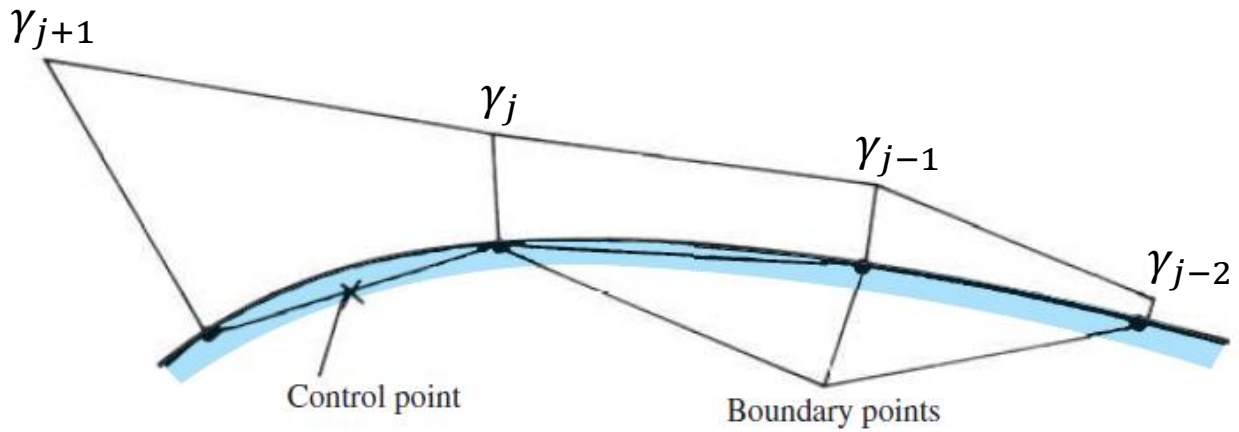

Example of linear distribution of γ over neighboring panels. The strength of the vortex sheet at the end point of panel $j-1$ is equal to the strength at the first point of panel j.

The numerical vortex panel method

A condition of no through-flow ($V_{n,i} = 0$) must be applied at the center of the i^{th} panel, on the *control point*. This yields N equations for $\mathrm{N} + 1$ unknowns. The extra equation needed is Kutta condition.

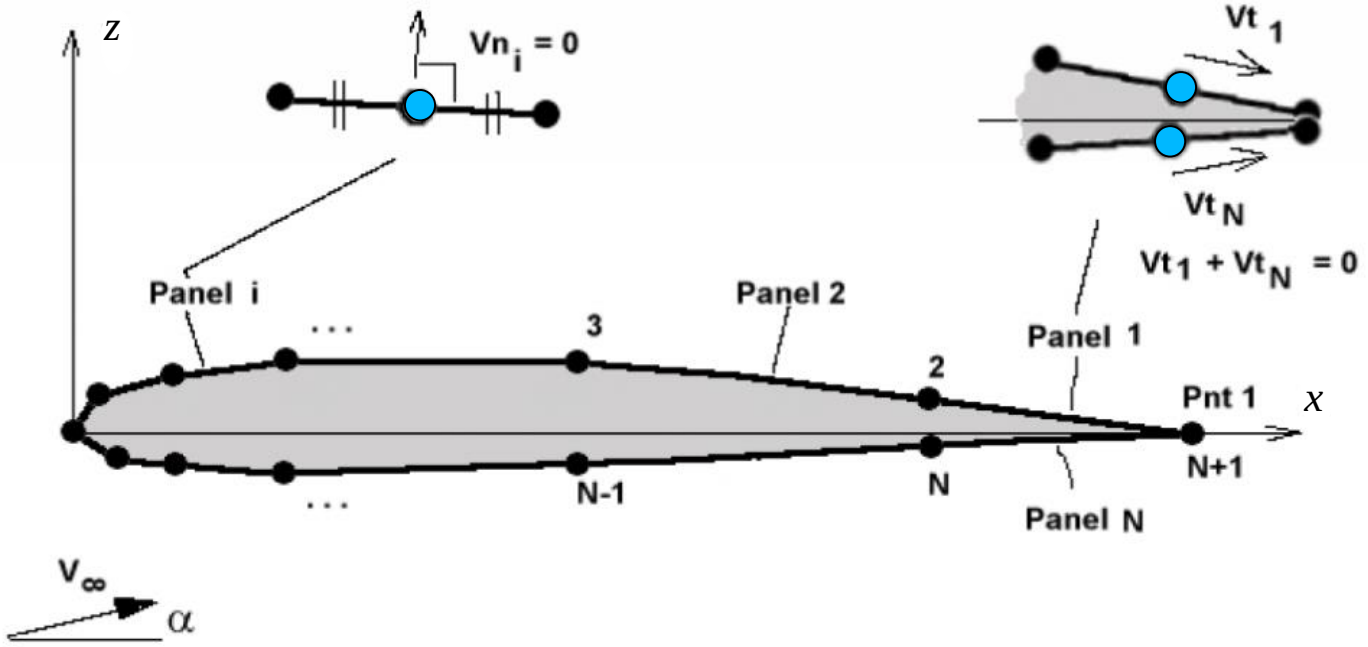

The numerical vortex panel method

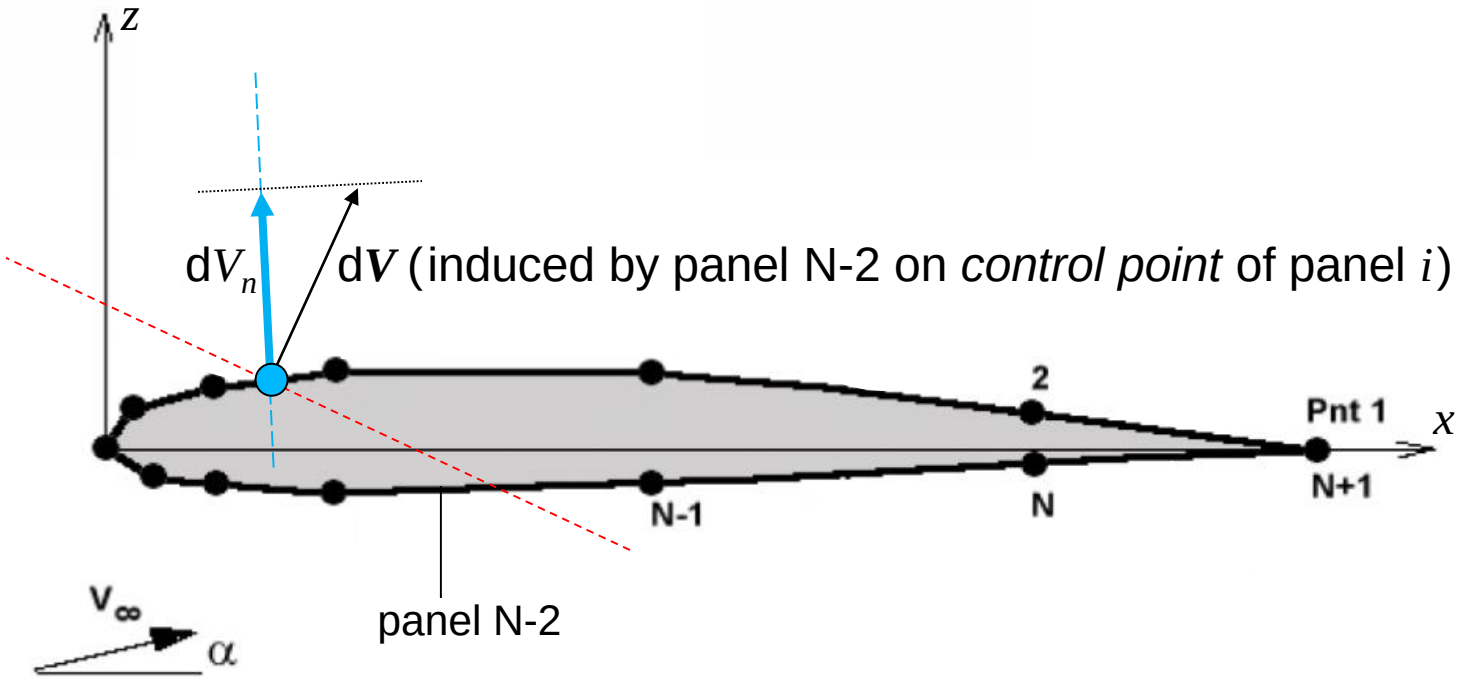

The numerical vortex panel method

For the generic panel i the equation to be enforced is:

$$V_{n,i} = \sum_{j=1}^{N+1} A_{i,j}\ \gamma_j + B_i\ V_\infty = 0$$

where $A_{i,j}$ represents the influence of the vorticity of panel j on the control point of panel i, and B_i represents the influence of the free-stream on panel i. Both $A_{i,j}$ and B_i are function of the geometry of the section, because of orientation and spacing of the panels.

The numerical vortex panel method

The system of linear equations eventually reads:

$$\begin{bmatrix} A_{1,1} & A_{1,2} & \cdots & \cdots & \cdots & A_{1,\mathrm{N}} & A_{1,\mathrm{N}+1} \\ A_{2,1} & A_{2,2} & & & & & \\ \cdots & & & & & & \\ \vdots & & & & & & \vdots \\ \cdots & & & & & & \\ A_{\mathrm{N},1} & A_{\mathrm{N},2} & \cdots & & \cdots & A_{\mathrm{N},\mathrm{N}} & A_{\mathrm{N},\mathrm{N}+1} \\ 1 & 0 & 0 & \cdots & 0 & 0 & 1 \end{bmatrix} \begin{bmatrix} \gamma_1 \\ \gamma_2 \\ \cdots \\ \vdots \\ \cdots \\ \gamma_{\mathrm{N}} \\ \gamma_{\mathrm{N}+1} \end{bmatrix} = -V_\infty \begin{bmatrix} B_1 \\ B_2 \\ \cdots \\ \vdots \\ \cdots \\ B_{\mathrm{N}} \\ 0 \end{bmatrix}$$

The numerical vortex panel method

Once the distribution strengths γ_i have been calculated, we can have surface tangential velocities at the center of each panel (V_i), and surface pressure coefficients, $c_{p,i} = \left(1 - \frac{V_i^2}{V_\infty^2}\right)$

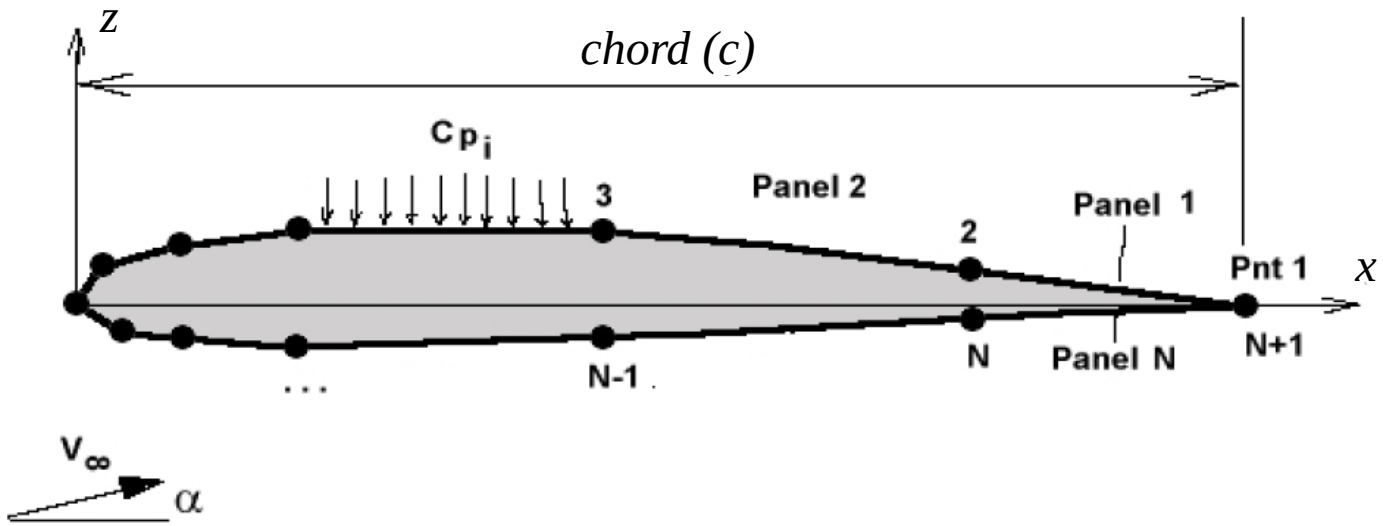

The numerical vortex panel method

The lift coefficient can be calculated, e.g. assuming a small angle of attack α (so that $\cos\alpha$ is close to one), as the integration of surface pressure coefficient acting in the z-direction, i.e.

$$c_l = \sum_{i=1}^{\mathrm{N}} c_{p,i} \frac{x_i - x_{i+1}}{c}$$

Pitching moment coefficient will similarly be the sum of the panel moments about the 1/4 chord point.

$$c_{m\,c/4} = \sum_{i=1}^{\mathrm{N}} c_{p,i} \frac{x_i - x_{i+1}}{c} \left[\frac{x_i + x_{i+1}}{2c} - \frac{1}{4} \right]$$

The numerical vortex panel method

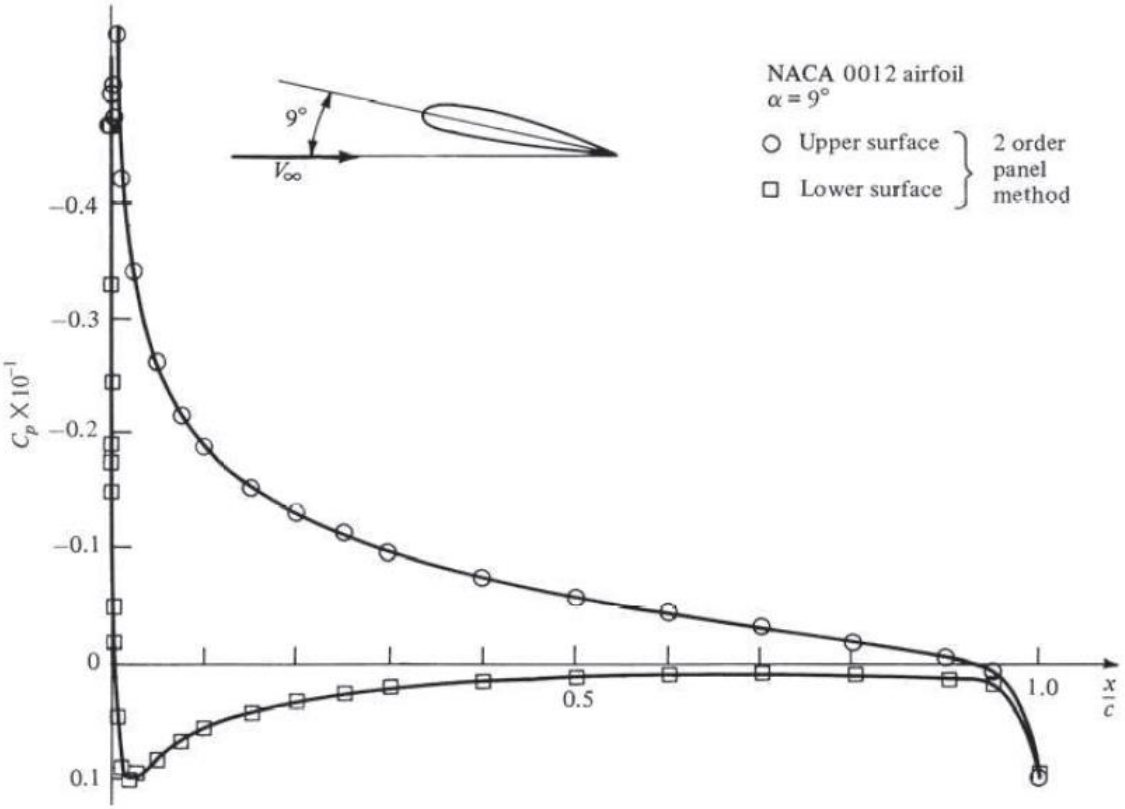

The *inverse* problem

For design purposes it is desirable to specify the surface pressure (or velocity) distribution, for example to achieve enhanced airfoil performances such as:

- preserve a laminar boundary layer over a considerable chordwise extent
- delay boundary-layer separation and hence reduce the form drag of the airfoil
- a relatively low suction peak on the upper surface of the airfoil would result in a higher critical Mach number for the airfoil, meaning that it could operate efficiently at a higher subsonic cruise speed than an airfoil with a conventional pressure distribution
- …

and calculate the shape of the airfoil that will produce the specified pressure (or velocity) distribution.

The *inverse* problem

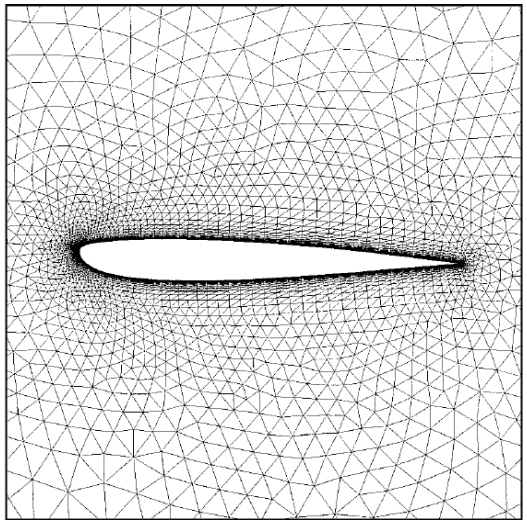

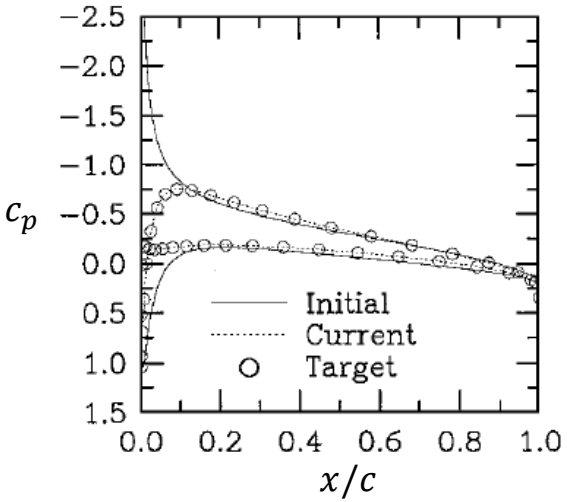

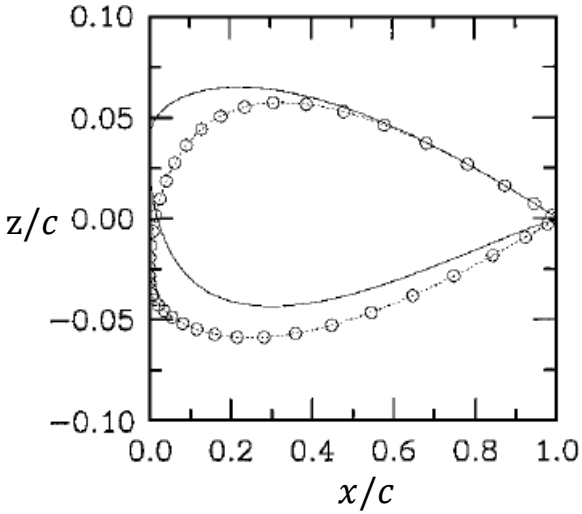

Adjoint optimization of an airfoil to match a specified pressure distribution (free-stream Mach number of 0.4, angle of attack of 2 deg., Reynolds number of 5×10^6)

The *inverse* problem

Further shape optimization objectives are:

- optimize lift coefficient
- minimize skin friction or form drag (or other types of drag)
- maximize the lift-to-drag ratio (aerodynamic efficiency)
- limit system vibrations (aeroelasticity problem)
- reduce aerodynamic noise
- stabilize (or mitigate) a shock
- …

Several optimization strategies are covered in the course by Prof. J. Pralits

3D wings

Lift for 3D wings

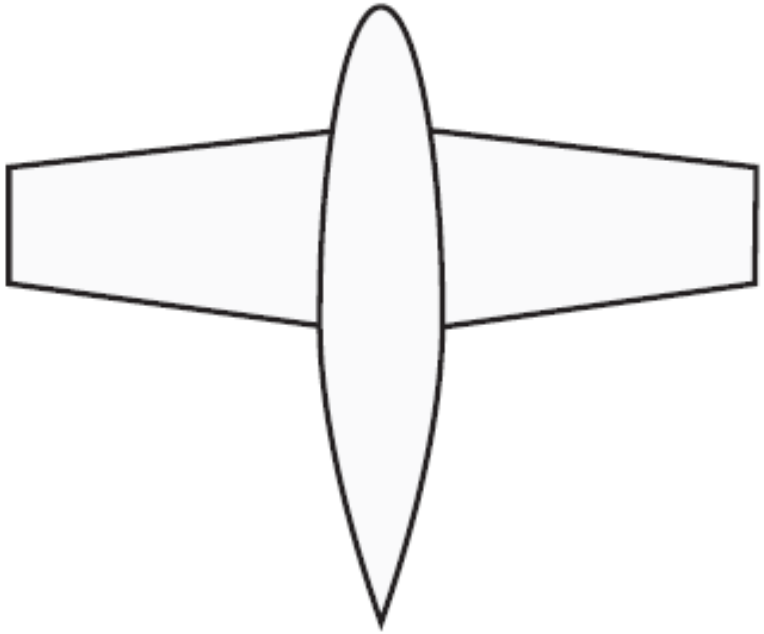

Lift on wing-body combination

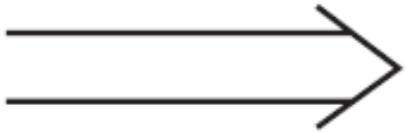

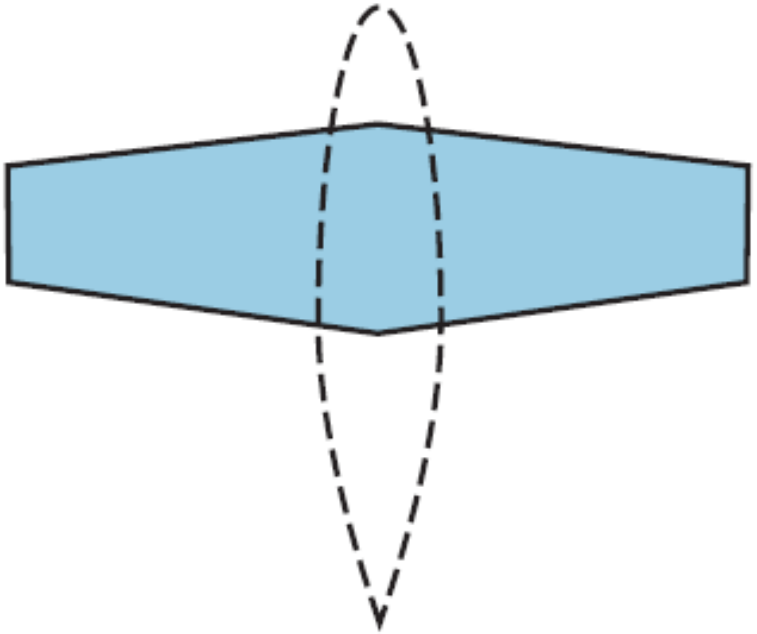

About the same as the lift on the wing of planform area S, which includes that part of the wing masked by the fuselage

Wing-tip vortices

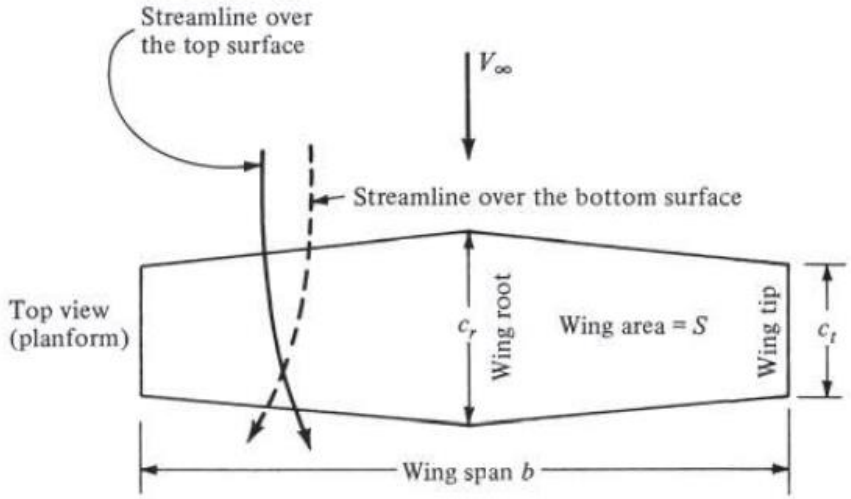

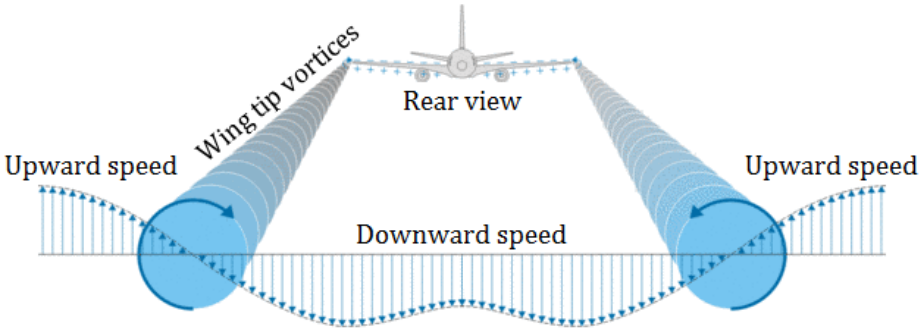

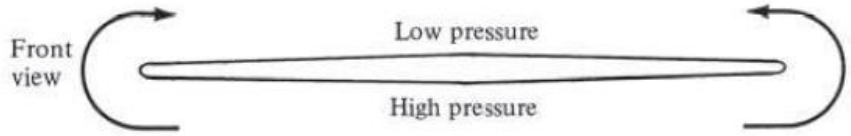

Downwash and induced drag, D_i'

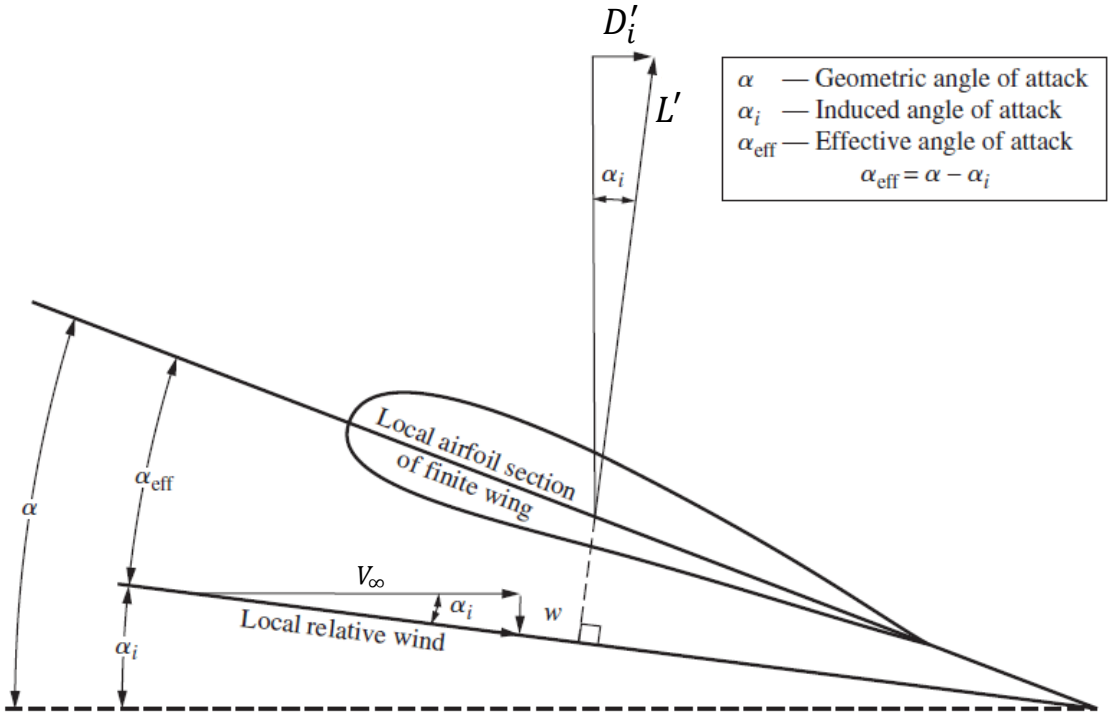

Effect of downwash on a *local* airfoil section of a 3D wing

Vortex line and Biot-Savart law

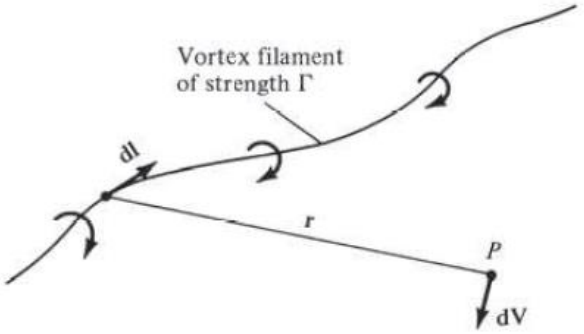

$$\mathbf{dV} = \frac{\Gamma}{4\pi}\frac{\mathbf{dl} \times \mathbf{r}}{|\mathbf{r}|^3}$$

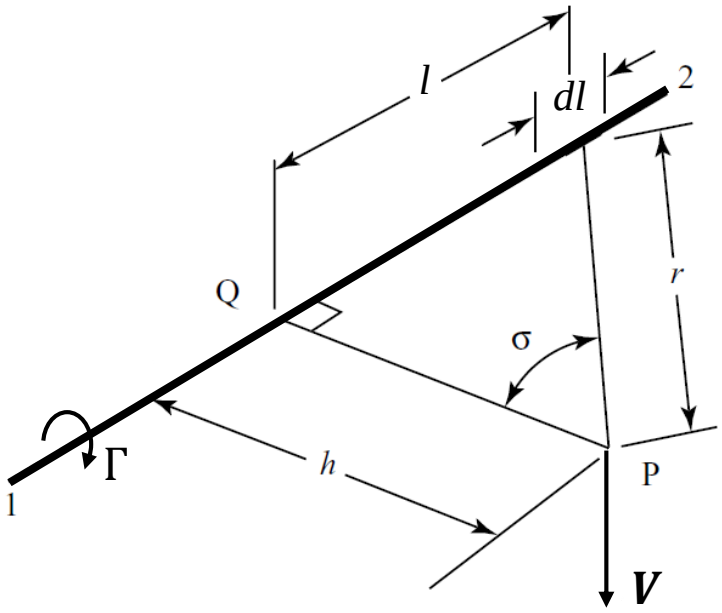

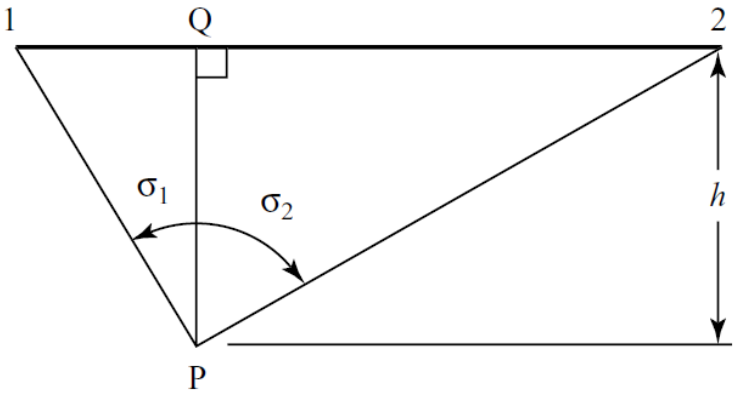

Vortex line and Biot-Savart law

If $1 \to -\infty$ and $2 \to +\infty$ then $V = \dfrac{\Gamma}{4\pi}\displaystyle\int_{-\infty}^{+\infty} \frac{\cos\sigma}{r^2}\,dl$

$$= \frac{\Gamma}{4\pi}\int_{-\infty}^{+\infty} \frac{\cos^3\sigma}{h^2}\,dl = \frac{\Gamma}{4\pi h}\int_{-\pi/2}^{+\pi/2} \cos\sigma\,d\sigma = \frac{\Gamma}{2\pi h}$$

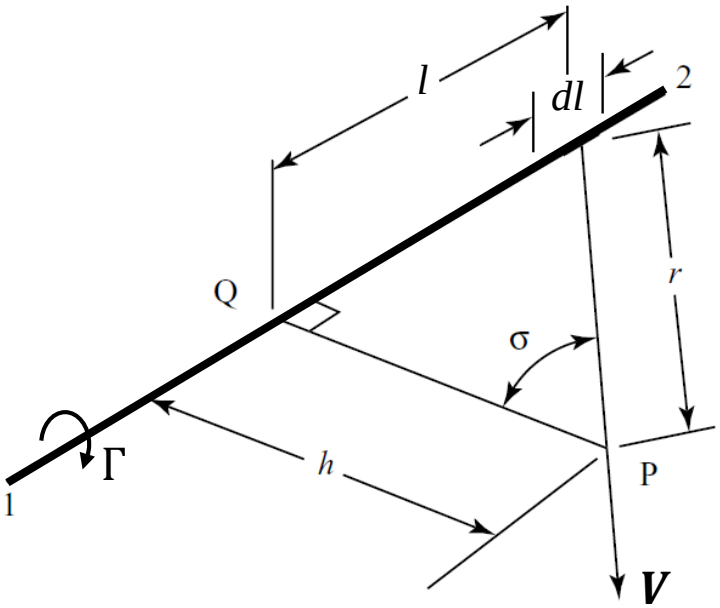

This result agree with the case of the 2D potential vortex!

$$l = h\,\tan\sigma \quad \to \quad dl = h\,\frac{1}{\cos^2\sigma}\,d\sigma$$

Vortex line and Biot-Savart law

If 1 and 2 are two values characterized by the two angles σ_1 and σ_2, the velocity in P has magnitude

$$V = \frac{\Gamma}{4\pi h}\int_{\sigma_1}^{\sigma_2} \cos\sigma \, d\sigma = \frac{\Gamma}{4\pi h}\left(\sin\sigma_2 - \sin\sigma_1\right)$$

If the end point 1 (or eventually both end points) of the segment 1-2 lies to the left of the point of interest P, then σ_1 is a negative angle. If the filament is **semi-infinite**, then

$$V = \frac{\Gamma}{4\pi h}$$

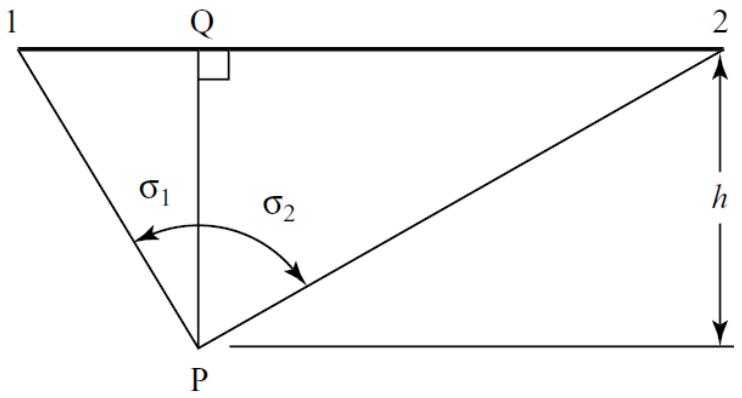

(half the value found for an infinite vortex filament!)

The horseshoe vortex

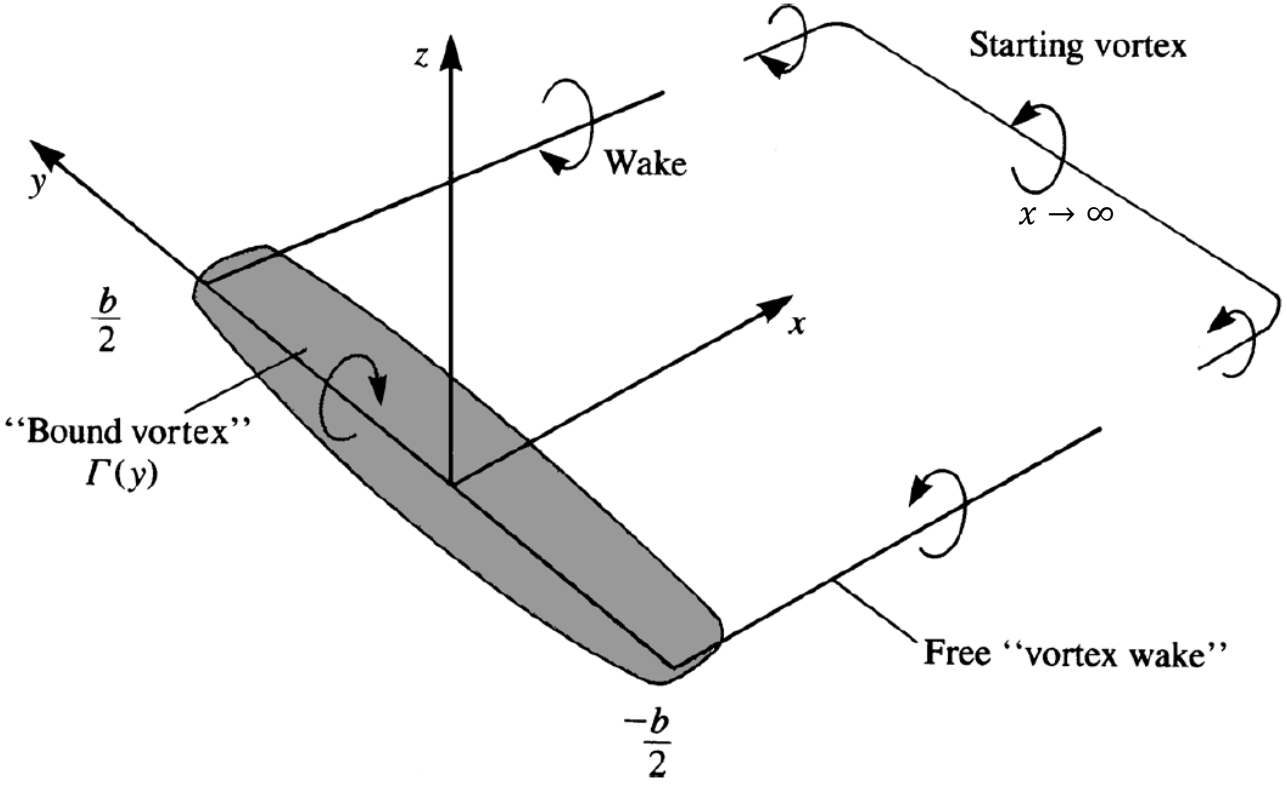

Simple horseshoe vortex model representation of a wing

The horseshoe vortex

Downwash distribution along y for a single horseshoe vortex (unphysical …)

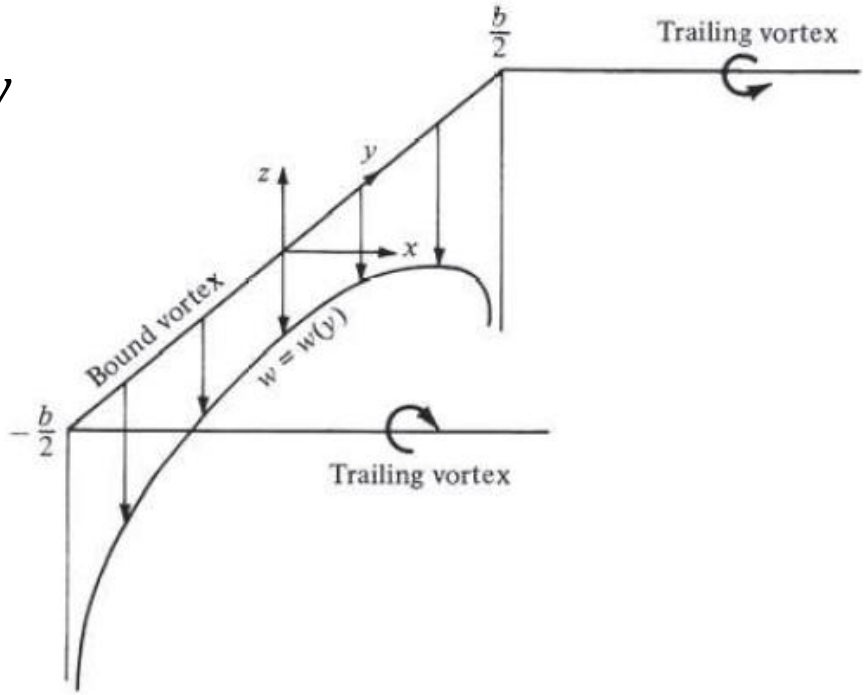

$$w(y) = -\frac{\Gamma}{4\pi(b/2+y)} - \frac{\Gamma}{4\pi(b/2-y)} = -\frac{\Gamma}{4\pi}\frac{b}{(b/2)^2 - y^2}$$

Prandtl's lifting line theory

Superposition of many horseshoe vortices, each with a different length of the bound vortex, but with all bound vortices lying on the **lifting line**

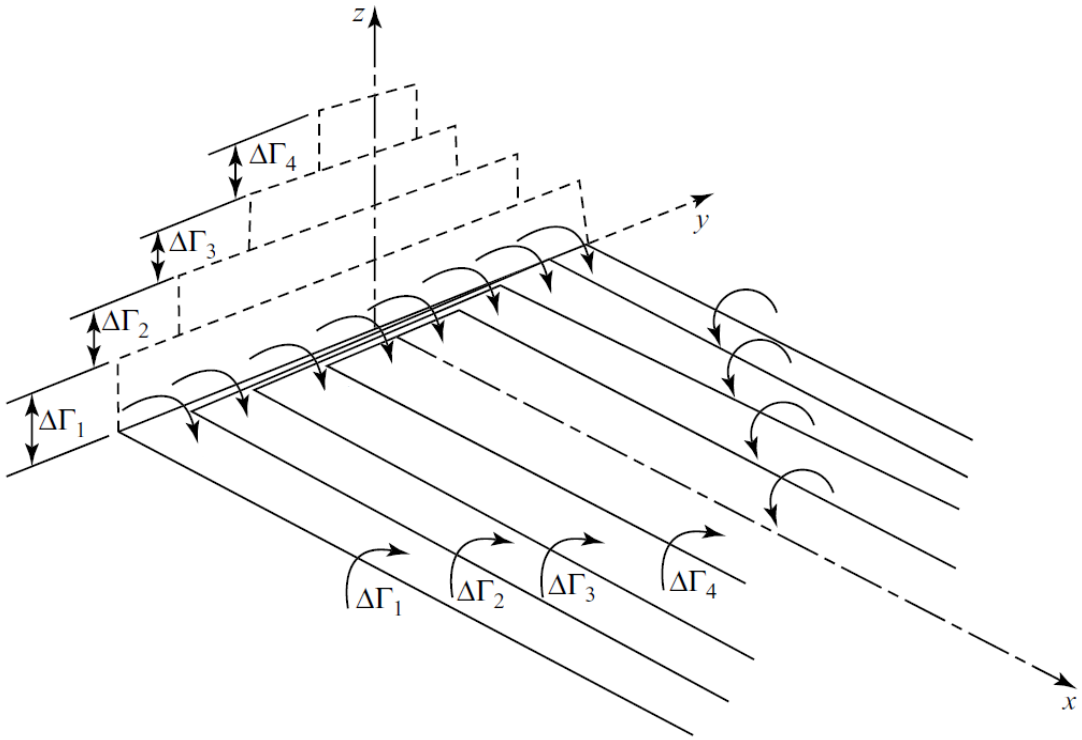

Prandtl's lifting line theory

Infinite horseshoe vortices superimposed along the lifting line

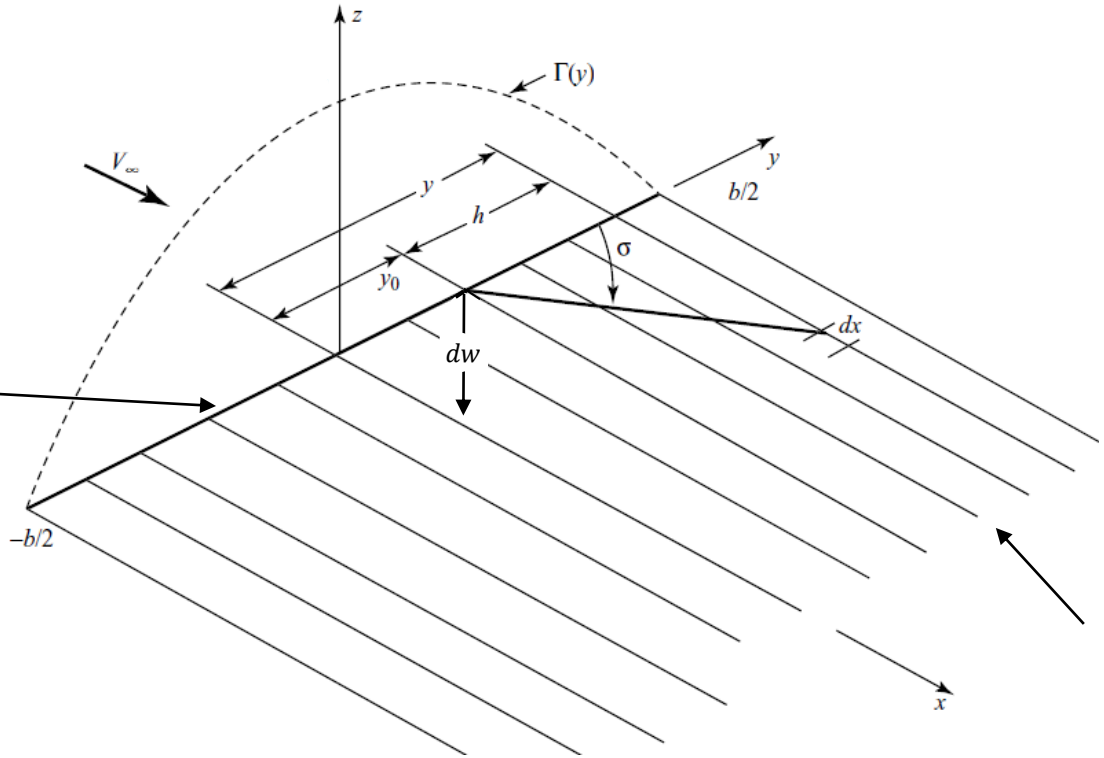

lifting line

continuous vortex sheet behind the lifting line

Goal of the analysis: find $\Gamma = \Gamma(y)$

Prandtl's lifting line theory

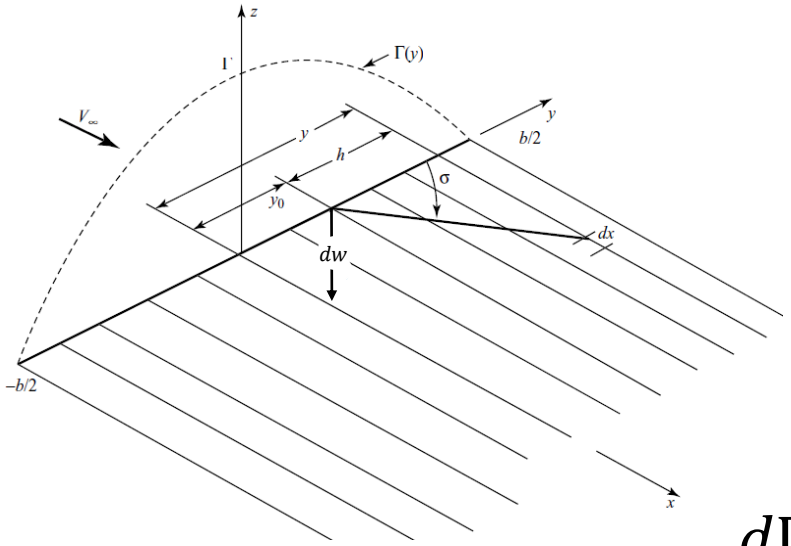

On y_0 the vertical velocity dw induced by the infinitesimal segment dx of a vortex filament positioned in a generic y is:

$$dw = \frac{d\Gamma}{4\pi(y - y_0)} = \frac{\frac{d\Gamma}{dy}dy}{4\pi(y - y_0)}$$

(notice that $\frac{d\Gamma}{dy} < 0$ at y_0 in figure)

$$\rightarrow \quad w(y_0) = \int_{-b/2}^{b/2} \frac{(d\Gamma/dy)}{4\pi(y - y_0)}dy$$

Prandtl's lifting line theory

From slide 95 the induced angle of attack at the generic section y_0 is

$$\alpha_i(y_0) = \tan^{-1}\left[\frac{-w(y_0)}{V_\infty}\right] \approx -\frac{w(y_0)}{V_\infty}$$

$$\alpha_i(y_0) = \frac{1}{4\,\pi\,V_\infty}\int_{-b/2}^{b/2}\frac{(d\Gamma/dy)}{(y_0 - y)}\,dy$$

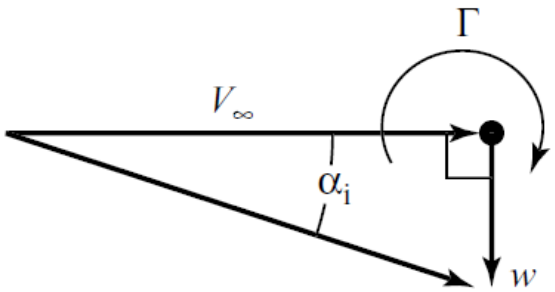

Velocity components at the lifting line

Prandtl's lifting line theory

Section lift coefficient:

if thin profile

$$c_l(y_0) = a_0\,(\alpha_{\text{eff}}(y_0) - \alpha_{l=0}) = 2\pi\,(\alpha - \alpha_i(y_0) - \alpha_{l=0})$$

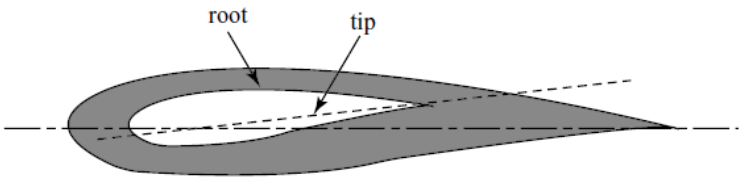

wash-out

geometric twist: $\alpha = \alpha(y_0)$

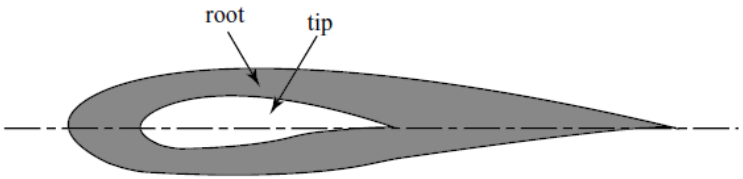

aerodynamic twist: $\alpha_{l=0} = \alpha_{l=0}(y_0)$

Fundamental equation of Prandtl's LLT

$$L'(y_0) = \frac{1}{2}\,\rho\,V_\infty^2\,c(y_0)\,c_l(y_0) \approx \rho\,V_\infty\,\Gamma(y_0)$$

$$c_l(y_0) = \frac{2\,\Gamma(y_0)}{V_\infty\,c(y_0)} = a_0[\alpha(y_0) - \alpha_i(y_0) - \alpha_{l=0}(y_0)]$$

$$\alpha(y_0) = \frac{2\,\Gamma(y_0)}{a_0\,V_\infty\,c(y_0)} + \alpha_{l=0}(y_0) + \frac{1}{4\,\pi\,V_\infty}\int_{-b/2}^{b/2}\frac{(d\Gamma/dy)}{(y_0 - y)}\,dy$$

$$\Gamma\left(y = \pm\frac{b}{2}\right) = 0$$

This is the ***monoplane equation***

Prandtl's lifting line theory

The fundamental equation of Prandtl's lifting line theory simply states that the geometric angle of attack is the sum of the effective angle plus the induced angle of attack. It is an integro-differential equation for $\Gamma = \Gamma(y_0)$, with y_0 ranging along the span from $-b/2$ to $+b/2$. Not easy to solve …

Consequences:

1. $L'(y_0) = \rho\, V_\infty\, \Gamma(y_0) \quad \rightarrow \quad L = \rho\, V_\infty \int_{-b/2}^{b/2} \Gamma(y_0)\, dy_0$
2. $D_i' = L' \sin\alpha_i \approx L'\, \alpha_i \quad \rightarrow \quad D_i \approx \rho\, V_\infty \int_{-\frac{b}{2}}^{\frac{b}{2}} \Gamma(y_0)\, \alpha_i(y_0)\, dy_0$
3. C_L and $C_{D,i}$ readily available

Drag

The total drag of a *subsonic* finite wing includes the induced drag, the skin friction drag and the pressure drag

$$D = D_i + \underbrace{D_{friction} + D_{pressure}}_{\text{also called } \textit{profile drag}\text{, and related to viscous effects}} \quad \rightarrow \quad C_D$$

At moderate angle of attack, the *profile drag* coefficient for a finite wing is essentially the same as for its airfoil sections.

The *profile drag* coefficient: $c_d = \frac{D_{friction} + D_{pressure}}{\frac{1}{2}\rho V_\infty^2 S}$ for a finite wing is available from *airfoil* data. Thus, the total drag coefficient takes the form: $C_D = c_d + C_{D,i}$

Elliptical lift distribution

Let us consider an elliptic circulation/lift distribution along y

$$\Gamma(y) = \Gamma_0 \sqrt{1 - \left(\frac{2\,y}{b}\right)^2}$$

$$\frac{\Gamma^2}{\Gamma_0^2} + \frac{y^2}{(b/2)^2} = 1$$

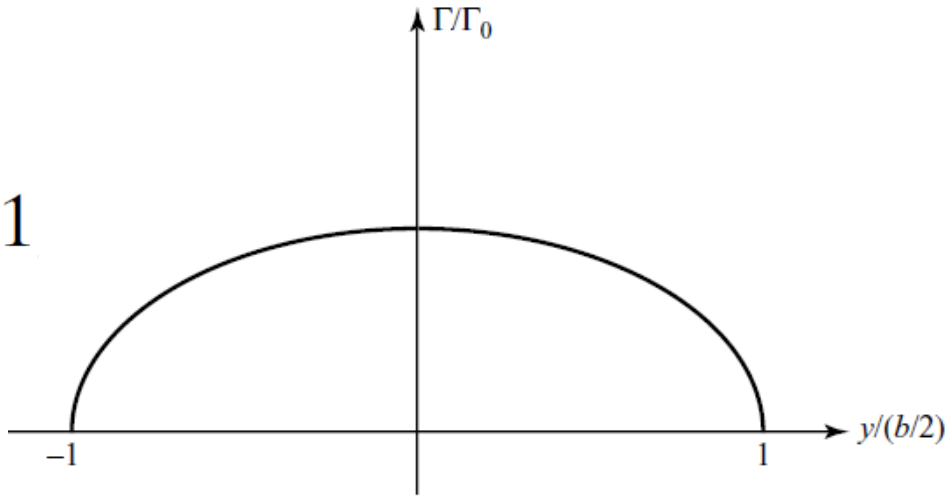

Elliptical lift distribution

Let us consider an elliptic circulation/lift distribution along y

$$\Gamma(y) = \Gamma_0 \sqrt{1 - \left(\frac{2\,y}{b}\right)^2}$$

$$\frac{d\Gamma}{dy} = -\frac{4\Gamma_0}{b^2} \frac{y}{(1 - 4y^2/b^2)^{1/2}}$$

$$\gamma = \left.\frac{d\Gamma}{dy}\right|_{y \to \pm\frac{b}{2}} \to \infty$$

vortex sheet of infinite strength at the tips

$$w(y_0) = \frac{\Gamma_0}{\pi b^2} \int_{-b/2}^{b/2} \frac{y}{(1 - 4y^2/b^2)^{1/2}(y_0 - y)}\, dy$$

(slide 103)

Elliptical lift distribution

Change of variables:

$$y = \frac{b}{2}\cos\theta \quad \rightarrow \quad dy = -\frac{b}{2}\sin\theta \; d\theta$$

with the variable θ going from π to 0.

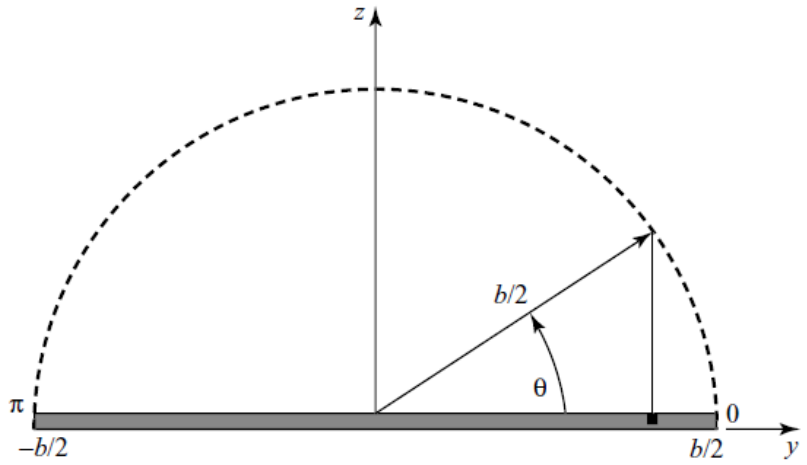

Elliptical lift distribution

Change of variables:

$$y = \frac{b}{2}\cos\theta \quad \rightarrow \quad dy = -\frac{b}{2}\sin\theta \; d\theta$$

with the variable θ going from π to 0. Then $\boxed{\Gamma(\theta) = \Gamma_0 \sin\theta}$ and

$$w(\theta_0) = -\frac{\Gamma_0}{2\pi b}\int_{\pi}^{0} \frac{\cos\theta}{\cos\theta_0 - \cos\theta}\, d\theta$$

$$w(\theta_0) = -\frac{\Gamma_0}{2\pi b}\int_{0}^{\pi} \frac{\cos\theta}{\cos\theta - \cos\theta_0}\, d\theta = -\frac{\Gamma_0}{2b}$$

(from Glauert's first integral with n = 1, slide 48)

Elliptical lift distribution

Constant downwash: $w(y) = -\dfrac{\Gamma_0}{2b}$

Induced angle of attack: $\alpha_i = -\dfrac{w}{V_\infty} = \dfrac{\Gamma_0}{2bV_\infty}$

For an elliptical lift distribution both the downwash and the induced angle of attack are constant along the span y (and both tend to zero as the span becomes infinite)

$$L = \rho V_\infty \Gamma_0 \int_{-b/2}^{b/2} \left(1 - \frac{4y^2}{b^2}\right)^{1/2} dy$$

$$= \rho V_\infty \Gamma_0 \frac{b}{2} \int_0^\pi \sin^2\theta \, d\theta = \rho V_\infty \Gamma_0 \frac{b}{4} \pi$$

Elliptical lift distribution

$$\Gamma_0 = \frac{4L}{\rho\, V_\infty b\, \pi} = \frac{4\left(\frac{1}{2}\rho\, V_\infty^2\, S\, C_L\right)}{\rho\, V_\infty b\, \pi} = \frac{2\, V_\infty S\, C_L}{b\, \pi}$$

$$\alpha_i = \frac{S\, C_L}{\pi\, b^2} = \frac{C_L}{\pi\, AR} \quad \text{with} \quad AR = b^2/S$$

Since α_i is constant, we have (cf. slide 107):

$$D_i \approx L\, \alpha_i = \rho\, V_\infty\, \alpha_i\, \Gamma_0\, \frac{b}{4}\pi \;\rightarrow\; C_{D,i} = \frac{D_i}{\frac{1}{2}\rho\, V_\infty^2\, S} = \frac{C_L^2}{\pi\, AR}$$

***"Lift-induced drag"* coefficient!**

Elliptical lift distribution

$$C_{D,i} = \frac{C_L^2}{\pi\, AR}$$

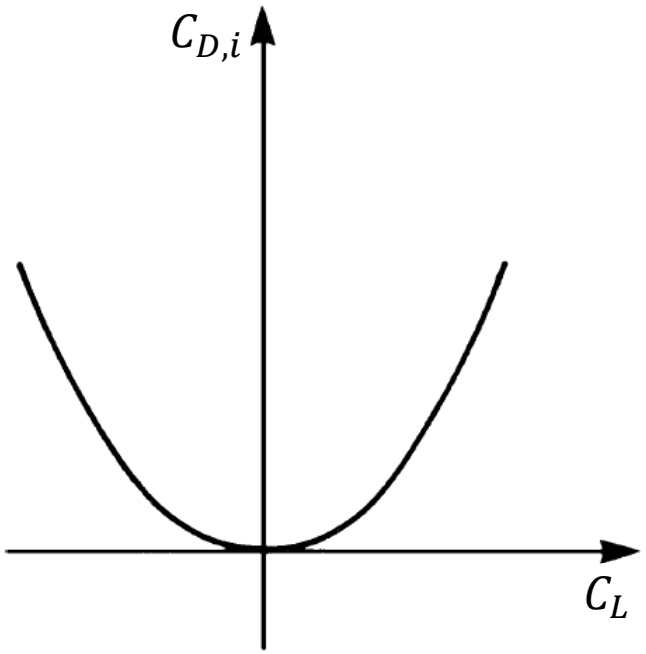

At zero lift $C_{D,i}$ is zero (and same for α_i)

As AR increases (to infinity for two-dimensional flow) $C_{D,i}$ decreases (to zero); same for α_i

At low speed (take-off or landing) L is large and D_i makes up a large part of the total drag (of the order of 60%). Even at relatively high cruising speeds, induced drag is typically 25% of the total drag

Elliptical lift distribution

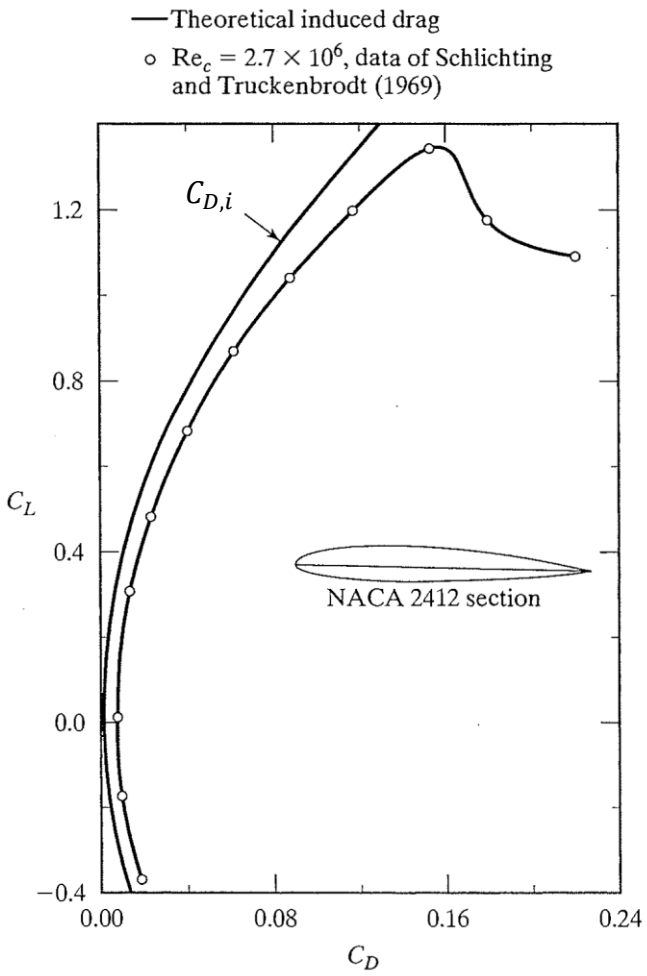

$$C_D = c_d + C_{D,i} = c_d + \frac{C_L^2}{\pi\, AR}$$

Drag polar for an elliptic untwisted wing of aspect ratio $AR = 5$

Lift slope for elliptical lift distribution

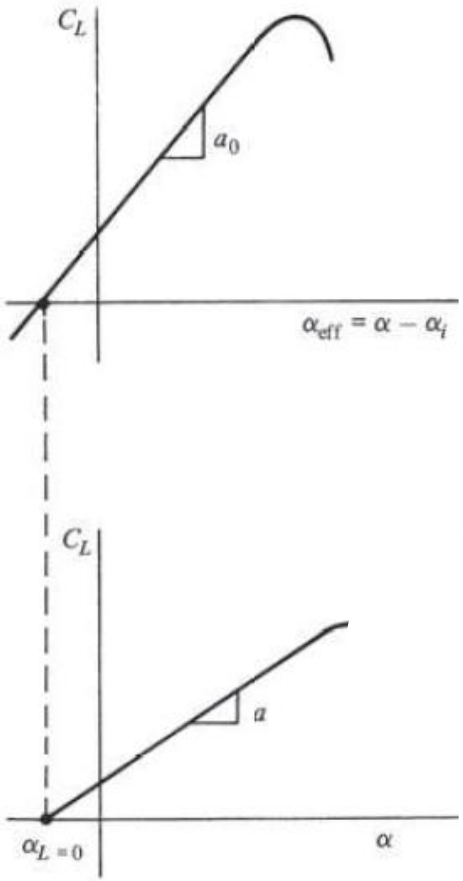

Ex. *Untwisted* wing, elliptical lift distribution

α_i constant along y

$\alpha_{\text{eff}} = \alpha - \alpha_i$ constant along y

Also, $\alpha_i = 0$ when $C_L = 0$, which means that at zero-lift $\alpha_{\text{eff}} = \alpha$, and thus $\alpha_{L=0} = \alpha_{l=0}$ (wing & airfoil)

Observations show that $a < a_0$, i.e. the finite wing has a reduced lift slope compared to an airfoil.
By how much?

Lift slope for elliptical lift distribution

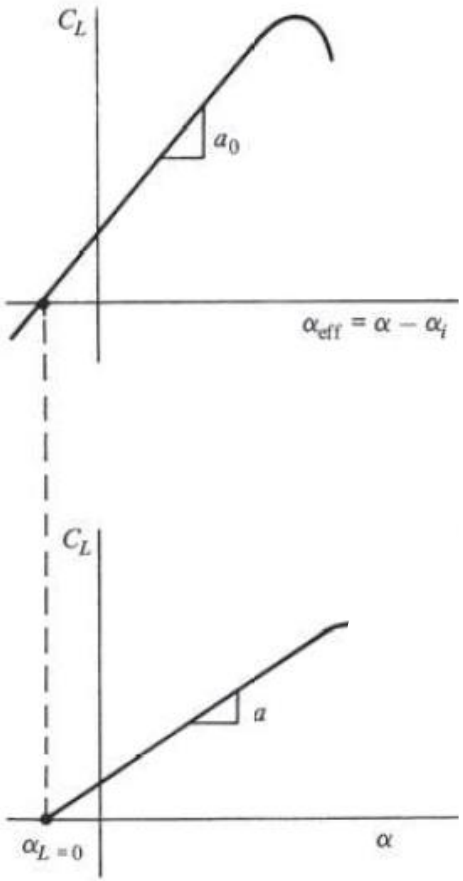

$$\frac{dC_L}{d(\alpha - \alpha_i)} = a_0$$

$$C_L = a_0(\alpha - \alpha_i) + constant$$

$$C_L = a_0\left(\alpha - \frac{C_L}{\pi\, AR}\right) + constant$$

$$C_L\left(1 + \frac{a_0}{\pi\, AR}\right) = a_0\alpha + constant$$

$$a = \frac{dC_L}{d\alpha} = \frac{a_0}{\left(1 + \frac{a_0}{\pi\, AR}\right)} = \frac{2\pi}{\left(1 + \frac{2}{AR}\right)}$$

for thin profile

Elliptical lift distribution: effect of AR on C_L

Thin profiles: $$a = \frac{2\pi}{\left(1 + \frac{2}{AR}\right)} = \frac{2\pi\, AR}{2 + AR} = \frac{C_L}{(\alpha - \alpha_{L=0})}$$

$$\frac{a}{2\pi} = \frac{C_L}{2\pi(\alpha - \alpha_{L=0})}$$

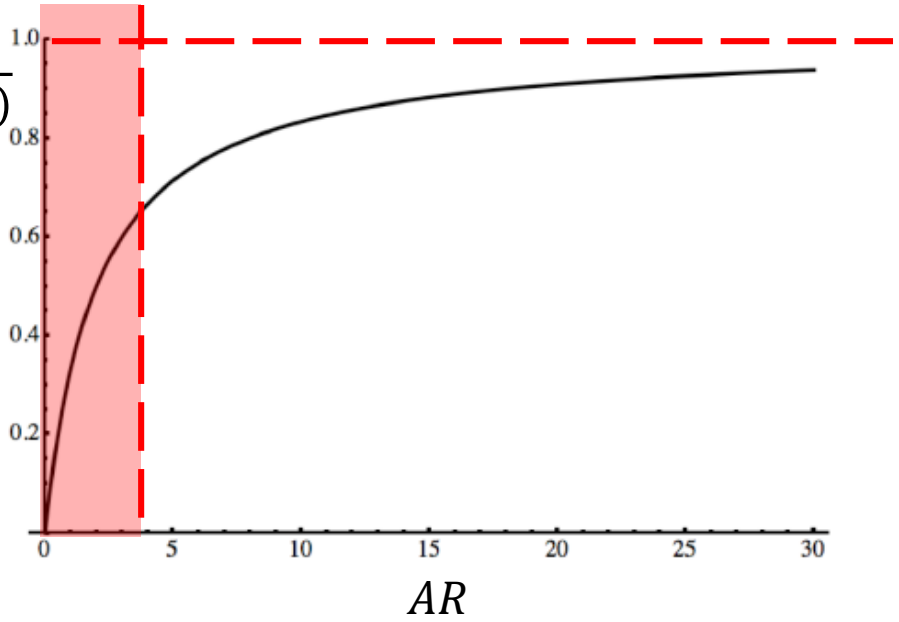

Elliptical lift distribution: effect of AR on $C_{D,i}$

$$\frac{AR}{2+AR} = \frac{C_L}{2\pi\,(\alpha - \alpha_{L=0})}$$

$$C_{D,i} = \frac{C_L^2}{\pi AR} = \frac{AR}{(2+AR)^2}\,4\pi(\alpha - \alpha_{L=0})^2$$

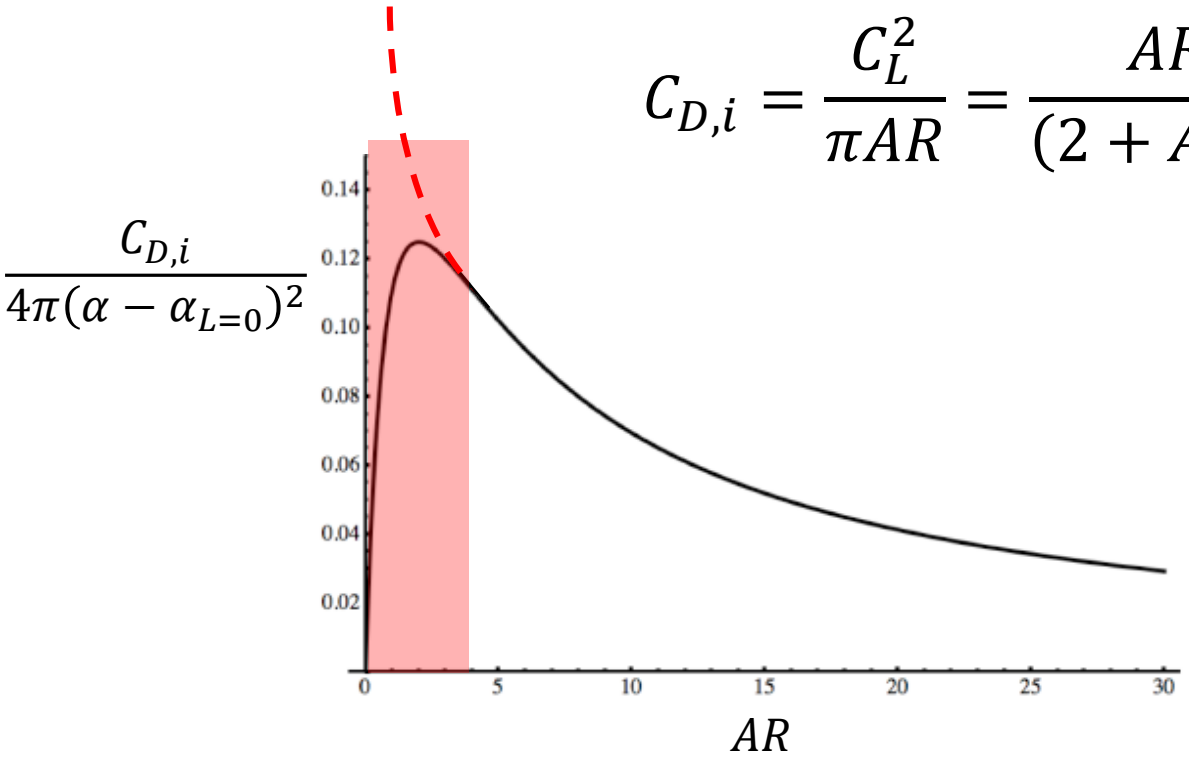

Prize exacted by the work needed to create the wake

Elliptical wing planform

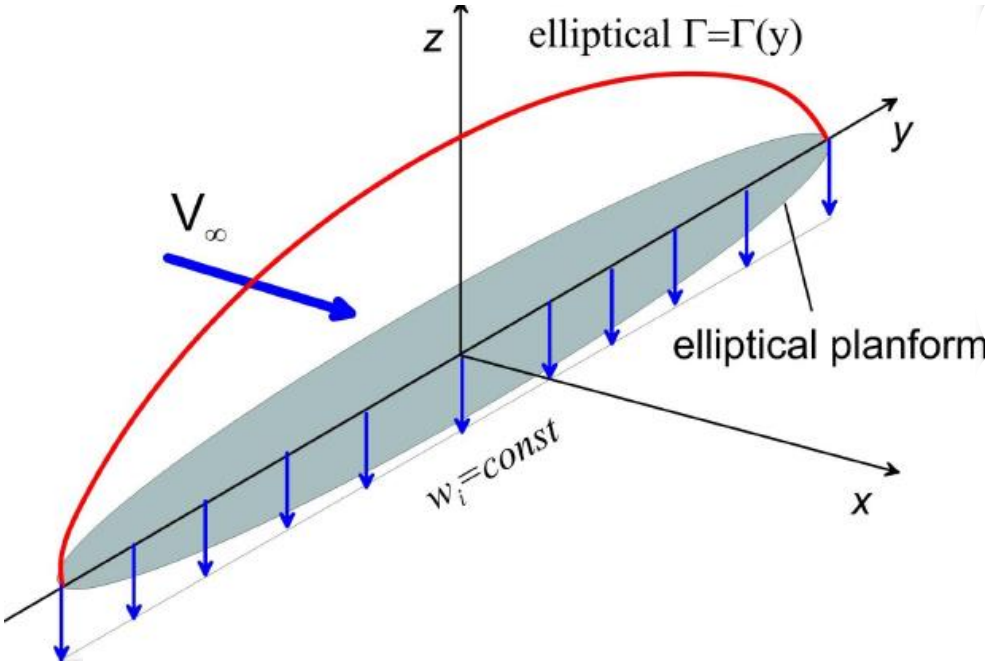

Untwisted wing:

no aero twist: $\alpha_{l=0}$ constant
no geom twist: α constant

$\alpha_{eff} = \alpha - \alpha_i$ constant

↓

$c_l = a_0(\alpha_{eff} - \alpha_{l=0})$: the *section* lift coefficient is constant along the span y

Local lift: $L'(y) = \frac{1}{2}\rho\, V_\infty^2\, c(y)\, c_l \rightarrow$ **the chord $c(y)$ is elliptical!**

Elliptical wing planform

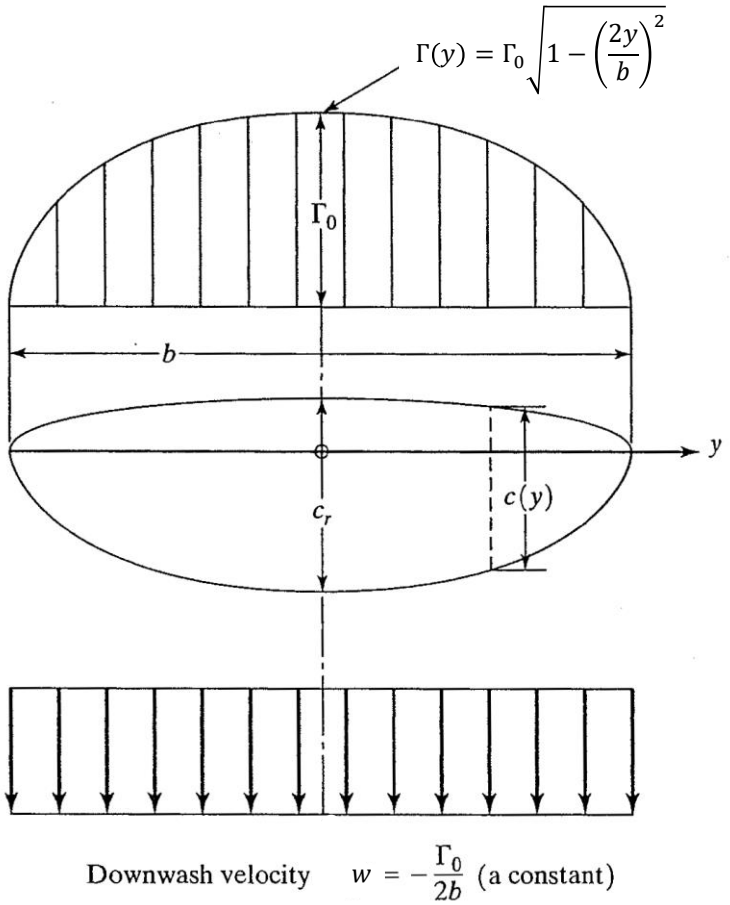

British *Spitfire*: the wing is formed from two ellipses of different minor axis. This shifts the major axis and the AC forward

Other untwisted wings

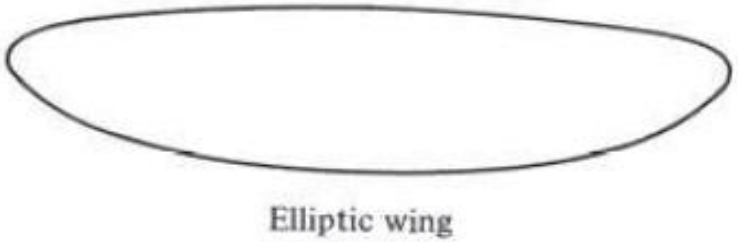

Elliptic wing

→ *Minimum induced drag* but expensive to manufacture

Rectangular wing

→ Lift distribution far from optimum

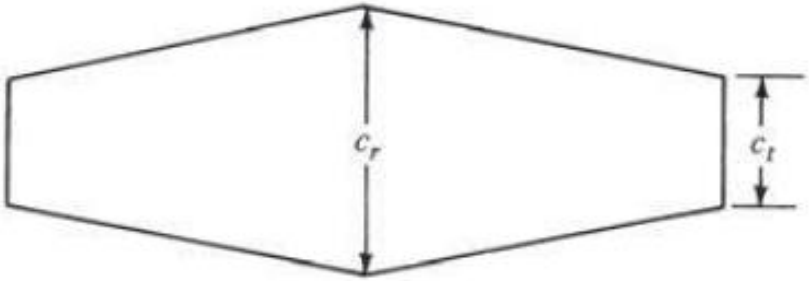

Tapered wing

→ Tapered planform (with *taper ratio* $\lambda \equiv \frac{c_t}{c_r}$) can be designed such that the lift distribution approximates the elliptic case

Other untwisted wings

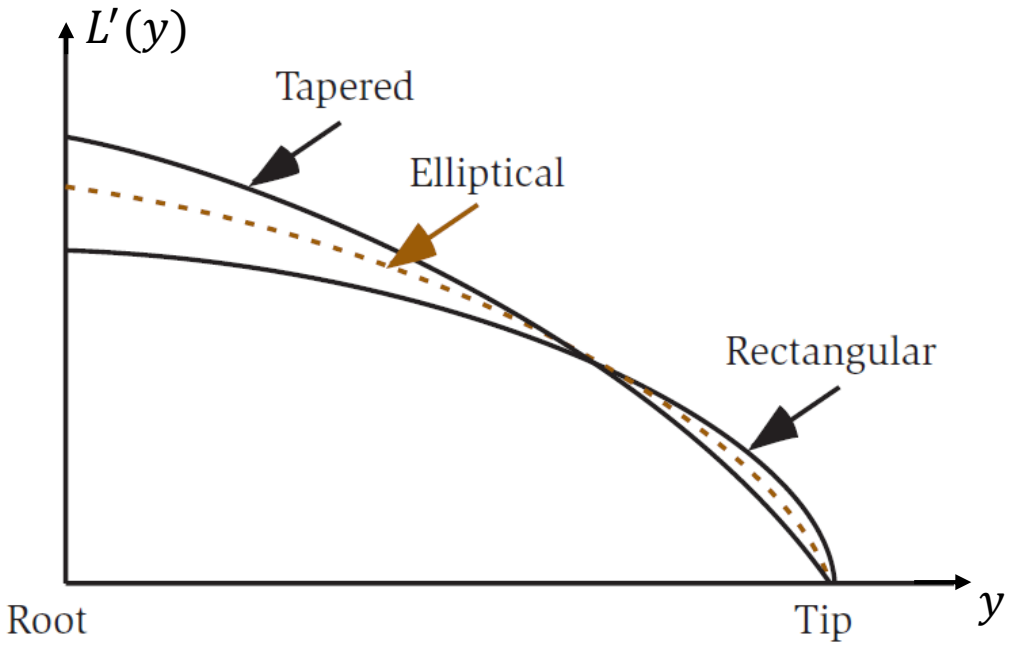

The rectangular wing has the highest loading at the tip

The linearly tapered wing “unloads” the tip, reducing the flexural moment there, and looses only a fraction of the lift compared to the elliptic wing. Reduced construction costs

Effect of *geometrical* wing twist

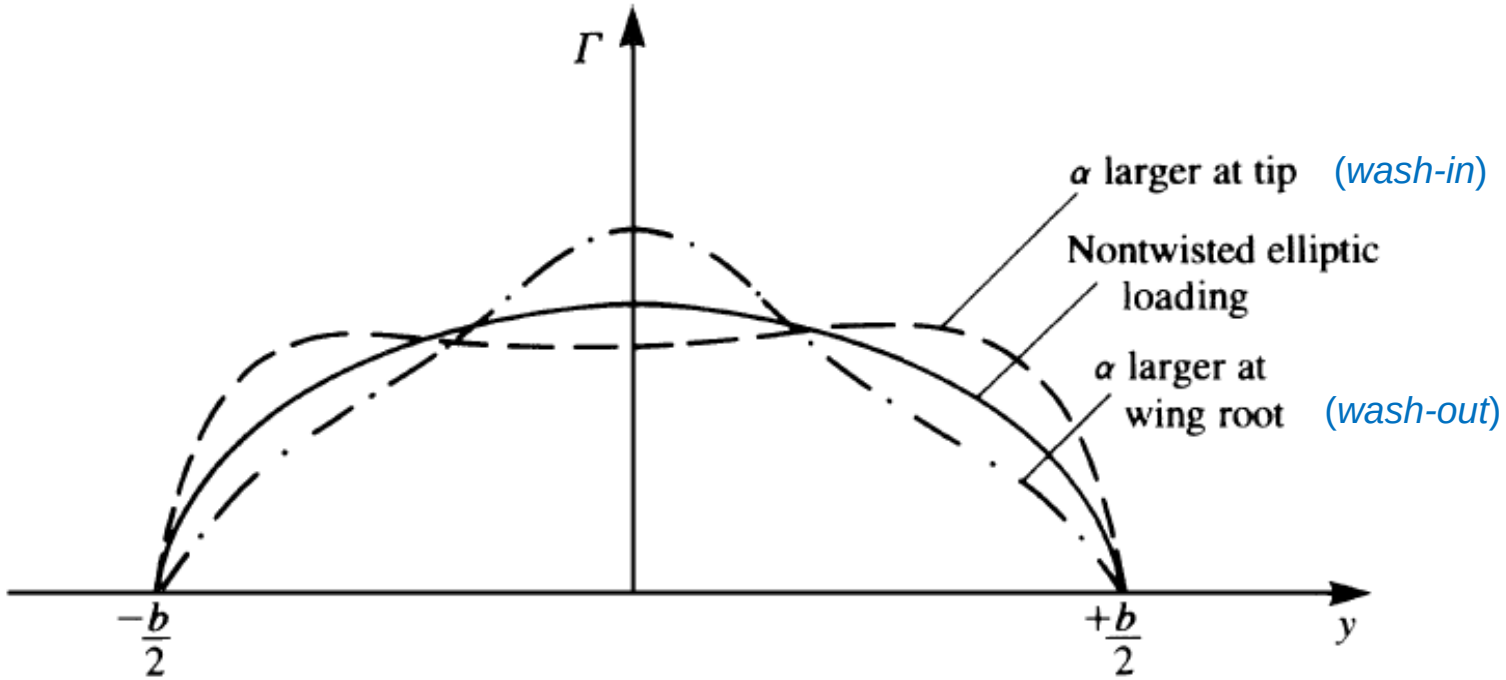

Spanwise loading of twisted elliptic wings

General circulation distribution

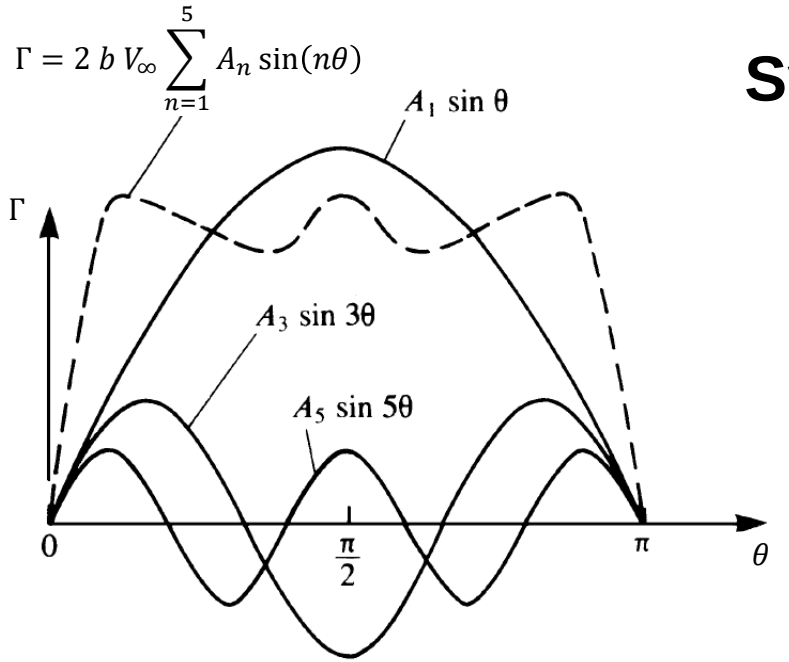

Symmetric loading

For an elliptic wing, using $y = \frac{b}{2}\cos\theta$, the circulation is $\Gamma = \Gamma_0 \sin\theta$. It is thus natural to express a *general* circulation distribution as a sine series:

$$\Gamma = 2\,b\,V_\infty \sum_{n=1}^{\infty} A_n \sin(n\theta)$$

General circulation distribution

The monoplane equation (slide 106) becomes:

$$\mu(\alpha - \alpha_{l=0}) \sin\theta_0 = \sum_{n=1}^{\infty} A_n \, (\mu n + \sin\theta_0) \sin(n\theta_0)$$

where $\mu = \frac{c\, a_0}{4b}$ (do the steps for yourselves and verify the equation above, using Glauert's first integral, slide 48)

This equation must be evaluated at N **spanwise stations** (i.e. at N values of θ_0) and solved for the N coefficients $A_1, A_2, A_3, \ldots A_N$. For symmetric loading only the *odd* coefficients are needed; typically, the first 4 or 5 coefficients are sufficient

General circulation distribution

Once the coefficients A_n are available:

$$C_L = \frac{2}{V_\infty S}\int_{-b/2}^{+b/2}\Gamma(y)\,dy = 2\,AR\sum_{n=1}^{\infty}A_n\int_0^{\pi} sin(n\theta)\sin\theta\,d\theta = A_1\pi\,AR$$

C_L depends only on the amplitude of the first harmonic!

$$\alpha_i(y_0) = \frac{1}{4\,\pi\,V_\infty}\int_{-b/2}^{+b/2}\frac{\left(d\Gamma/dy\right)}{y_0-y}\,dy = \cdots = \sum_1^N n\,A_n\frac{\sin(n\theta_0)}{\sin\theta_0}$$

$$C_{D,i} = \frac{2}{V_\infty S}\int_{-b/2}^{+b/2}\Gamma(y)\,\alpha_i(y)\,dy = \cdots = \pi\,AR\,A_1^2\left[1+\sum_2^N n\left(\frac{A_n}{A_1}\right)^2\right]$$

$$= \frac{C_L^2}{\pi\,AR}\left[1+\sum_2^N n\left(\frac{A_n}{A_1}\right)^2\right] = \frac{C_L^2}{\pi\,AR}\left[1+\delta\right]$$

(Glauert's integrals again!)

General circulation distribution

$$C_{D,i} = \frac{C_L^2}{\pi\, AR}\,[1+\delta]$$

δ is the *induced drag factor*

$\delta \in [0, 0.2]$

$$e = (1+\delta)^{-1} \leq 1$$

span efficiency factor

$$C_{D,i} = \frac{C_L^2}{\pi\, e\, AR}$$

For the elliptical lift distribution it is $\delta = 0$ and $e = 1$, which corresponds to *minimum induced drag* → the elliptical lift distribution characterizes the ***optimal planar*** wing planform

General circulation distribution: moments

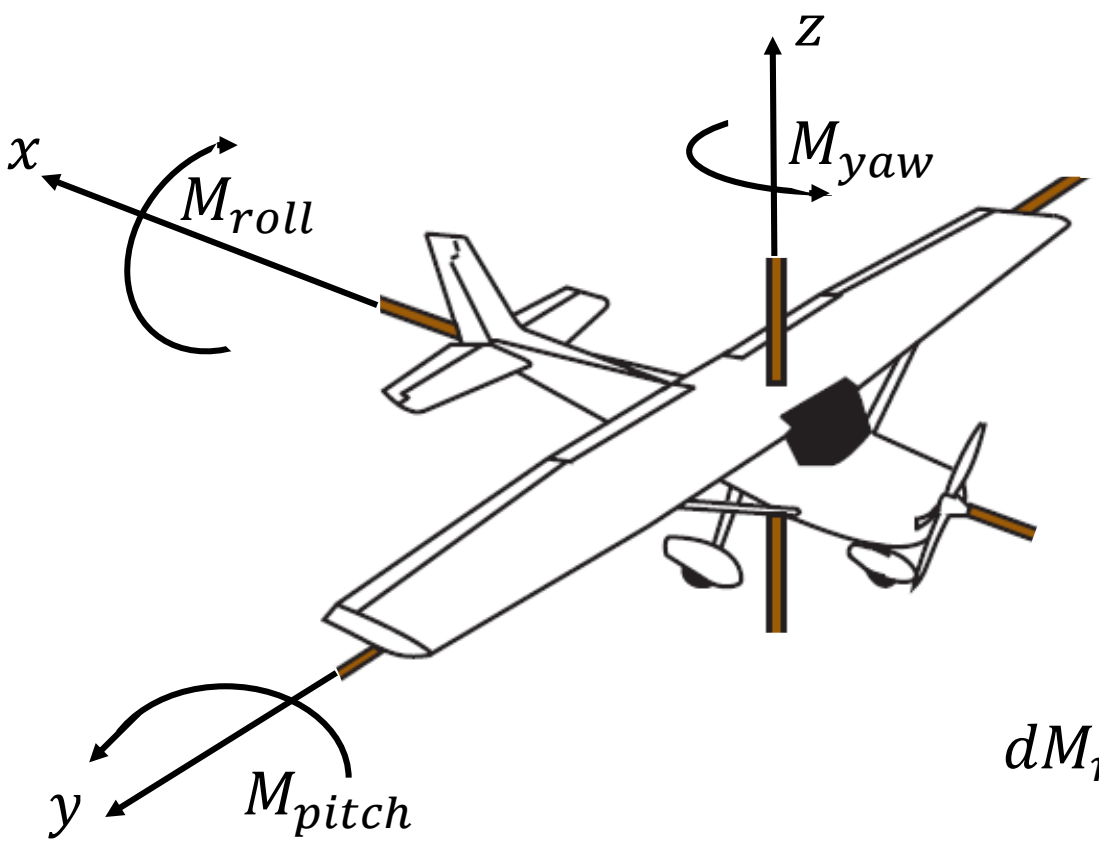

$$dM_{roll} = y\, dL$$

$$dM_{yaw} = -y\, dD$$

General circulation distribution: moments

Pitching moment is available from 2D wing profile analysis (slide 65; careful, coefficients A_i are not the same!!)

Roll moment:

$$M_{roll} = \rho\, V_\infty \int_{-b/2}^{b/2} y\, \Gamma(y)\, dy = \ \ldots$$

$$= \frac{\rho\, V_\infty^2\, b^3}{4} \sum_{n=1}^{\infty} A_n \int_0^{\pi} \sin(n\theta) \sin(2\theta)\ d\theta = \frac{\pi\ A_2\, \rho\, V_\infty^2\, b^3}{8}$$

$$\boxed{C_{M\,roll} = \frac{\pi}{4} A_2\, AR}$$

$C_{M\,roll}$ depends only on the amplitude of the second harmonic!

General circulation distribution: moments

Yaw moment (*accounting only for induced drag*):

$$M_{yaw} = -\int_{-b/2}^{b/2} y\, dD_i = -\int_{-b/2}^{b/2} y \left[\alpha_i\, \rho\, V_\infty\, \Gamma(y)\, dy\right] = \cdots$$

$$= -\frac{\rho\, V_\infty^2\, b^3}{2} \sum_{n=1}^{\infty} \sum_{m=1}^{\infty} n\, A_n\, A_m \int_0^{\pi} \sin(n\theta) \sin(m\theta) \cos(\theta)\; d\theta =$$

$$= -\frac{\pi\, \rho\, V_\infty^2\, b^3}{8} \sum_{n=1}^{\infty} (2n+1)\, A_n\, A_{n+1}$$

$$C_{M\,yaw} = -\frac{\pi}{4} AR \sum_{n=1}^{\infty} (2n+1)\, A_n\, A_{n+1}$$

$C_{M\,yaw}$ depends on the amplitude of all harmonics!

Generic wing

$$C_{D,i} = \frac{C_L^2}{\pi\, e\, AR}$$

The span efficiency factor e for a **nonplanar** wing can be larger than one, i.e. the induced drag can be **less** than the ideal value

Another "efficiency factor", called the *Oswald efficiency factor*, e_0, takes into account the variation with C_L of the total drag, including the viscous profile drag. It is defined in practice by *curve fitting* a known total drag polar

$$C_D = C_{D_{min}} + \frac{C_L^2}{\pi\, e_0\, AR}$$

Generic wing

$C_{D_{min}} \approx C_{D_0}$

C_{D_0}: zero-lift drag coefficient

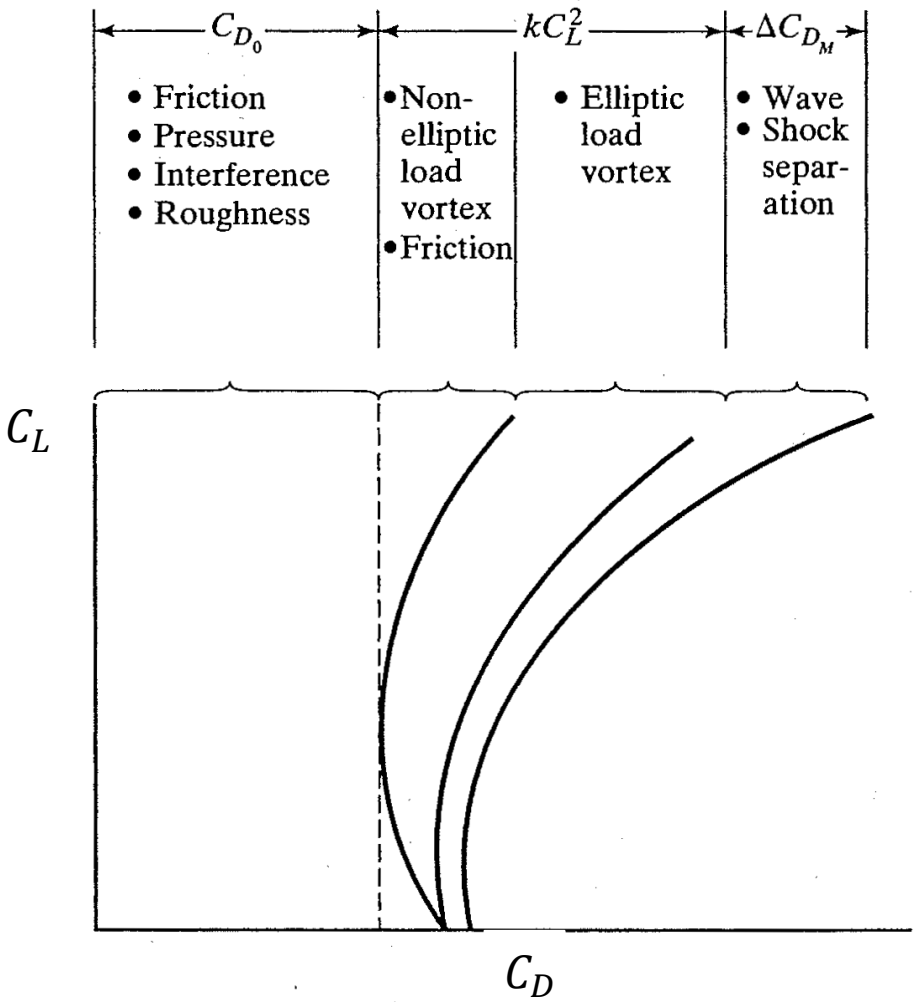

Rectangular wing: effect of AR

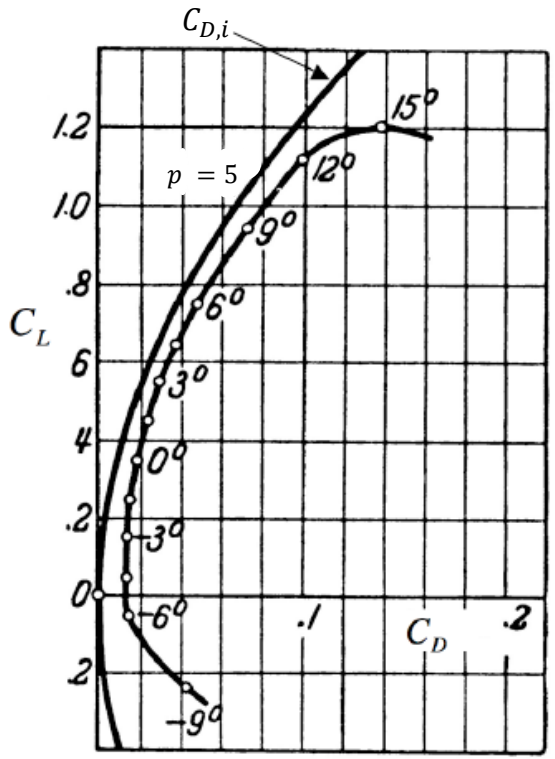

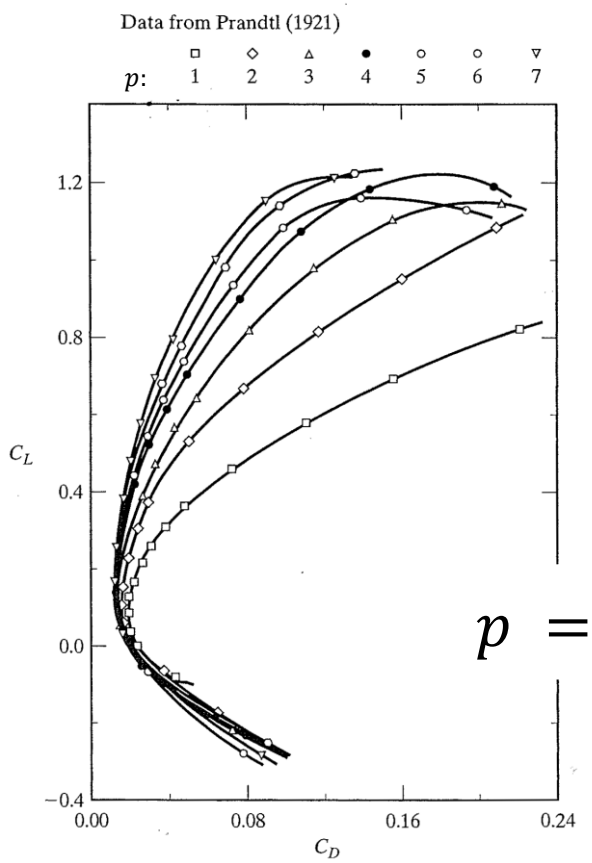

$$p = \frac{2}{\pi} AR$$

Measured drag polar for a **rectangular wing** with $p = 5$ (left) and for rectangular wings of varying aspect ratio (right)

Rectangular wing: effect of AR

AR varies typically from 6 to 22 for standard subsonic airplanes and gliders; it has a **strong influence** on $C_{D,i}$

Let us consider two finite wings with same profile but different aspect ratio:

$$C_{D\,1} = c_d + \frac{C_L^2}{\pi\, e\, AR_1}$$

$$C_{D\,2} = c_d + \frac{C_L^2}{\pi\, e\, AR_2}$$

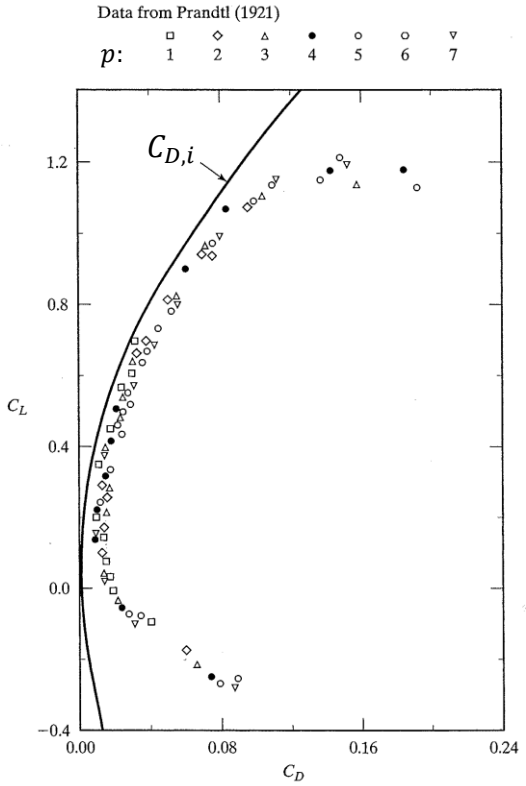

Drag polar converted to $AR = 5\left(\frac{\pi}{2}\right)$

Rectangular wing: effect of AR

Assume that the two wings operate at the same C_L; also, since the airfoil section is the same for both wings, c_d is the same. The variation of δ (and e) between the two wings is small

Hence

$$C_{D\,1} = C_{D\,2} + \frac{C_L^2}{\pi\, e}\left(\frac{1}{AR_1} - \frac{1}{AR_2}\right)$$

i.e. the data of a wing with AR_2 can be scaled to the case of wings of any other aspect ratio

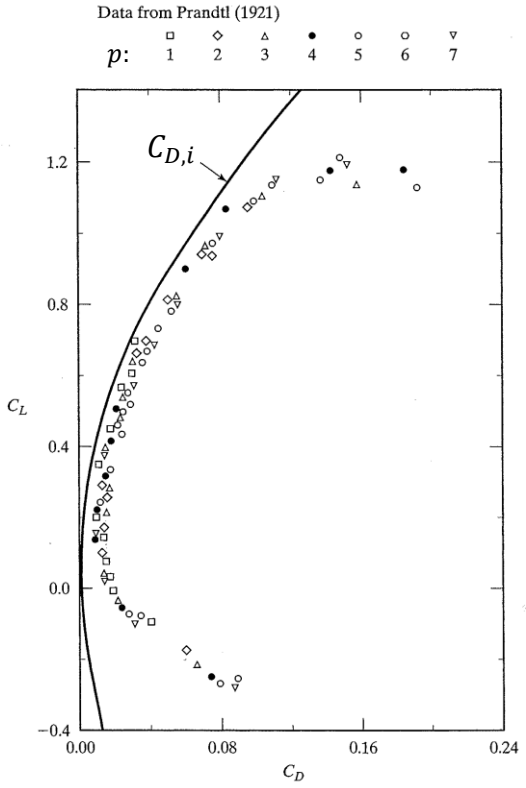

Drag polar converted to $AR = 5\left(\frac{\pi}{2}\right)$

Lift slope for a wing of general planform

$$a = \frac{a_0}{1 + \left(\frac{a_0}{\pi\, AR}\right)(1 + \tau)}$$

τ is the *induced lift factor*

$\tau \in [0, 0.25]$

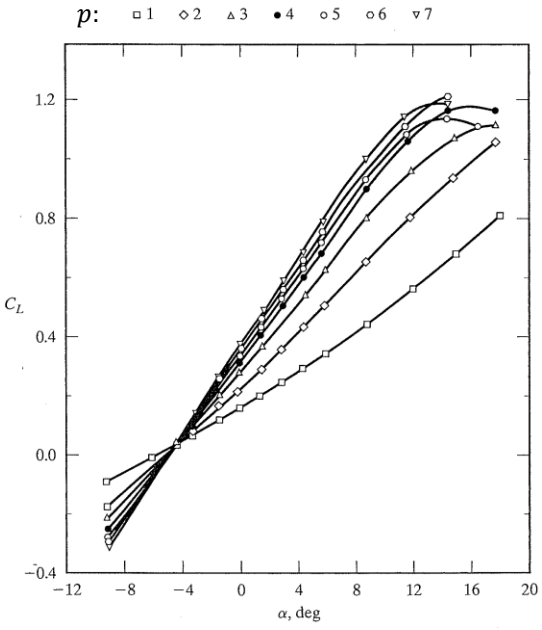

Prandtl's (1921) rectangular wing data

Lift slope for a wing of general planform

Downwash → effective angle of attack of finite wing ↘ and lift ↘

If a section at $y = y_0$ of a finite wing were to have the same lift as the same profile of an infinite wing at angle of attack α_{2D}, its angle of attack would have to be increased by

$$\alpha_i(y_0) = \frac{C_L}{\pi AR}\left[1 + \sum_2^N n \, \frac{A_n}{A_1} \frac{\sin(n\theta_0)}{\sin\theta_0}\right] = \frac{C_L}{\pi AR}\left[1 + g(y_0)\right].$$

Neglecting the correction factor $g(y_0)$, two wings (with different AR's) have the same lift C_L of an infinite wing if their angles of attack are

$$\alpha_1 \approx \alpha_{2D} + \frac{C_L}{\pi \, AR_1} \quad \text{and} \quad \alpha_2 \approx \alpha_{2D} + \frac{C_L}{\pi \, AR_2}$$

Lift slope for a wing of general planform

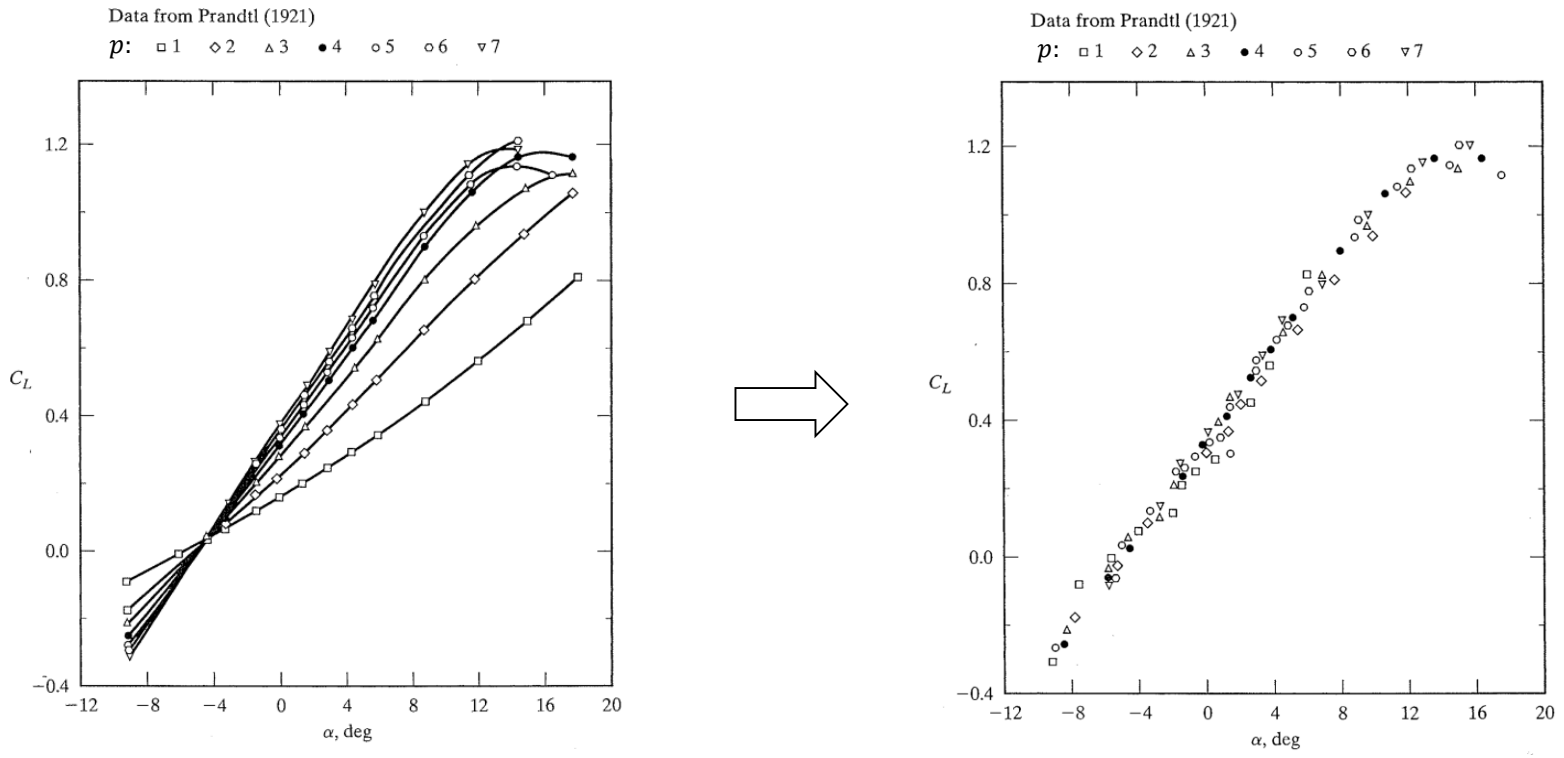

Lift data converted to $p = 5$ using $\alpha_1 = \alpha_2 + \frac{C_L}{\pi}\left(\frac{1}{AR_1} - \frac{1}{AR_2}\right)$

When can Prandt's LLT be applied?

Prandtl's classical lifting line theory yields reasonable results for straight wings at moderate to high aspect ratio. However, it is *inappropriate* for

- low-aspect-ratio straight wings ($AR < 4$, as a rule of thumb)
- swept wings
- delta wings

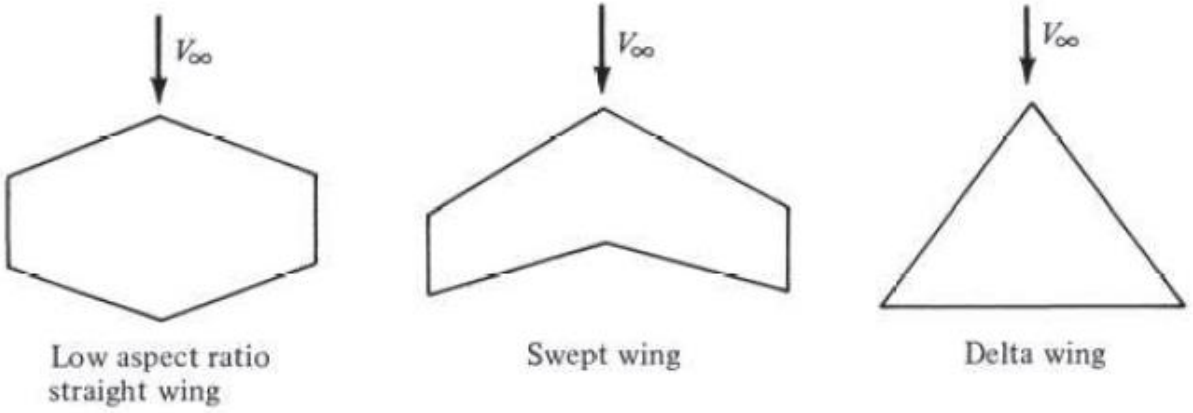

Empirical corrections

Low-aspect-ratio straight wings

$$a = \frac{a_0}{\sqrt{1 + \left(\frac{a_0}{\pi\, AR}\right)^2} + \frac{a_0}{\pi\, AR}}$$

H.B. Helmbold (1942)

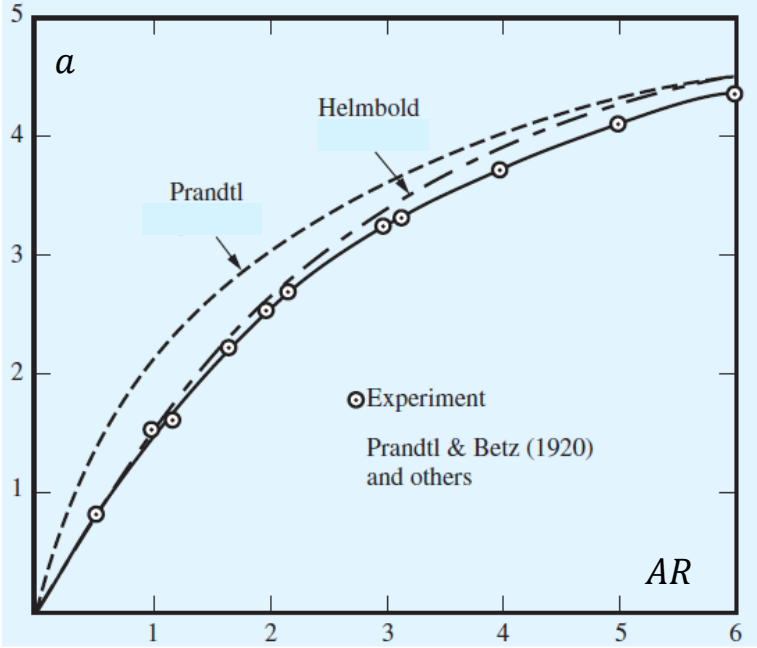

Empirical corrections

Swept wings

$$a = \frac{a_0 \cos \Lambda}{\sqrt{1 + \left(\frac{a_0 \cos \Lambda}{\pi\, AR}\right)^2} + \frac{a_0 \cos \Lambda}{\pi\, AR}}$$

D. Kuchemann (1978)

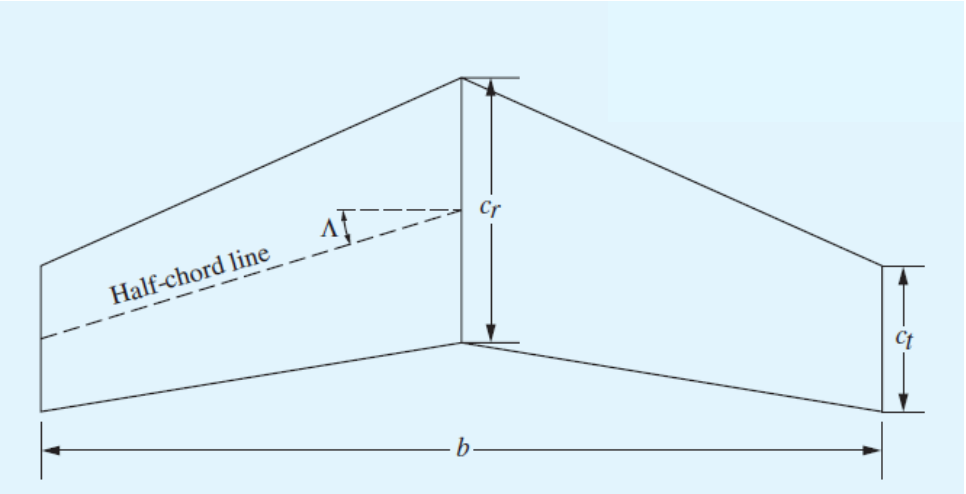

Numerical methods

For low-aspect-ratio wings, swept wings, and delta wings, *lifting-surface* theory must be used. In modern aerodynamics, such lifting-surface theory is implemented by the *vortex panel* or the *vortex lattice* techniques.

Another approach is *aerodynamic strip theory*, which treats each section of the wing as 2D. It takes information from a 3D panel code or from LLT, and uses the *effective angle of attack*; thus, in some way, it includes the effect of the three-dimensionality of the wing.

Numerical methods: vortex panel

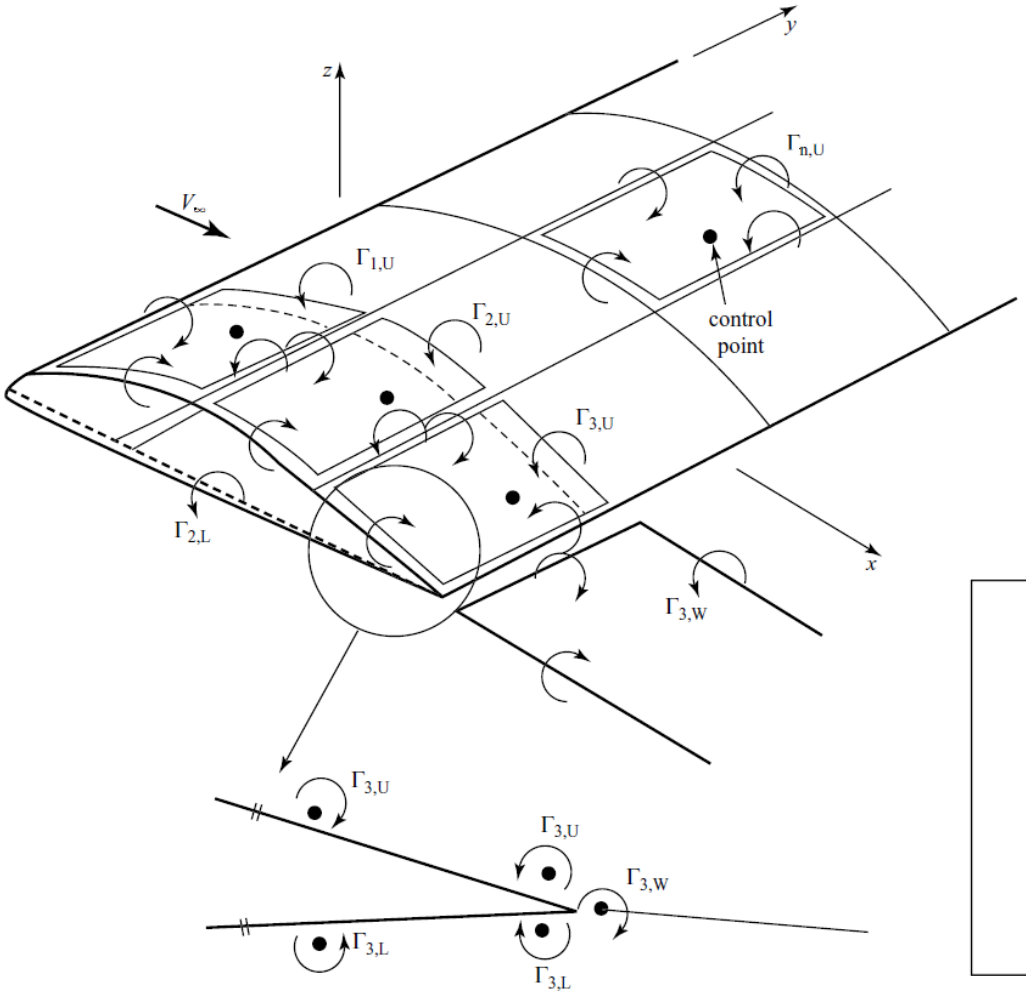

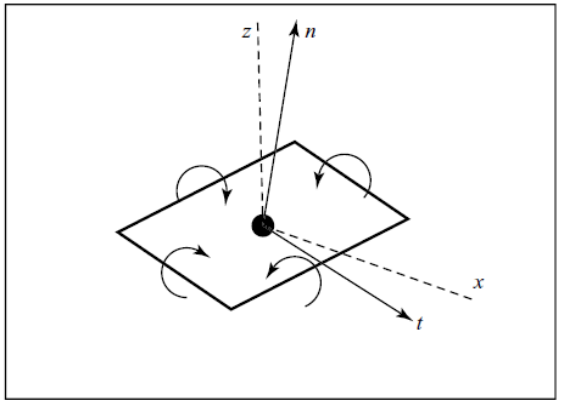

(*n* refers to surface normal in this figure; *t* refers to the tangent direction at the control point)

Numerical methods: vortex lattice

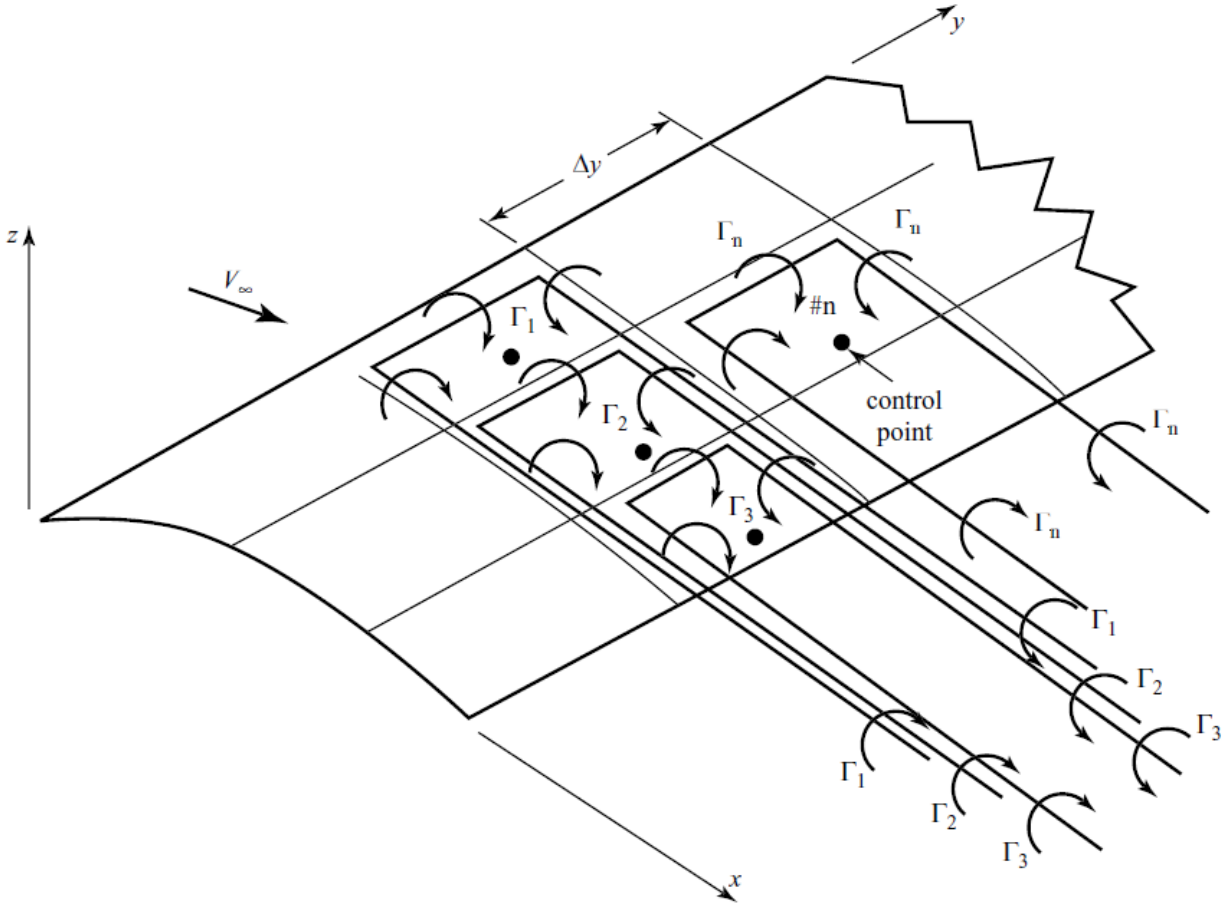

Vortex lattice method (Thomas, 1976)

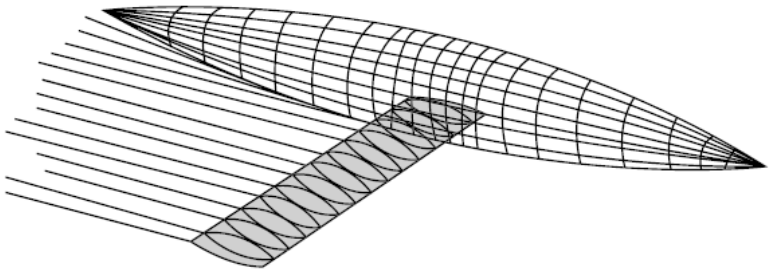

Representative paneling for three-dimensional wing vortex lattice

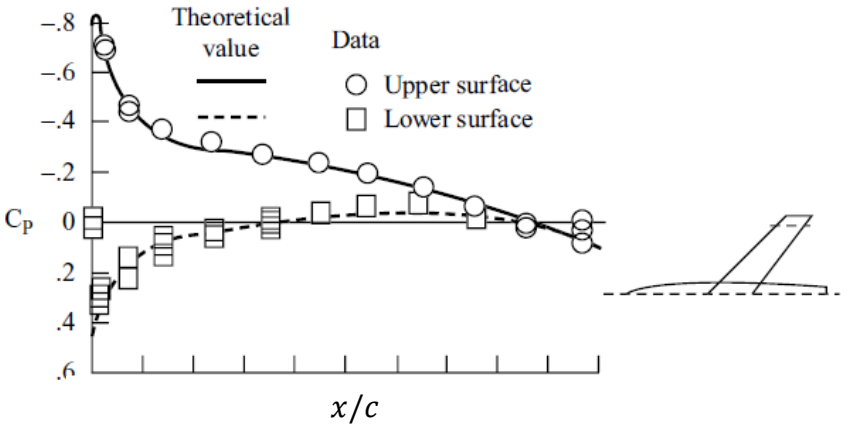

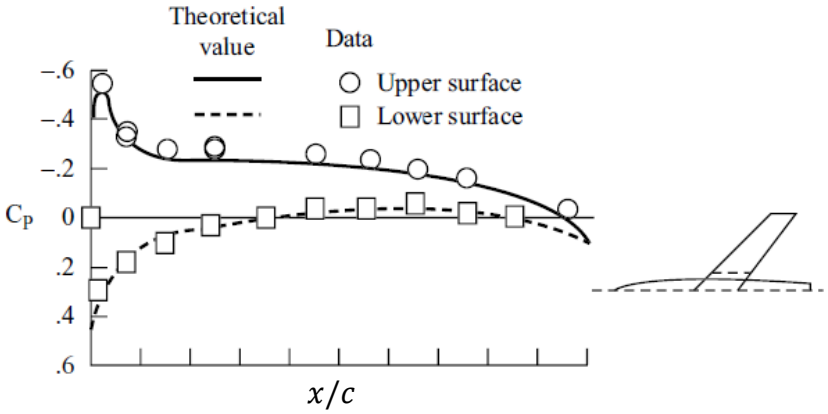

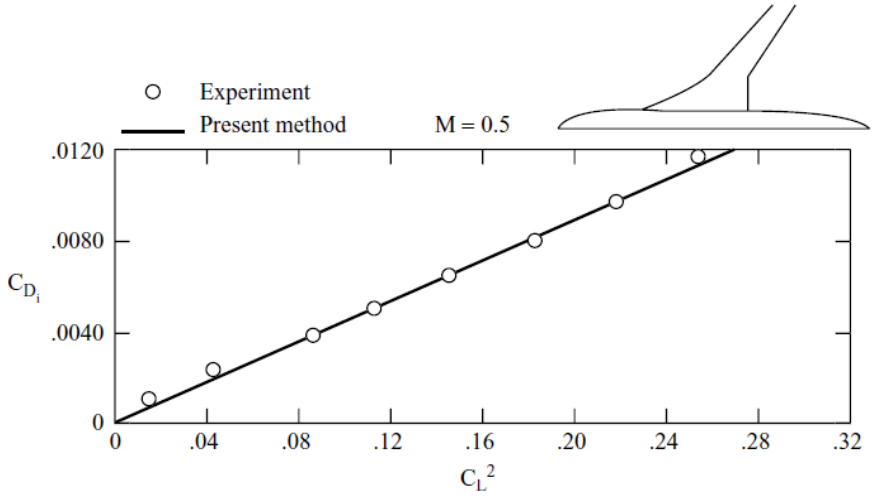

Induced drag for Lockheed ATT-95 aircraft

Far field calculations

The same analytical results already obtained for lift and induced drag can be recovered by applying the integral form of the momentum equation over a large control volume (assuming inviscid, steady flow, with no body forces)

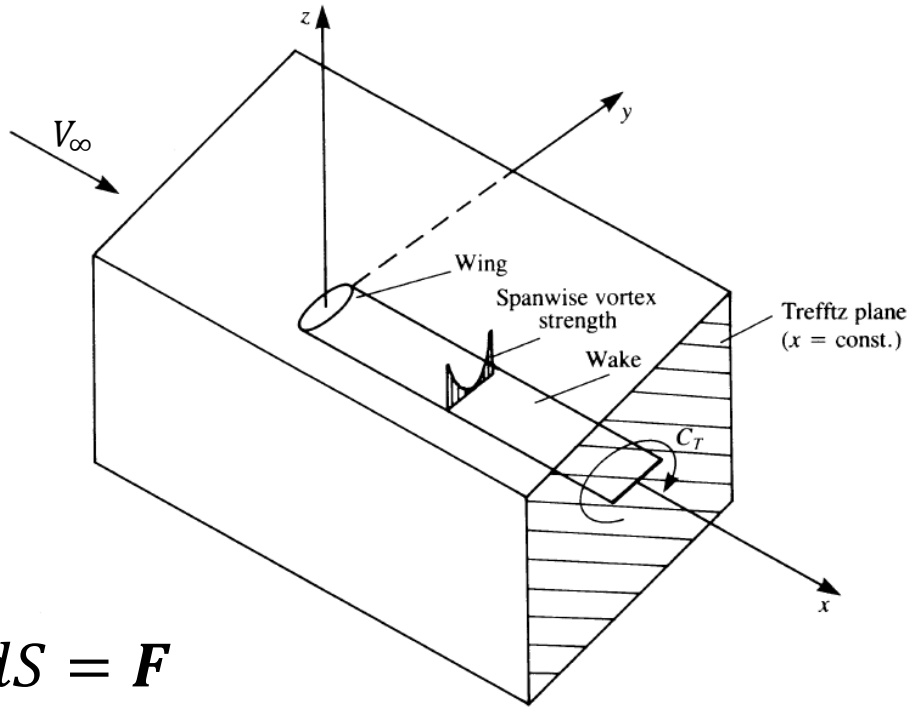

$$\int_S \rho \boldsymbol{V} (\boldsymbol{V} \cdot \boldsymbol{n}) \, dS + \int_S p \boldsymbol{n} \, dS = \boldsymbol{F}$$

Far field calculations

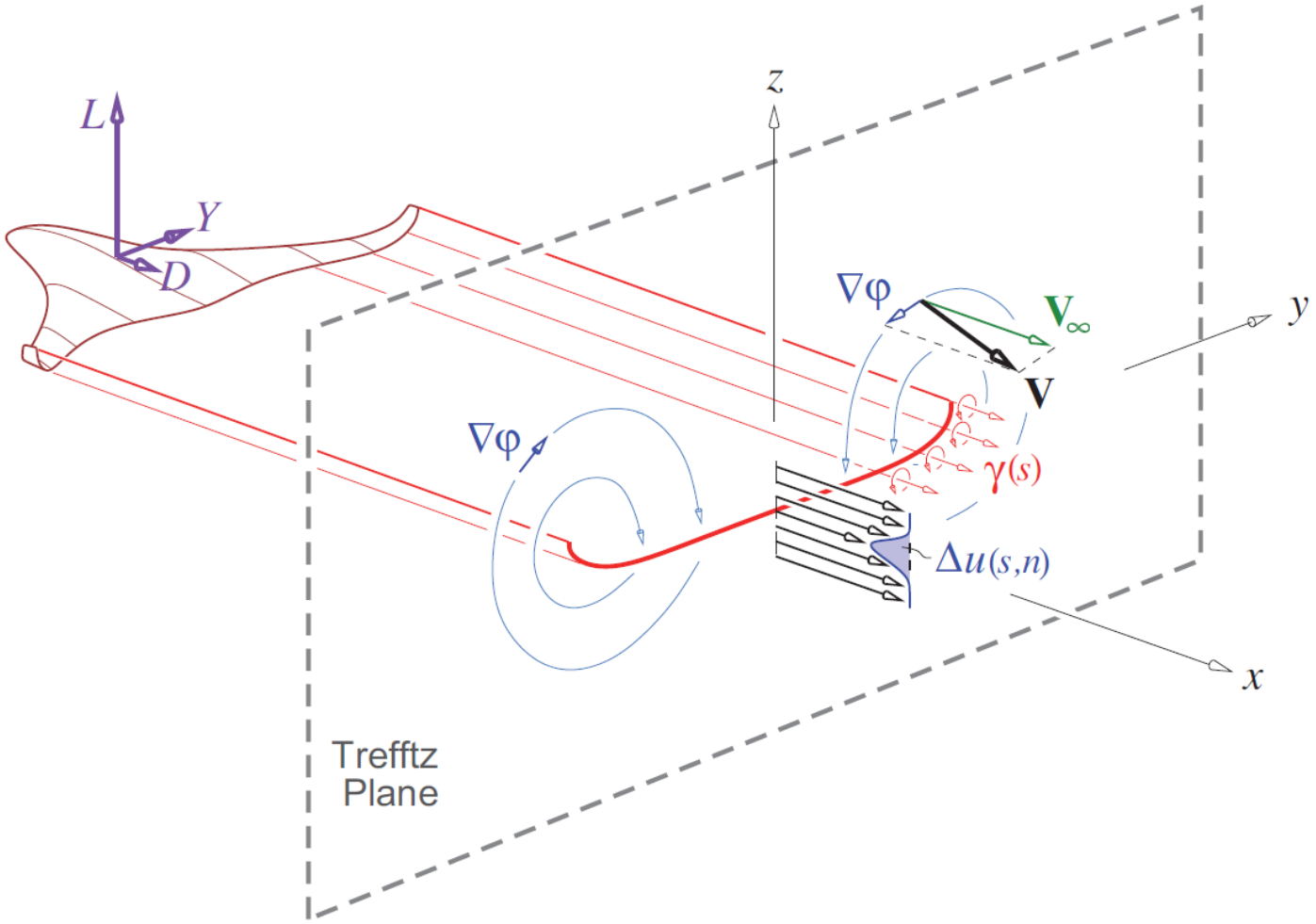

Far field calculations

For the simplest case (elliptic lift distribution), the *Trefftz's plane approach* yields the same lift and drag already found, i.e.

$$L = \frac{\pi\, b}{4}\, \rho\, V_\infty\, \Gamma_0 \qquad D_i = \frac{\pi}{8}\, \rho\, \Gamma_0^2$$

However, the approach allows consideration of more complex configurations

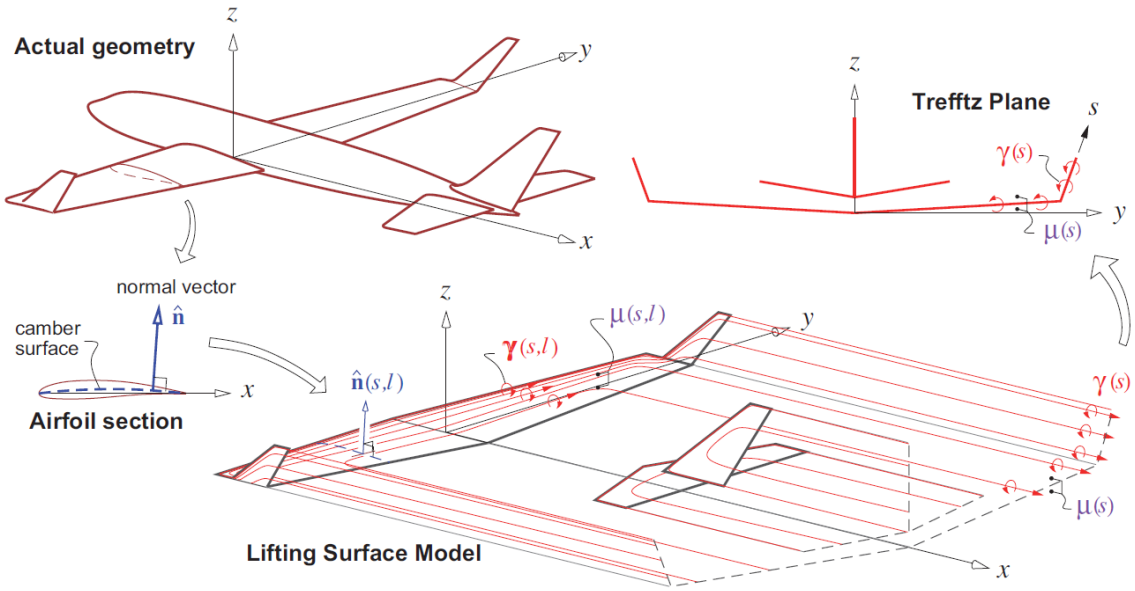

Vortex filaments and lifting line theory

Exercises

1. The rectangular vortex filament in the figure has strength $\Gamma = 200\ m^2/s$. The rectangle is in the plane A-B-C-D. Find the magnitude of the velocity in P.

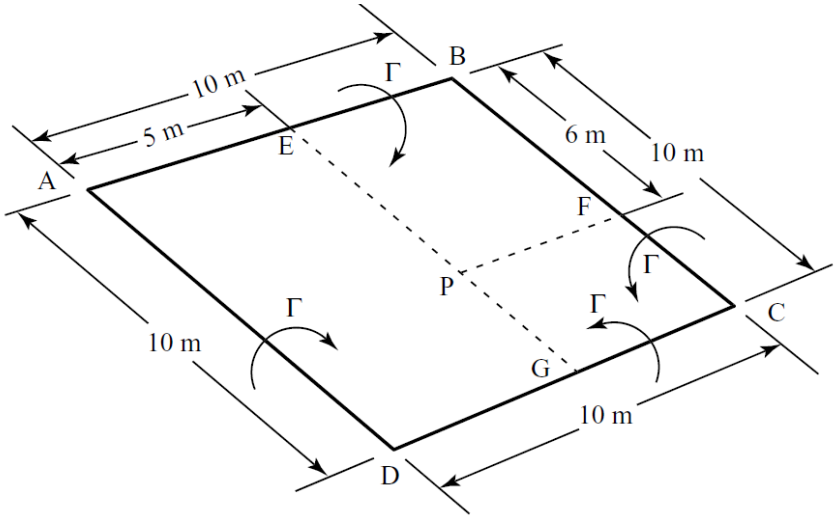

2. Revise all the worked-out examples in the book by Anderson at the end of section 5.3.

3. Revise the completely solved problem proposed in the slides which follow. Then repeat the exercise using the excel worksheet provided by Dr. Joel Guerrero.

Solved exercise

Use the mooplane equation to compute the aerodynamic coefficients for a wing

The monoplane equation *(slide 127; $\theta_0 = \phi$)* will be used to compute the aerodynamic coefficients of a wing for which aerodynamic data are available. The geometry of the wing to be studied is illustrated in Fig. 7.13. The wing, which is unswept at the quarter chord, is composed of NACA 65–210 airfoil sections. Referring to the data of Abbott and von Doenhoff (1949), the zero-lift angle of attack (α_{0l}) is approximately $-1.2°$ across the span. Since the wing is untwisted, the geometric angle of attack is the same at all spanwise positions. The aspect ratio (AR) is 9.00. The taper ratio λ (i.e., c_t/c_r) is 0.40. Since the wing planform is trapezoidal,

$$S = 0.5(c_r + c_t)b = 0.5c_r(1 + \lambda)b$$

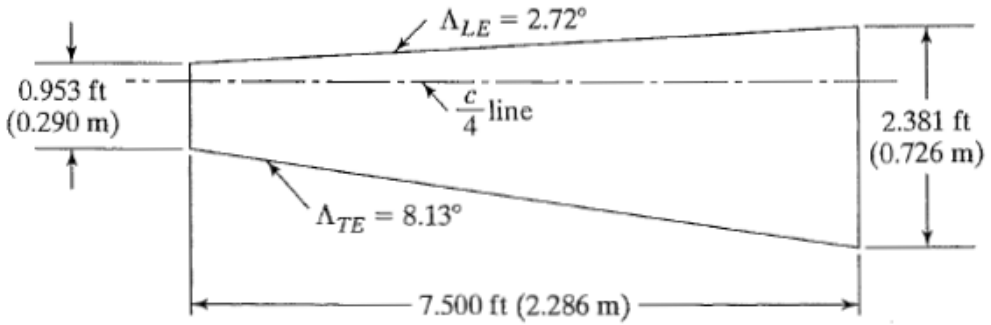

Figure 7.13 Planform for an unswept wing, AR = 9.00. λ = 0.40, airfoil section NACA 65–210.

Solved exercise

and

$$AR = \frac{2b}{c_r + c_t}$$

Thus, the parameter μ in *slide 127* becomes

$$\mu = \frac{ca_0}{4b} = \frac{ca_0}{2(AR) \cdot c_r(1 + \lambda)}$$

$s = b/2$

Solution: Since the terms are to be evaluated at spanwise stations for which $0 \leq \phi \leq \pi/2$ [i.e., $-s \leq y \leq 0$ (which corresponds to the port wing or left side of the wing)],

$$\mu = \frac{a_0}{2(1 + \lambda)AR}[1 + (\lambda - 1)\cos\phi]$$

$$= 0.24933(1 - 0.6\cos\phi) \qquad \textbf{(7.30)}$$

where the equivalent lift-curve slope (i.e., that for a two-dimensional flow over the airfoil section a_0) has been assumed to be equal to 2π. It might be noted that numerical solutions for lift and the vortex-drag coefficients were essentially the same for this geometry whether the series representing the spanwise circulation distribution included four terms or ten terms. Therefore, so that the reader can perform the required calculations with a pocket calculator, a four-term series will be used to represent the spanwise loading. Equation (7.26) is

Solved exercise

$$\mu(\alpha - \alpha_{0l}) \sin\phi = A_1 \sin\phi(\mu + \sin\phi) + A_3 \sin 3\phi(3\mu + \sin\phi) + A_5 \sin 5\phi(5\mu + \sin\phi) + A_7 \sin 7\phi(7\mu + \sin\phi) \quad \textbf{(7.31)}$$

Since there are four coefficients (i.e., A_1, A_3, A_5, and A_7) to be evaluated, equation (7.31) must be evaluated at four spanwise locations. The resultant values for the factors are summarized in Table 7.1. Note that, since we are considering the left side of the wing, the y coordinate is negative.

For a geometric angle of attack of 4°, equation (7.31) becomes

$$0.00386 = 0.18897A_1 + 0.66154A_3 + 0.86686A_5 + 0.44411A_7$$

TABLE 7.1 Values of the Factor for Equation (7.31)

Station	ϕ	$-\frac{y}{s}$ $(= \cos\phi)$	$\sin\phi$	$\sin 3\phi$	$\sin 5\phi$	$\sin 7\phi$	μ
1	22.5°	0.92388	0.38268	0.92388	0.92388	0.38268	0.11112
2	45.0°	0.70711	0.70711	0.70711	−0.70711	−0.70711	0.14355
3	67.5°	0.38268	0.92388	−0.38268	−0.38268	0.92388	0.19208
4	90.0°	0.00000	1.00000	−1.00000	1.00000	−1.00000	0.24933

Solved exercise

for $\phi = 22.5°$ (i.e., $y = -0.92388s$). For the other stations, the equation becomes

$$0.00921 = 0.60150A_1 + 0.80451A_3 - 1.00752A_5 - 1.21053A_7$$
$$0.01611 = 1.03101A_1 - 0.57407A_3 - 0.72109A_5 + 2.09577A_7$$
$$0.02263 = 1.24933A_1 - 1.74799A_3 + 2.24665A_5 - 2.74531A_7$$

The solution of this system of linear equations yields

$$A_1 = 1.6459 \times 10^{-2}$$
$$A_3 = 7.3218 \times 10^{-5}$$
$$A_5 = 8.5787 \times 10^{-4}$$
$$A_7 = -9.6964 \times 10^{-5}$$

Using equation (7.27), the lift coefficient for an angle of attack of 4° is

$$C_L = A_1\pi \cdot AR = 0.4654$$

The theoretically determined lift coefficients are compared in Fig. 7.14 with data for this wing. In addition to the geometric characteristics already described, the wing had a dihedral angle of 3°. The measurements reported by Sivells (1947) were obtained at a Reynolds number of approximately

Solved exercise

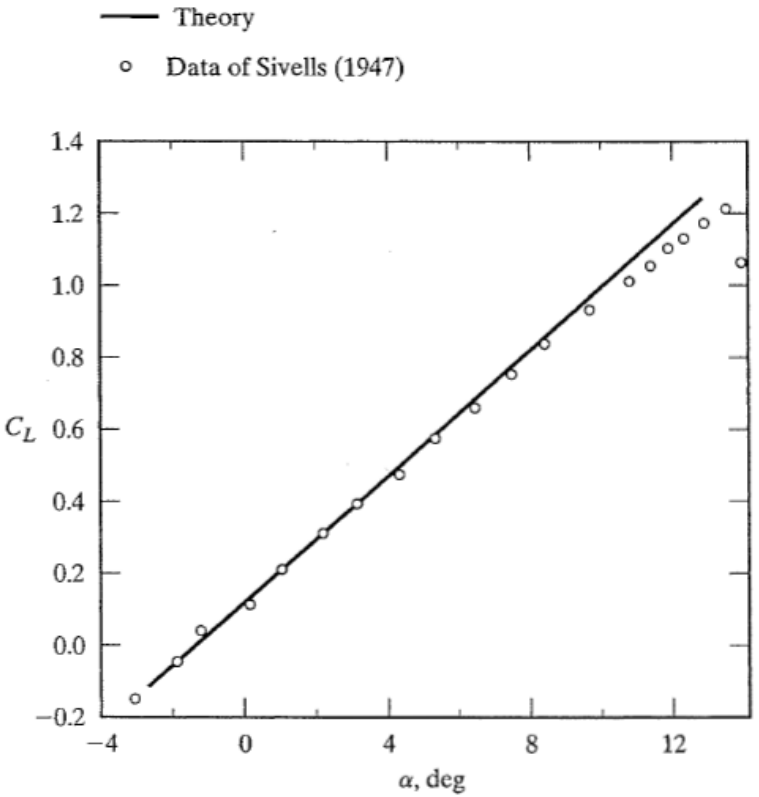

Figure 7.14 Comparison of the theoretical and the experimental lift coefficients for an unswept wing in a subsonic stream. (Wing is that of Fig. 7.13.)

Solved exercise

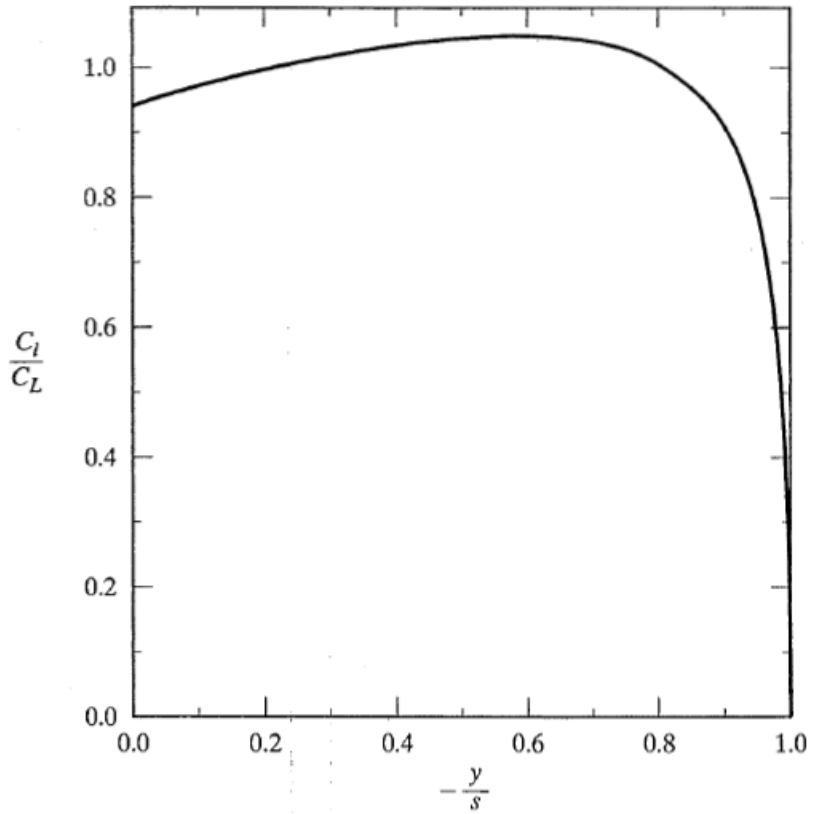

Figure 7.15 Spanwise distribution of the local lift coefficient, $AR = 9, \lambda = 0.4$, untwisted wing composed of NACA 65–210 airfoil sections.

Solved exercise

4.4×10^6 and a Mach number of approximately 0.17. The agreement between the theoretical values and the experimental values is very good.

The spanwise distribution for the local lift coefficient of this wing is presented in Fig. 7.15. As noted by Sivells (1947), the variation of the section lift coefficient can be used to determine the spanwise position of initial stall. The local lift coefficient is given by

$$C_l = \frac{\rho_\infty U_\infty \Gamma}{0.5 \rho_\infty U_\infty^2 c}$$

which for the trapezoidal wing under consideration is

$$C_l = 2(AR)(1 + \lambda)\frac{c_r}{c} \sum A_{2n-1} \sin(2n - 1)\phi \qquad \textbf{(7.32)}$$

The theoretical value of the induced drag coefficient for an angle of attack of 4°, as determined using equation (7.29), is

$$C_{D,i} = \frac{C_L^2}{\pi \cdot AR}\left(1 + \frac{3A_3^2}{A_1^2} + \frac{5A_5^2}{A_1^2} + \frac{7A_7^2}{A_1^2}\right)$$

$$= 0.00766(1.0136) = 0.00776$$

Solved exercise

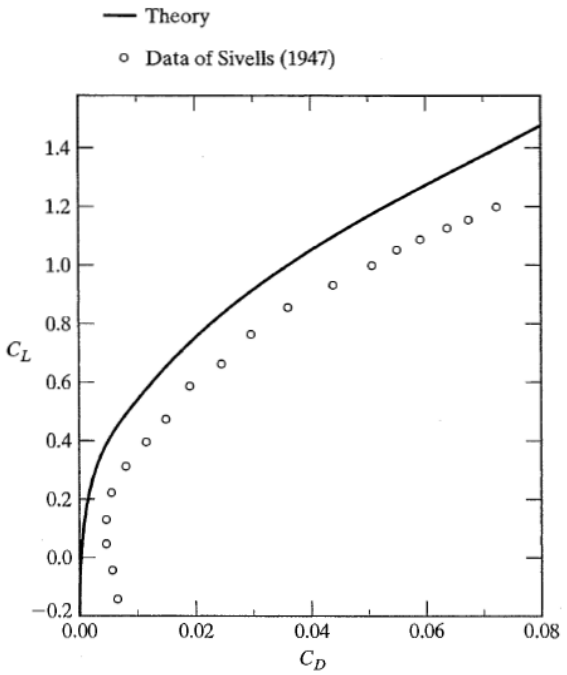

Figure 7.16 Comparison of the theoretical induced drag coefficients and the measured drag coefficients for an unswept wing in a subsonic stream. (Wing is that of Fig. 7.13.)

The theoretically determined induced drag coefficients are compared in Fig. 7.16 with the measured drag coefficients for this wing. As has been noted earlier, the theoretical relations developed in this chapter do not include the effects of skin friction. The relatively constant difference between the measured values and the theoretical values is due to the influence of skin friction.